Direct Contact Membrane Distillation of Saline Wastewater for Recycling

vorgelegt von
Sana Abdelkader
geb. Tunis, Tunesien

von der Fakultät III – Prozesswissenschaften
der Technischen Universität Berlin
und der
Höheren Schule für Lebensmittelindustrie Tunis der Carthage Universität, Tunesien
(im Rahmen des Doppel-Promotionsabkommens)
zur Erlangung des akademischen Grades

Doktorin der Ingenieurwissenschaften
- Dr.-Ing. –

genehmigte Dissertation

Promotionsausschuss:

Vorsitzender:	Prof. Dr. Hamdi Mokhtar (INSAT, Tunesien)
Gutachter:	Prof. Dr.-Ing. Mongi Seffen (ESSTHS, Tunesien)
Gutachter:	Prof. Dr. Martin Denecke (Universität Duisburg-Essen)
Gutachter:	Dr. Joachim Koschikowski (Fraunhofer ISE)
Gutachter:	Prof. Dr.-Ing. Sven-Uwe Geissen (TU Berlin)
Gutachter:	Prof. Dr.-Ing. Latifa Bousselmi (CERTE, Tunesien)

Tag der wissenschaftlichen Aussprache: 11. Dezember 2018
an der Höheren Schule für Lebensmittelindustrie Tunis, Tunesien

Berlin 2018

Dissertation Report
On

Direct Contact Membrane Distillation of Saline Wastewater for Recycling

Presented by

Sana Abdelkader

In the frame of an international joint supervision convention of a doctoral thesis

Submitted to the:

National Higher School of Food Industries **(ESIAT)**, Tunisia

and

Technical University Berlin **(TUB)**, Germany
Faculty III - Process Sciences
Department of Environmental Technology, Chair of Environmental Process Engineering

For the attainment of the academic degree of:

DOCTOR (Dr.-Ing.)

Disciplines:
Food Industries (ESIAT)
Environmental Science and Technology (TUB)

Jury members:
Chairman: Prof. Dr. Hamdi Mokhtar (INSAT, Tunisia)
Evaluator: Prof. Dr.-Ing. Mongi Seffen (ESSTHS, Tunisia)
Evaluator: Prof. Dr. Martin Denecke (University of Duisburg-Essen, Germany)
Examinator: Dr. Joachim Koschikowski (Fraunhofer ISE, Germany)
Supervisor: Prof. Dr.-Ing. Sven-Uwe Geissen (TU Berlin)
Supervisor: Prof. Dr.-Ing. Latifa Bousselmi (CERTE, Tunisia)

Centre of Water Research and Technologies (CERTE), Tunisia

Defense date: 11. December 2018

To my precious and dearest family

To my beloved parents

Ali and Aida

This work would not have been possible without your unconditional love and support, your guidance and your constant belief in me.

A heartfelt Thank You to each and every one of you.

Acknowledgements

I would like to thank all those who helped me and contributed to the preparation and completion of this thesis.

I would like to express my sincere gratitude to my supervisor **Professor Latifa Bousselmi**, head of the research laboratory "Wastewater and Environment (LabEaUE)" at the Center for Water Research and Technologies (CERTE), for her valuable guidance and support throughout the elaboration of this thesis. Her great mentorship, positive outlook and encouragements inspired me and enabled me to carry out this thesis successfully.

I would like also to thank my supervisor **Professor Sven-Uwe Geissen**, head of the "Chair of Environmental Process Engineering" at the Technische Universität Berlin (TUB), for his valuable support and for his constructive suggestions and recommendations during the planning and development of this research work.

I extend my sincere thanks to all members of the jury for the honor they do me by agreeing to read my manuscript and to participate in the defense of this thesis.

My sincere thanks to **Dr. Ali Boubakri**, assistant professor at CERTE, for his help, interest and kind support during the realization of this work.

My thanks also go to my colleagues at the "Chair of Environmental Process Engineering (TUB)" for their support. My special thanks go to **Dr. Gesine Götz** for her constant encouragement and motivation and for the relevance of her advices.

I would like to express my gratitude to **Dr. Joachim Koschikowski**, head of the "Water Treatment and Separation" research group at Fraunhofer-Institute for Solar Energy Systems (ISE), for his support, scientific advice and valuable collaboration. My sincere thanks go also to all the members of the "Water Treatment and Separation" research group at Fraunhofer ISE, for their generosity, their time, resources and expertise which helped me greatly in the elaboration of this work.

I would like also to thank **Dr. Malini Balakrishnan**, senior fellow at The Energy and Resources Institute (TERI), and her research group for giving me the opportunity to work in collaboration with their team and for their interest in my work.

Last but not least, I would like to express my gratitude to all the colleagues and friends who have granted me their moral and intellectual support throughout my thesis. I express my gratitude to all my colleagues at the CERTE, those who kindly agreed to help and to provide their valuable support.

Tunis, August 2018

Sana Abdelkader

Abstract

Freshwater availability is suffering from an increasing pressure created by the growing demand, depleting resources and the environmental pollution. Saline wastewater and saline industrial effluents are creating a complex issue due to their contribution in the pollution and the alteration of both surface water and groundwater properties. Thus, attention is drawn to investigating complete treatment systems for water recovery, especially in the industry. Desalination of saline wastewater presents a possibility to supply households, industry and agriculture with water. Hence, the development of cost effective and efficient treatment processes has become an obligation.

In this work, the first step was to test two biological processes, namely aerobic and anaerobic processes, in combination with two membrane treatments (microfiltration and ultrafiltration) for saline wastewater treatment. It was observed during the tests that both the biological treatments and the membrane filtration performances were significantly affected by the NaCl concentration increase in the feed solutions.

Membrane Distillation (MD) is a competitive technology for water desalination which forms an appealing solution for industrial wastewater treatment. It is getting an increasing attention thanks to its advantages in terms of energy consumption and final permeate quality. In this study, the second step was to apply Response Surface Methodology (RSM) to optimize the Direct Contact Membrane Distillation (DCMD) treatment of synthetic saline wastewater. The aim was to enhance the process performance and the permeate flux by optimizing the operating parameters.

Despite its advantages, one of the most challenging issues in DCMD is membrane fouling and wetting. Therefore, the DCMD treatment of real industrial effluent was a focus in the present research work. Saline dairy effluent discharged from hard cheese industry was first pretreated by macrofiltration (MAF) and ultrafiltration (UF) and then processed by DCMD to investigate the extent of the aforementioned issues. Effluents pretreated by UF have led to the best process performance with stable DCMD permeate flux values at different operating conditions. Fouling has occurred in all the experiments, though their effect on the flux behavior and membrane wetting was different from one feed to the other. The utility theory was applied on the different scenarios that have been experimented using the studied system in order to identify the best demonstrated improvements in terms of process performance and cost-effectiveness.

Zusammenfassung

Die Verfügbarkeit von Süßwasser leidet unter einem zunehmenden Druck, der durch die wachsende Nachfrage, die Erschöpfung der Ressourcen und die Umweltverschmutzung entsteht. Salzwasser und salzhaltige Industrieabwässer stellen ein komplexes Problem dar. So wird die Aufmerksamkeit auf die Untersuchung kompletter Aufbereitungssysteme zur Wasserrückgewinnung, insbesondere in der Industrie, gelenkt. Die Entsalzung von salzhaltigem Abwasser bietet die Möglichkeit, Haushalte, Industrie und Landwirtschaft mit Wasser zu versorgen. Daher ist die Entwicklung kostengünstiger und effizienter Behandlungsverfahren zu einer Verpflichtung geworden.

In dieser Arbeit war der erste Schritt, zwei biologische Prozesse zu testen, nämlich aerobe und anaerobe Prozesse, in Kombination mit zwei Membranbehandlungen (Mikrofiltration und Ultrafiltration) zur Behandlung von Salzwasser. Bei den Tests wurde festgestellt, dass sowohl die biologischen Behandlungen als auch die Membranfiltrationsleistungen durch den Anstieg der NaCl-Konzentration in den Feed-Lösungen signifikant beeinflusst wurden. Die Membran-Destillation (MD) ist eine wettbewerbsfähige Technologie zur Wasserentsalzung, die eine attraktive Lösung für die industrielle Abwasserbehandlung darstellt. Dank seiner Vorteile in Bezug auf Energieverbrauch und Endpermeatqualität erfährt es eine zunehmende Aufmerksamkeit. In dieser Studie wurde im zweiten Schritt die Response Surface Methodology (RSM) zur Optimierung der Direktkontakt Membrandestillation (DCMD) Behandlung von synthetischem Salzwasser angewendet. Ziel war es, die Prozessleistung und den Permeatfluss durch Optimierung der Betriebsparameter zu verbessern. Trotz seiner Vorteile ist Membranverschmutzung und Benetzung eines der schwierigsten Themen bei der DCMD. Daher war die DCMD-Behandlung von realem industriellem Abwasser ein Schwerpunkt der vorliegenden Forschungsarbeiten. Das aus der Hartkäseindustrie eingeleitete salzhaltige Milchabwasser wurde zunächst durch Makrofiltration (MAF) und Ultrafiltration (UF) vorbehandelt und anschließend von der DCMD verarbeitet, um das Ausmaß der oben genannten Probleme zu untersuchen. Die mit UF vorbehandelten Abwässer haben zu bester Prozessleistung mit stabilen DCMD-Permeatfluss bei unterschiedlichen Betriebsbedingungen geführt. Fouling ist in allen Experimenten aufgetreten, obwohl ihr Einfluss auf das Flussverhalten und die Benetzung der Membranen von einem Feed zum anderen unterschiedlich war. Die Utility-Theorie wurde auf die verschiedenen Szenarien angewendet, die mit dem untersuchten System experimentiert wurden, um die an den besten nachgewiesenen Verbesserungen in Bezug auf Prozessleistung und Kosteneffizienz zu identifizieren.

Résumé

La disponibilité de l'eau douce souffre d'une pression croissante créée par la demande progressive, l'épuisement des ressources et la pollution de l'environnement. Les eaux usées salines et les effluents industriels salins créent un problème complexe en raison de leur contribution à la pollution et à l'altération des propriétés des eaux de surface et des eaux souterraines. Ainsi, l'attention est attirée sur l'étude de systèmes complets de traitement pour la récupération de l'eau, en particulier dans l'industrie. Le dessalement des eaux usées salines offre la possibilité d'approvisionner en eau les ménages, l'industrie et l'agriculture. Par conséquent, la mise au point de procédés de traitement rentables et efficaces est devenue une obligation.

Dans ce travail, la première étape consiste à tester deux procédés biologiques, à savoir les procédés aérobie et anaérobie, en combinaison avec deux traitements membranaires (microfiltration et ultrafiltration) pour le traitement des eaux usées salines. Il a été observé au cours des essais que les traitements biologiques et les performances de filtration ont été significativement affectées par l'augmentation de la concentration en NaCl dans les effluents.

La distillation à membrane (MD) est une technologie compétitive qui constitue une solution attrayante pour le traitement des eaux usées industrielles salines. Elle fait ainsi l'objet d'une attention croissante grâce à ses avantages en termes de consommation d'énergie et de qualité de perméat final. Dans cette étude, la deuxième étape consiste à appliquer la méthode d'optimisation par les plans à surfaces de réponses (RSM) pour optimiser le traitement des eaux usées salines synthétiques par distillation à membrane à contact direct (DCMD). L'objectif est d'améliorer les performances du procédé et le flux de perméat en optimisant les paramètres opératoires.

Malgré ses avantages, l'un des problèmes les plus difficiles à résoudre dans la DCMD est l'encrassement et le mouillage des membranes. Par conséquent, la DCMD des effluents industriels réels a été étudié dans ce travail. Les effluents laitiers salins rejetés par une industrie fromagère ont d'abord été prétraités par macrofiltration (MAF) et ultrafiltration (UF), puis traités par DCMD pour étudier l'ampleur des problèmes susmentionnés. Les effluents prétraités par l'UF ont permis d'obtenir les meilleures performances avec des valeurs de flux de perméat stables dans différentes conditions de fonctionnement. L'encrassement s'est produit dans toutes les expériences, bien que leur effet sur le comportement du flux et le mouillage de la membrane ait été différent selon la qualité de l'effluent initial. La théorie de l'utilité a été appliquée aux différents scénarios expérimentaux en utilisant le système de traitement étudié afin d'identifier les meilleures améliorations en termes de performance du processus et de rentabilité.

TABLE OF CONTENTS

1 LITERATURE SURVEY

1.1 INTRODUCTION AND OBJECTIVES

The increasing domestic and industrial demand for clean and fresh water is creating an ever-growing pressure on the global security since water has numerous interlinkages with all the aspects in our life in terms of economic development, energetic demand, environmental security and industrial growth which is getting even more critical with the actual witnessed climate change (**UN report, 2015**). Water scarcity is an urgent problem that needs innovative and adapted solutions in order to satisfy the world's current and future population. According to the UN report "**Water and Energy**" (**2014**), it is expected that the growing global water demand will contribute in the aggravation of the actual issue of water scarcity and unavailability all over the world since it is expected, by 2050, to push 40% of the global population under water scarcity level.

Water desalination is considered as one of the most prevalent solution to overcome the aforementioned problem. However, it presents one of the most energy-consuming processes with 75.2 Terawatt hour per year, which presents 0.4% of the global electricity demand. The high energy consumption characterizes the common desalination technologies: membrane separation processes (Reverse Osmosis: RO) and thermally driven processes (Multistage Flush: MSF, Adsorption Desalination: AD, etc.) (**Shahzad et al. 2017**). Water desalination and more precisely wastewater treatment and desalination is providing an interesting alternative to partially overcome the need for more water resources by creating an alternative water resource through the reuse of the discharged effluents and to integrate them in the industrial or domestic water cycles via multiple desalination technologies like Membrane Distillation (MD) which is offering the production of high quality permeates by the means of lower energy consumption in comparison to the conventional and well established desalination processes (**Miller, 2003; Samblebe, 2006**).

In this context, MD comes as an emerging water treatment technology that is having a growing interest since it is associating the advantages of both membrane and thermal processes to avoid large amounts of energy consumption without compromising the final treated water quality and with an interesting ability to process multiple saline feed water qualities. MD has the particularity of operating under low hydrostatic pressure and low operating temperature (below the feed boiling temperature) without overlooking the particular nature of the driving force which is the transmembrane water vapor pressure difference (**El-Bourawi et al. 2006**).

In this framework comes the present work that is focusing on the saline wastewater treatment:

- The first part of this work is focusing on the treatment of synthetic saline wastewater using different combinations of biological and filtration processes: aerobic biological treatment and anaerobic biological treatment coupled with both microfiltration and ultrafiltration membrane processes by ceramic and polymeric membranes. With a particular emphasis on the salt concentration, the salt content was varied in all of the aforementioned treatments and by using new and a particular kind of membranes made in TERI University laboratories, India. In this section, different treatment processes and wastewater qualities were analysed and investigated to show the effect of each parameter on the processes performance, the treated water quality and on the studied membrane filtration.
- To deal with the efflunts desalination, the second part of this study is focusing on investigating the optimization of synthetic saline wastewater treatment by Direct Contact Membrane Distillation (DCMD) by maximizing the process response in terms of permeate flux through the application of Response Surface Methodology (RSM). This objective will be achieved by the identification of the optimum levels of the operating independent variables, namely, the temperature difference, feed velocity, salt concentration and glucose concentration.
- Considering on one hand the importance of the food industry effluents treatment as well as the possibility of water recovery and on the other hand the lack of researches treating those effluents by membrane distillation, this present work investigates also the capability of Direct Contact Membrane Distillation (DCMD) of treating raw and pretreated saline dairy effluent. The emphasis of these investigations was on the fouling and wetting phenomena that occur during the processing of three feed qualities: i) raw effluent ii) pretreated by macrofiltration (MAF) and iii) followed by ultrafiltration (UF). For the sake of accuracy, the DCMD experiments were performed under various operating conditions. This allows to reveal new insights related to the impact of such conditions on the DCMD process. The major constitutions of this work are listed in the following: An experimental environment is setup to assess the efficiency of DCMD for treating saline dairy effluent.The membranes pore sizes and the effluent pretreatment type are varied in order to analyze their effect on the performance of The DCMD process. The feed velocity and temperature difference are also varied for this purpose and the obtained results are discussed in order to explore the efficiency of DCMD process in this type of industry.The novelty of this research

work consists in investigating the conception of a complete treatment system based on DCMD for a specific real industrial effluent (dairy wastewater). This system takes into consideration the effluent pretreatment with two different technologies.

- The performance analysis of saline dairy wastewater DCMD process is extended so as to consider its cost-effectiveness when in it is associated with two types of pretreatment. To this purpose, we take into consideration a set of parameters (i.e. criteria) that impact the applicability of the DCMD process in industry in order to assess its performance. Having introduced these criteria, a set of indicators are defined and are used in our analysis through the application of the utility theory. Then, a mathematical model is developped to assess the performance of the scenarios that have been experimented using our setup. Finally, the results are discussed based on our case study in order to analyze the cost-effectiveness of the DCMD process with respect to the two pretreatment options.

1.2 SALINE WASTEWATER

Saline wastewater has generally two major origins, namely, sewage and industrial effluents. On one hand, the contamination of surface water and groundwater with salts affects the domestic and municipal wastewater quality since this used resources will end up in the sewage system , this contamination could be attributed to the salinization of the groundwater bodies in some coastal areas (i.e. Mediterranean basin) by seawater and aquifers recharge that is aggravated by the overexploitation of the natural water resources for irrigation and/or domestic activities (**Demir et al., 1999; Panno et al., 2002; Khaska et al., 2013**).Moreover, in some cases the salinity of the groundwater is caused by evaporates dissolution in the groundwater that is driven by gravity (**Bethke et al., 1990**).

On the other hand, some industrial activities are important contributors in the generation of saline effluents because of the high salt concentration consumption (mainly NaCl) in their processes that induces the discharge of large amounts of saline effluents in the environment. Some of the most influencing industries that could be listed in this context are: the chemical industry and agro-food industry as well as leather, textile and petroleum industries (**Antileo et al., 1997**; **Diaz et al., 2002**; **Lefebvre et al., 2006.a**). In addition to the aforementioned saline effluents sources, the water softening (desalination) stations have their share in the generation of non-negligible amounts of hyper saline brines following the application of water desalination technologies (generally, Reverse Osmosis RO) **(Lattemann et al., 2008**).

According to the UN report (**2017**), untreated and poorly treated wastewater discharge in the environment is still a common practice in some countries leading to direct negative impact. This influence affects not only the human health but also the fauna and flora since we cannot dissociate the discharged effluents from the water cycle (**Figure 1**). This dilemma gets even more complex and critical when the wastewater contains high salt levels in addition to the organic pollutants (**Lefebvre et al., 2006.a**).

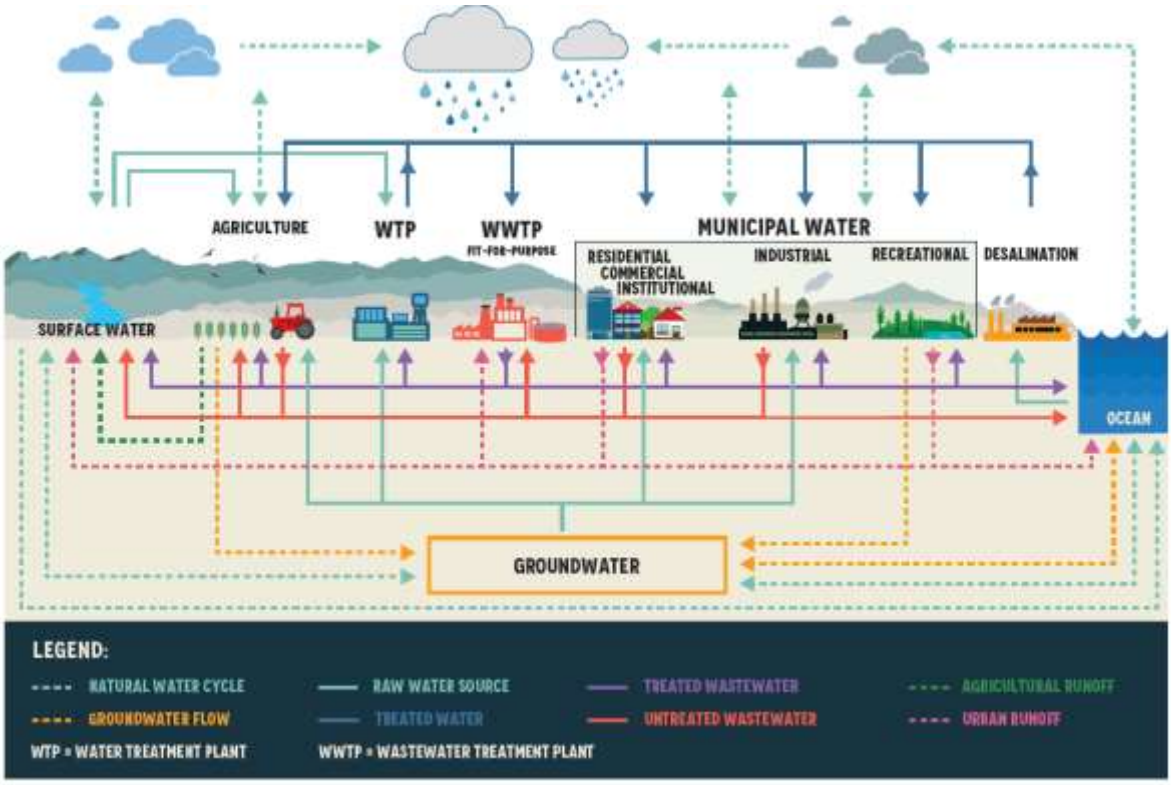

***Figure 1**: Wastewater in the water cycle (source: UN report 2017).*

1.2.1 Saline effluents treatment

1.2.1.1 Biological processes

Aerobic activated sludge process and anaerobic digestion are generally the most applied processes for wastewater treatment that can lead to good effectiveness in terms of Chemical Organic Carbon COD reduction levels (**Sundaresan et al., 2008**; **Saleh et al., 2004**).

Membrane bioreactors (MBRs) which are the combination of membrane separation and the activated sludge process, are now widely used in wastewater treatment with well recognized advantages (**Judd and Judd, 2006**). Meanwhile, their performance is also known to be limited by fouling, which constrains both operating flux and ultimately, the membrane lifetime (**Ji et al., 2006**) due to soluble and bound colloidal/macromolecular substances in the sludge biomass which is referred to as soluble and bound extracellular polymeric substances (EPS), respectively (**Bura et al., 1998; Nuengjamnong et al., 2005**; **Ji et al., 2006)**.

There are two fundamental strategies for cells to survive under osmotic stress:

- The increase of the intracellular ion concentration in order to balance the external osmotic pressure, and all intracellular enzymes have to adapt to the new conditions. This strategy is followed by the anaerobic halophilic bacteria, whose entire physiology has been adapted to high saline environments (**Kempf et al., 1998**).
- Many microorganisms accumulate osmotically active solutes called "compatible solutes". The high external osmotic pressure is balanced within the cells by organic compatible solutes to protect and enhance the bacterial growth in high osmolality environments (**Kempf et al., 1998**).

The complexity of saline wastewater treatment derives mainly from the fact that the usual biological processes has shown in some cases limited performance mainly linked to the effluents salt concentration (**Wang et al., 2005**). Moreover, it is well known that in high salt content levels, the microorganism's osmotic stress is increased which could have inhibitory or toxic effects on the sludge bacteria. This could lead to the cells plasmolysis and/or the inhibition of their activity, thereby reducing the effectiveness of biological treatment in terms of chemical oxygen demand (COD) removal (**Reid et al., 2006**; **Luo et al., 2015**).Hence, it was found in previous research that in MBR treatment the microbial community is altered due to salinity changes and the effluent salinity significantly affects the physical and biochemical properties of the activated sludge, leading to several changes in the MBR treatment performance: the settlement phase, the bio-flocculation, the membrane surface charge, hydrophobicity and filterability (**Kargi and Dincer, 1996; Dincer and Kargi, 2001**).

Reid et al. (2006), revealed in their study that effluents witnessing salinity shocks over a certain range (0.1–4 g/L) are likely to become even more challenging to an MBR than effluents having readily stable salinity levels.

Therefore, and according to them, coastal-based installations that are struggling with seawater intrusion and other treatment plants that are dealing with the treatment of certain saline

effluents may benefit from the use of buffer tanks, or possibly pre-sedimentation which would enhance the MBR treatment by reducing the effluents' organic load.

Several studies have examined the anaerobic treatment of different saline industrial effluents such as those generated by seafood, tanning and textile industries in addition to saline sewage wastewater (**Lefebvre et al., 2006.a; Moharram et al., 2015**).

Ozalp et al. (2003) proposed the use of an up-flow anaerobic sludge bed reactor (UASBR) and they measured an 85% total organic carbon (TOC) removal in synthetic sewage wastewater with NaCl concentration of 15 g/l. In their study, the hydraulic retention time (HRT) was 24h and the reactor gradually reached 15 g NaCl/L over a period of 109 days. Besides, it is worth mentioning that TOC analysis was used due to difficulties encountered in carrying out COD analyses because of the interference of chlorides in highly saline samples.

Rovirosa et al. (2004) studied the treatment of saline wastewater by using a laboratory down-flow anaerobic fixed bed reactor. The results showed that an HRT of 24 h was required to obtain total COD, organic-N, total-P and fecal coliform concentration reduction efficiencies higher than 72%, 51%,39% and 98%, respectively, with sea salts concentrations in the range from 5 g/L to 15 g/L.

Gebauer (2004) studied anaerobic treatment of sludge from saline fish farm effluents and followed the COD removal in undiluted sludge with 35%salinity varied between 40% and 54% depending on the operating condition. Another research focusing on the treatment of saline wastewater of tannery soak liquor in an up-flow anaerobic sludge blanket reactor (UASB) showed that 78% COD removal can be obtained at 5 days HRT and 71 g/L total dissolved solids (TDS) as salinity (**Lefebvre et al., 2006.b**).

To overcome the limitations observed in the anaerobic digestion, some studies focused on investigating the influence of the operating conditions on the process efficiency. For instance, **Vyrides and Stuckey** (**2009.b**) studied the possibility of compatible solutes addition to the anaerobic saline medium and found that glycine betaine had the best effect on its performance and that under high salinity conditions (2% and 4% NaCl) there has been more production of extracellular polymeric substances (EPS) and the mean floc size was relatively bigger.

Moreover, **Shi et al.** (**2014**) reported in their study that sequential anaerobic–aerobic treatments of saline pharmaceutical wastewater achieved high COD removal rates that reached 94.7% and 91.8%.The use of salt-tolerant (halophilic) microorganisms was also investigated to study how effective the biological treatment could be when treating saline effluents with the selected microbial groups through the enhancement of the COD removal rates (70% to 84%

with effluents having an NaCl concentration of 3%) with emphasis on the microorganism's survival capability in osmotic stress (**Kapdan et al., 2007; Zhang et al., 2014**).

1.2.1.2 Membrane processes

Membrane treatment includes multiple separation classes according to the substances rejected by the membranes which is mainly controlled by the membranes pore size (**Figure 2**). Macrofiltration, microfiltration and ultrafiltration could be considered as pretreatments to the saline effluents desalination since they have no effect on the salt concentration reduction, but they could provide good suspended solids and colloids removal rates which improve the saline effluents quality for further desalination (**Lefebvre et al., 2006.a**).

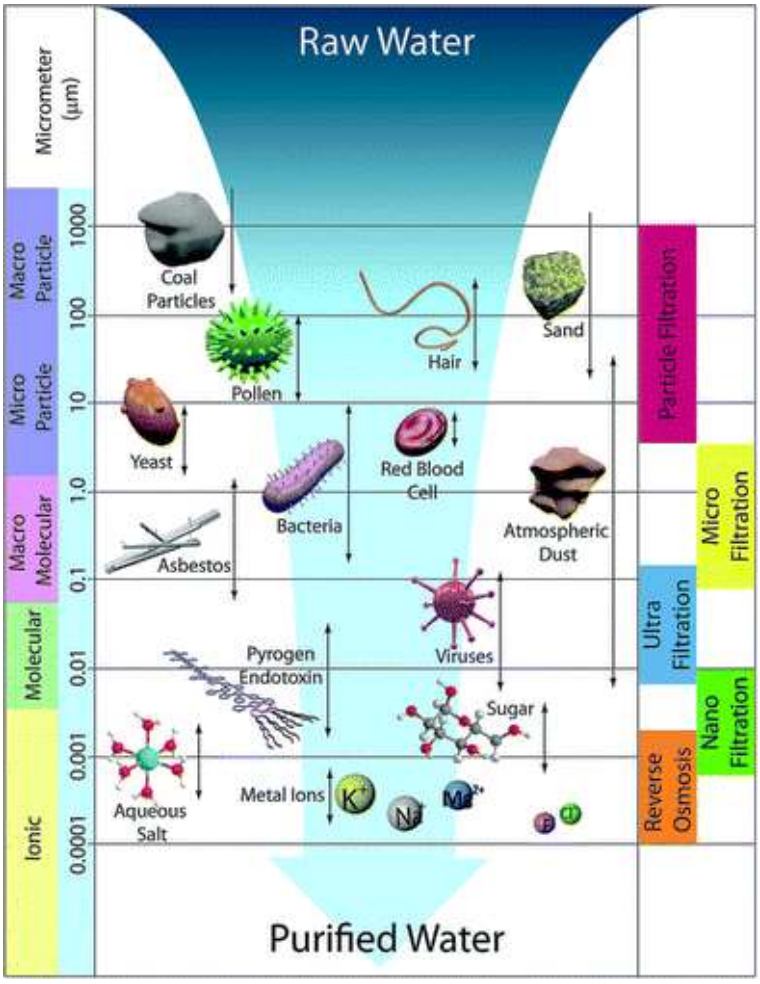

***Figure 2**: Schematic illustration of the different membrane filtration types according to the retained particle's size. (Source: lee and al. 2016)*

Nanofiltration, as a membrane separation technology using both electric charge (Donnan effect) and pore size (sieving effect), could separate low molecular weight solutes (e.g. glucose, saccharides, amino acid, and peptide) from inorganic salt solutions, and simultaneously concentrate organic solutes and remove inorganic salt, showing a good potential in desalination and/or the recovery of valuable organic substances (permeation of monovalent salts) (**Mohammad et al., 2010**). Moreover, the salt ions could easily pass through the membrane at high salt concentrations; even the nominal monovalent salt rejection was often negative in mixtures of salts and large charged organic molecules or mixed monovalent–multivalent salts, thus greatly decreasing osmotic pressure difference across membrane (**Luo et al., 2009; Mohammad et al., 2010**).

The most commonly applied desalination technology is Reverse Osmosis (RO) which showed good performance but has an important disadvantage which is the process high energy consumption which reflects on the process cost, since for a typical reverse osmosis seawater desalination plant, it is required to provide 3 to 10 kWh of electric energy in order to produce one cubic meter of freshwater and most of the required energy is used to pressurize the feed streams and such operating pressure is related to feed salinity degree (**Dashtpour et al., 2012**). For instance, the applied pressure could vary between 15 to 30 bars for brackish water and could range between 55 to 70 bars for seawater desalination (**Dashtpour et al., 2012**). Another issue that is common in membrane treatments, and especially in RO, is the membrane fouling which highly affects the water recovery rates that can drop to 25% to 45% when treating seawater (**Charcosset, 2009**).

When observing the membrane processes performance, it appears to be a complex function of the feed water characteristics and the chemical and physical properties of the membrane itself. These complex interactions make process control difficult as the feed water mixture can change in time (**Tchobanoglous and al., 2003**).

1.2.1.3 Other processes

Different physico-chemical technologies were employed for the treatment of saline effluents such as thermal processes which include the solar evaporation as the simplest technique and the multi-effect evaporation which could have a competitive cost in comparison to membrane processes (mainly RO) in some regions where there is high availability of energy with low cost (**Lefebvre and al. 2006.a).**

Chemical oxidation was also applied as one of the viable options for the treatment of saline effluents, for example, Boron-Doped Diamond anodes were utilized for electrochemical

oxidation of industrial saline streams which has led to good removal rates in terms of TOC and ammonia and consequently increased the effluent's biodegradability and demonstrated that electro-oxidation could be considered as a good alternative for pretreatment before biological processes application (**Anglada et al., 2010**).

Ion exchangers are also used to desalinate water by removing the effluents ionic content through anionic and cationic resins that catches the ions and then the resins are subjected to a regeneration phase (backwashing) which leads both to cost increase of the process and the generation of high concentration streams (**McGhee, 1991**).

Another possible treatment is the coagulation/flocculation process which could be a pretreatment in the case of high salinity effluents in order to reduce the colloidal COD by the means of coagulant agents. However, this process doesn't decrease the salt concentration which requires further treatments for salt removal (**Lefebvre et al., 2006.a**).

Nevertheless, the existing alternative desalination treatment approaches, such as crystallization, extraction, ion-exchange and electrodialysis, are usually too expensive to be effectively put in industrial applications and the cost of treatment can eventually undermine the economic viability of the whole process with progressing tightening of environmental regulations (**Jianquan et al., 2013**).

1.2.2 Cheese industry wastewater

Treating real industrial wastewater, more precisely food industry effluents, presents a challenging issue when it comes to water recovery and reuse due to their complex and generally fluctuating compositions and characteristics (**Blaschek et al., 2007**). Among the food processing industries, we find dairy industries which consume variable water quantities and generate effluents that have variable characteristics and qualities depending on the final product and the steps of the process design (**Rivas et al., 2010**).

1.2.2.1 Cheese whey wastewater composition

Cheese making procedures generate effluents that are mainly composed of the water volumes that are utilized for cheese manufacture and the cleaning process in addition to cheese whey that could have different qualities depending on the processed raw milk characteristics and on whether there has been a valorization step of the cheese whey in the industry (**Table 1**) (**Carvalho et al., 2013**).

Saline cheese whey effluents are often characterized, in addition to their salt content, by a variable organic load due to the presence of whey proteins and traces of other milk fat and

proteins which are found with variable proportions in the discharged wastewater after hard cheese manufacture (**Blaschek et al., 2007**).Whey proteins are mainly composed of: β-lactoglobulin (60%), α-lactalbumin (20%), Immunoglobulin G (10%), Bovine Serum Albumin: BSA (3%) and Lactoferrin (0.1%) (**Singh et al., 2014**). Their molecular masses are respectively: 18.3 kDa, 14.2 kDa, 161 kDa, 66.4 kDa and 76.1 kDa. Concerning the other milk proteins, they are casein micelles (molecular weight ranging from 10^6 to $>10^9$ Da) and they are consisting in aggregates formed through hydrophobic and electrostatic repulsive interactions of casein proteins and micellar calcium phosphates. Among the caseins, which are responsible of the whitish color of cheese whey, we find α_{S1}-casein, α_{S2}-casein and β-casein (**Singh et al., 2014**).

Table 1: *Compilation of cheese whey wastewater characteristics (adapted from Carvalho et al., 2013 and Kezia et al., 2015).*

pH/EC	Lactose	Proteins	Fats	COD	TOC	Total solids	Reference
7±2/-	-	-	-	1.62 ±0.56	0.55 ±0.09	-	**Fang et al.,1991**
4.3-8.7/-	-	2.3-33.5	0.4-5.7	5.4-77.3	-	3.9-58.9	**Kalyuzhnyi et al., 1997**
5.92	44.37 ±0.88	9.06	-	71.41	35.4	62.44±2.9	**Yang et al., 2003**
7.83-7.9	-	-	0.33-0.95	11.8-17.6	-	-	**Janczukowicz et al., 2008**
-/ 110-127	4.5±1	0.3±0.05	-	-	-	114±5	**Kezia et al., 2015**
4-4.6/ 11.3-13.5	0.178-0.182	(939-947) 10^{-6}	1.83-3.76	8.8-25.6	-	7-8.3	**Rivas et al., 2010**
-	0.18 ±0.003	(943±6) 10^{-6}	-	18.5±1.4	-	7.7±0.6	**Rivas et al., 2011**
-/ 66-74	8±0.6	3.6±0.3	-	-	-	77±7	**Kezia et al., 2015**

All parameters are expressed in (g/L) except EC (mS/cm).

As illustrated in **Table 1**, the cheese whey wastewater has a fat content that varies in a wide range and this fraction comes originally from the raw milk lipids which are present in the milk serum under a dispersed form of globules that have different diameters varying generally between <1µm to almost 20µm with a mean size of 3 to 4µm and the fat globules size distribution is closely linked to the medium (milk or whey) homogenization, since it induces the breakdown of the fat globules and the change of their native structure (**Argov et al., 2008**; **Singh et al., 2014**).

1.2.2.2 Cheese whey wastewater treatment

Generally, cheese whey wastewater is conventionally treated chemically (coagulation/ flocculation) and/or via biological processes (aerobic and anaerobic digestion) to reduce its Chemical Oxygen Demand (COD) significantly with removal rates that can reach 99% in some cases (**Carvalho et al., 2013**). However, in the presence of high salt content, biological effluent treatment showed limited performance due to the alteration of the biomass properties and growth which causes the instability and reduction of the organic removal process especially with the presence of salt built-up (**Jang et al., 2013**).

1.3 MEMBRANE DISTILLATION

1.3.1 Process description

MD is an emerging water treatment technology that focuses mainly on water streams desalination. This technology is known as a thermally driven process that includes membrane separation via the transport of water vapor molecules through a hydrophobic microporous membrane (**Figure 3**). MD has interesting advantages thanks to the fact that it summarizes both benefits of membrane and thermal processes through its relatively low energy consumption and the generation of water with high quality **(El-Bourawi et al., 2006**). Additionally to its high salt rejection rates, MD is characterized by good rejection rates of non-volatile and low adsorptive organic compounds (**Carnevale et al., 2016; Plattner et al., 2017**).

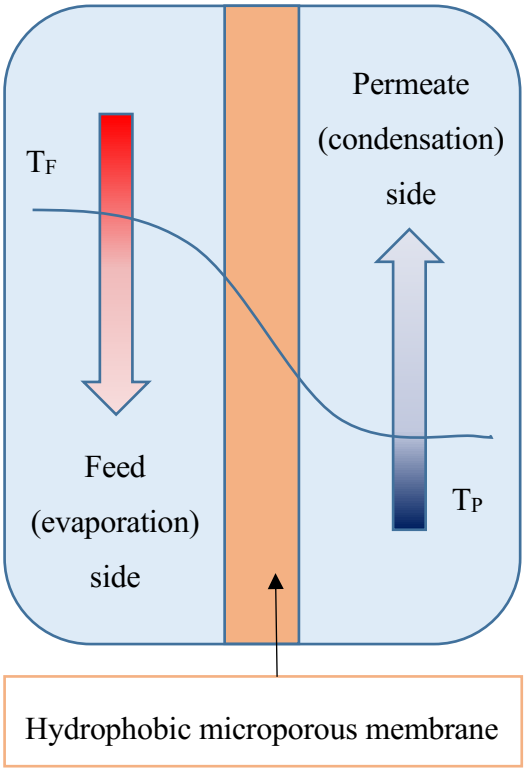

Figure 3: *Schematic of MD process*

As shown in **Figure 3**, MD process is based on the presence of two separate hydraulic loops: first, one evaporation side where the feed is being heated (T_F) and circulated continuously and has to enter in direct contact with the hydrophobic membrane and second, one condensation side where the permeate is being cooled (T_P) and circulated continuously which creates a temperature gradient between the two membrane's sides following which the water vapor molecules start passing from the first side to the second one through the microporous barrier that prevents the liquid streams from being transferred to the opposite side due to surface tension forces and consequently liquid/vapor interfaces are created on the membrane(**Khayat et al., 2011**).

One of the most important characteristics of MD is the ability of operating under low hydrostatic pressure and low operating temperature since the feed stream temperature could be inferior to its boiling temperature, which makes MD an attractive option for water desalination, and another particularity of MD process is the nature of the driving force that is based on the transmembrane water vapor pressure difference between the two streams (**Alkhudhiri et al., 2012**). Since the feed in MD process doesn't require to be heated up to high temperature levels, the use of the waste heat in the plants (via heat recovery heat exchangers) or alternative energy

resources (i.e. solar energy, etc…) for this purpose is a possible option that helps in dwindling the MD process cost (this could include low amount of additional heating if needed) especially when the thermal energy resources are limited (**Guan et al., 2015**). One of the possibilities to recover heat for MD process operation is the concentration cascades design that is formed of multiple MD units with countercurrent cross-flow continuous water circulation where the heat is recycled for each cascade in order to achieve maximum heat recovery with good water recovery levels that can reach 50% to 60% without additional heat resources (**Lee et al. 2011; He et al., 2013**).

1.3.2 Membrane distillation configurations

Depending on the methodology following which the water vapor is recovered and collected in the cool side of the porous hydrophobic membrane (the permeate side) we can distinguish multiple MD configurations where the way of inducing the vapor pressure gradient across the membrane is different (Figures 4 and 5) (**Drioli et al., 2014**).

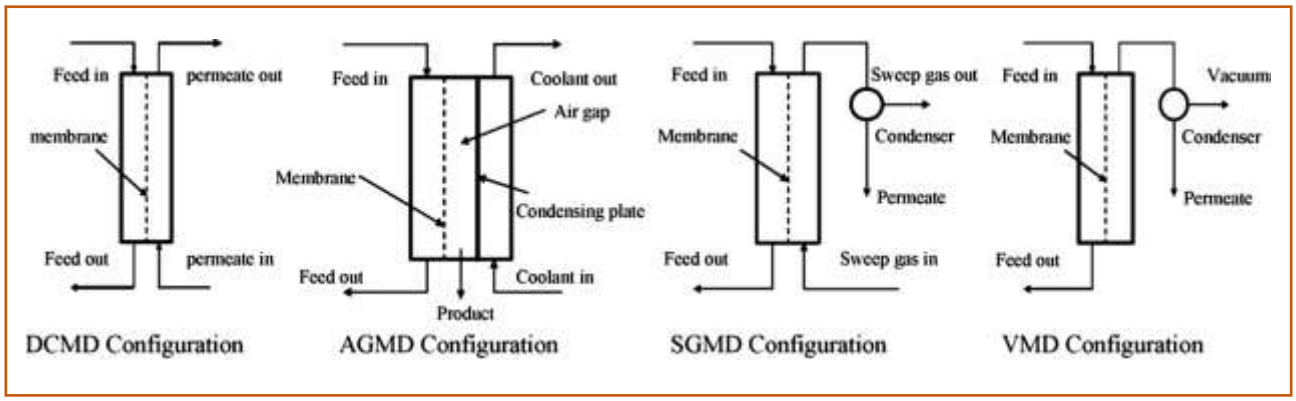

***Figure 4**: Common types of membrane distillation configurations (adapted from El-Bourawi et al., 2006)*

1.3.2.1 Direct Contact Membrane Distillation (DCMD)

This is the simplest configuration of MD, where the permeate stream is kept in direct contact with the opposite side of the hydrophobic membrane (**Figure 4**). In this case, both feed and permeate streams are being circulated using pumps and the created vapor pressure across the membrane induces the vapor molecules to pass through the membrane and to be condensed directly in the cooler water stream (**Khayat et al., 2011**).

1.3.2.2 Air-gap Membrane Distillation (AGMD)

In this configuration, a condensing surface (or plate) is placed after an air gap between the membrane surface and coolant stream (**Figure 4**). The vapor molecules which pass through the membrane cross the air gap and condensate on the cold waterproof surface to be collected afterwards as the MD permeate and consequently the membrane has no wetting risks on the permeate side (**Drioli et al., 2014; Ashoor et al., 2016**).

1.3.2.3 Sweeping-gas Membrane Distillation (SGMD)

The liquid stream in the permeate side is replaced in this configuration by an inert gas which sweeps the membrane on the permeate side and the condensation of water vapor molecules is performed outside the membrane module (**Figure 4**), such configuration is useful when treating feed streams that contains volatile compounds and the obtained permeate quality will be independent of the membrane wetting (**El-Bourawi et al., 2006**; **Alkhudhiri et al., 2012; Drioli et al., 2014**).

1.3.2.4 Vacuum Membrane Distillation (VMD)

In this particular configuration vacuum is created on the permeate side using a vacuum pump which creates on this side a pressure lower than the saturation pressure of the volatile molecules in the feed stream and afterwards the vapor condensation is made outside the membrane module like in the SGMD configuration (**Figure 4**). VMD configuration provides high permeate fluxes but it can present higher risks of membrane wetting and fouling in some cases (**El-Bourawi et al., 2006; Khayat et al., 2011; Drioli et al., 2014)**.

1.3.2.5 Osmotic Membrane Distillation (OMD)

The major difference between OMD and the previous MD configuration is that OMD is a non-thermal process that operates at constant and relatively low temperature and the driving force (vapor pressure gradient) is created by the water activity difference between the two liquid streams (**Figure 5**) which enter in direct contact with the membrane surface on both sides (on one side the feed stream and on the other typically a brine stream) which is realized under atmospheric pressure.

This configuration could be interesting when treating viscous and/or thermally sensitive feed streams (**Babu et al., 2006; Warczok et al., 2007**).

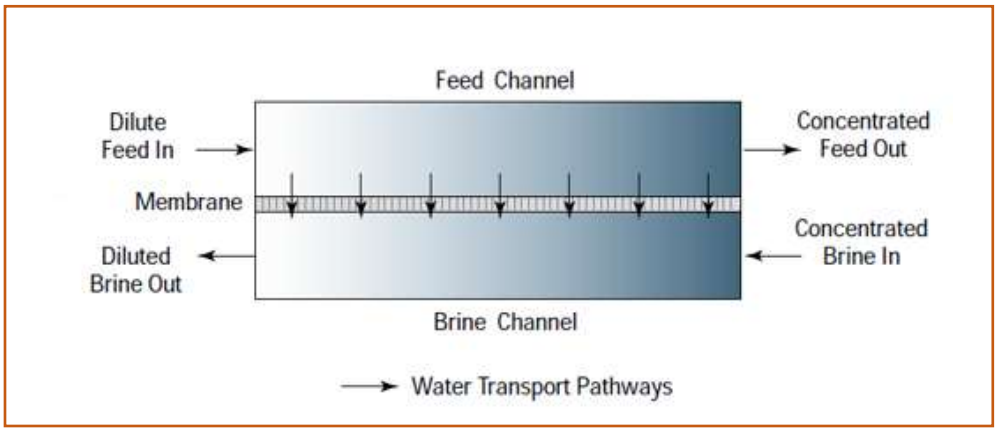

***Figure 5**: Schematic of Osmotic Membrane Distillation (OMD) (source: Hogan et al., 1998)*

1.3.3 Transport phenomena in Direct Contact Membrane Distillation (DCMD)

In Membrane distillation, the water vapor molecules transport through the microporous hydrophobic membrane involves two types of transport mechanisms, namely, heat transfer and mass transfer which are governing the process performance.

1.3.3.1 Heat transfer

According to **El-Bourawi et al**. (**2006**), the heat transfer could be divided into four distinct steps: the first step is the heat transfer from the circulating feed stream to the membrane surface which is made through the membrane thermal boundary layer on the feed side; the second step is realized by conductive heat transfer across the membrane matrix and its pores that are generally filled with gas; the third step is the heat transfer related to the vaporization latent heat which is considered as the efficient heat in the membrane distillation process; the fourth step of heat transfer does occur from the permeate side membrane surface to the circulating permeate stream and this through membrane's thermal boundary layer.

The first and fourth heat transfer steps are associated to the temperature polarization effect which is equivalent to a heat transfer resistance on both membrane sides resulting in a decrease in the MD driving force that could even reach 80% and this due to the lower temperature difference on the membrane surface in comparison to the bulk temperature difference (**Lawson et al., 1996; Martinez-Diez et al., 1999**).

1.3.3.2 Mass transfer

In direct contact membrane distillation, the mass transfer, which is expressed generally in mass flux (J), is created through the vapor pressure gradient between the feed and permeate streams

that enter in direct contact with the two membrane surfaces. During the mass transfer mechanism, three different steps could be distinguished (**Onsekizoglu, 2012**): the water that enters in contact with the membrane surface on the feed side is evaporated to transfer afterwards across the hydrophobic membrane through the pores and finally the water vapor condensates at the permeate side on the membrane vapor/liquid interface.

1.3.4 Membranes in DCMD

One of the most important characterizations of MD process is the hydrophobic microporous membrane through which water vapor is transferred due to a temperature gradient created between the feed and the permeate streams. (**Camacho et al., 2013; Ashoor et al., 2016**).

The membranes utilized in MD process are generally made from polytetrafluoroethylene (PTFE), polypropylene (PP) or polyvinylidene fluoride (PVDF) with low resistance to mass transfer and in order to ovoid heat losses across the membrane, it should also have low thermal conductivity with good resistance to high temperatures and chemicals (**Alkhudhiri et al., 2012).**

In addition to the aforementioned specifications, supplementary characteristics should be available in the hydrophobic membrane in order to have good performance of the membrane distillation process. Among the important membrane properties, we can distinguish: membrane thickness, porosity and nominal pore size as well as liquid entry pressure (wetting pressure) (**Drioli et al., 2009**). Membrane thickness has an inversely proportional relationship with the permeate flux since increasing the thickness has direct positive effect on the membrane mass transfer resistance increase (**Alkhudhiri et al., 2012).** The membrane porosity in MD membranes varies between 30% and 85% and it is equivalent to the percentage of the pores volume divided by the total membrane volume which means that when increasing the membrane's porosity the permeate flux increases (**Alkhudhiri et al., 2012; El-Bourawi et al., 2006).**Membrne nominal pore size is a sensitive parameters since a choice has to be made to operate with the appropriate pore size (having dimensions that are large enough to have good permeate fuxes) and, at the same time, maintaining a good permeate quality since membranes with large pore sizes are more vulnerable to wetting (**Drioli et al., 2014**). Thus, an optimum pore size should be considered depending on the feed quality to avoid the pores wettability (**El-Bourawi et al., 2006**). As for the membrane Liquid Entry Pressure (LEP), this parameter has significant effect on the process performance and presents an important indication of the membrane quality and the MD process performance, since the feed pressure should not exceed the membrane's LEP in order to maintain the its hydrophobic character (**Alkhudhiri et al.,**

2012). Moreover, the membrane's LEP is significantly affected by the feed concentration and organic content and other solutes in the feed stream such us ethanol which usually reduces the membranes hydrophobicity (**Alkhudhiri et al., 2012; Gostoli, 1989**).

The enhancement of MD process has drawn attention to the improvement of the membrane hydrophobicity using multiple techniques such as the utilization of hydrophobic surface modifying macromolecules on poly(vinylidene fluoride) hydrophobic composite membranes which has led to promising results in sea water MD treatment (**Prince et al., 2014.a**). Moreover, multiple studies have focused on the enhancement of the driving force for the water vapor transport in MD process through the development of hydrophobic membranes that have high resistance to pore wetting which did lead to significantly higher flux levels along with high rejection rates (**Prince et al., 2012; Prince et al., 2014.b; Efome et al., 2016**).

1.3.5 Fouling and wetting in DCMD

One of the challenges that faces MD is the capability of treating real industrial effluents that could contribute in the creation of new alternative water resources for the industry, knowing that the feed quality has an important impact on the membrane fouling, by the means of the variable organic and/or mineral components that are present in the feed streams (**Ashoor et al., 2016**).

According to **Tijing et al.** (**2015**),there are different parameters that affect and govern the membrane fouling in MD process which could be classified into four different groups, namely: the feed water characteristics (organic load, ionic strength, pH, etc.), the operational conditions (flow rate, liquid streams temperature, etc.) the membrane properties (pore size, hydrophobicity, etc.) and the foulant characteristics (such as its concentration, molecular size, solubility, hydrophobicity, etc.). The effluent's organic content is one of the most affecting factors responsible of the membrane alteration in membrane processes, especially in MD, by its deposition on the hydrophobic membrane surface during the process and which increases the possibilities of fouling phenomena (**Naidu et al., 2014**).

In addition to the organic fouling, mineral fouling (scaling) could also occur during MD process and has significant effect on the flux decline such as in the case of $CaCO_3$ precipitation on the membrane surface which reduces the membrane permeability and rises the temperature polarization effect in addition to its influence on the membrane wettability after the formation of a deposit on the membrane surface (**Gryta, 2008**).

1.3.6 Pretreatment and membrane cleaning

Multiple strategies could be considered to reduce membrane fouling in MD among which we find effluent pretreatment using multiple methods that include sedimentation, acidification and degasification, coagulation/flocculation, thermal processes and membrane pretreatments which have shown an undeniable positive effect in the MD process enhancement and such filtration pretreatments are gaining more attention due to their ability to efficiently remove of different particles and large macromolecules in the feed stream (**Tijing et al., 2015**).

The membrane chemical cleaning could also be considered as a solution to remove the deposited fouling layer, periodically. Nevertheless, cleaning could also contribute in the membrane wettability and such risk imposes a limited membrane cleaning without complete dissolution of the deposit (**Gryta, 2008**). The chemical cleaning involves generally the circulation of heated acids and basic solutions to address the both the inorganic (rinsing with acid solution) and the organic fouling (rinsing with basic solutions) which could relatively allow to regain the initial flux in the case where the fouling layer is deposited on the membrane surface but if the fouling is located inside the membrane pores, the flux recovery would be very difficult to achieve and the membrane will lose in hydrophobicity with the repeated cleaning (**Tijing et al., 2015**).

1.3.7 Fields of application

Based on its high separation performance, MD is being investigated and applied for water, and in some cases, nutrients recovery from various types of effluents, taking into consideration the effect of the experimental parameters (**Izquierdo-Gil et al., 1999; Singh et al., 2013; Jia et al., 2017**). In addition to its high salt rejection rates, MD is characterized by good rejection rates of non-volatile and low adsorptive organic compounds (**Carnevale et al., 2016; Plattner et al., 2017**).

With respect to MD applications, MD is showing promising performances when it comes to water desalination and some food processing applications. There have been multiple investigations to separate different types of components from water: non-volatile compounds (ions, colloids and macromolecules) or traces volatile organics for environmental purposes (wastewater treatment and reuse, desalination, etc.) also MD is tested for food processing (juice and milk concentration) and biomedical applications **(El-Bourawi et al., 2006; Onsekizoglu, 2013**).

1.3.7.1 Water desalination

With respect to water desalination, some mathematical theoretic models were developed to simulate the membrane distillation process for multiple membrane module configurations in order to enhance their performances (**Laganà et al., 2000; Boukhriss et al., 2015; Deshpande et al., 2017**). According to Khayat et al. (**Khayet et al., 2007**), the application of response surface methodology to optimize salt aqueous solutions treatment by direct contact membrane distillation is suitable to assess the permeate fluxes for both commercial- and laboratory-made membranes. Moreover, they had proposed an algorithm which can help in the searching step for optimum localization considering as factors the stirring rate, the feed temperature and the salt concentration. Another optimization study carried by **Cheng et al. (2016)** using response surface methodology (via the application of quadratic rotation-orthogonal composite design) has proven that both operating conditions and membrane module parameters optimization can lead to a remarkable improvement of the process performance. The recorded enhancement was in terms of average permeate flux, water productivity per unit volume of module, water production per unit energy consumption, and comprehensive index.

1.3.7.2 Wastewater treatment

The interest in membrane distillation systems has led to more emphasis on the process optimization in order to achieve the highest possible permeate fluxes, in other terms higher recovery rates. In their study, **Zhang et al.** (**2016**) found that an optimization of saline wastewater treatment by vacuum membrane distillation using PP hollow fiber membrane had increased the water recovery percentage to 88.6% with an improvement of the permeate quality in terms of electrical conductivity and total suspended solids removals in comparison to one-stage vacuum membrane distillation.

The MD process has been successfully studied for purification of waste waters of pharmaceutical and textile industries as well as underground waters contaminated with heavy metals. More recently, the feasibility of applying membrane distillation process for recovering potable water from arsenic, uranium and fluoride contaminated brackish waters has been proposed. High quality permeates with dissolved solids concentrations less than 20 ppm (more than 99% rejection of salts) along with arsenic, fluoride and uranium contaminant reductions in the range of 96.5– 99.9% were reported (**Yarlagadda et al., 2011**).

1.3.8 Utility theory

Utility theory is a well-known and well-established notion that is applied in different fields for decision making purposes through the analyses of an individual's preference-indifference relation (**Kaplinski, 2013**).

On the practical level, utility theory takes into consideration assumptions about a person's preferences which gives the opportunity to present them numerically in useful ways and to help the decision maker in choosing his preferences among multiple complicated alternatives (**Fishburn, 1968**). Utility theory could be utilized to analyze the customer’s attitudes towards taking the risk and this can explain the mechanism behind the decision-making process, with emphasis on the merge of the economic and psychological aspects (**Kaplinski, 2013**).

In order to fulfill this objective, a utility function, which is a mathematical function, could be developed to show the preference of an individual who is facing various complex alternatives (**Cohon, 1978**).

The utility theory has been applied in this work to assess the performance of the saline dairy effluent DCMD treatment with respect to two types of pretreatments in order to evaluate the two pretreatment scenarios in term of cost-effectiveness.

2 MATERIAL AND METHODS

2.1 STUDIED SALINE EFFLUENTS

2.1.1 Synthetic saline wastewater

The Synthetic wastewater used throughout the studies was composed of 1 g/L $C_6H_{12}O_6$, 1 g/L NH_4Cl, 0.3 g/L KH_2PO_4, 2 g/L $MgCl.{}_6H_2O$, 0.2 g/L $CaCl_2.2H_2O$, 1 g/L $C_2H_3NaO_2.3H_2O$, and various concentrations of salt (0–3% NaCl).

Trace elements solution was composed of 3 g/L $MgSO_4.7H_2O$, 0.5 g/L $MnSO_4.2H2O$, 1 g/L NaCl, 0.1 g/L $FeSO_4.7H2O$, 0.1 g/L $CaCl_2.2H_2O$, 0.18 g/L $ZnSO_4.7H_2O$, 0.01 g/L $CuSO_4.5H_2O$, 0.01 g/L H_3BO_3, 0.01 g/L $Na_2MoO_4.2H_2O$, 0.25 g/L $NiCl_2.6H_2O$. One milliliter of stock trace element solution was added to 1 L of synthetic feed wastewater. The pH was adjusted to pH=7 by adding required amounts of 5% phosphoric acid and/or 5% KOH (**Kapdan and Erten, 2007**). All chemicals were analytical grade and were used as received.

In section (**3.2.**), a new feed solution was prepared for each experiment in the optimization study and various concentrations of NaCl and glucose ($C_6H_{12}O_6$) were added to simulate different saline wastewater compositions. The chosen ranges of variation of *COD* and [*NaCl*] have average levels and are as follows: the *COD* varies from 0.3 to 10 gO_2/L and the [*NaCl*] from 10 to 30 g/L. The *COD* and [*NaCl*] variation ranges are including different effluent qualities in terms of salinities and organic loads (**Kapdan and Erten, 2007**).

2.1.2 Saline cheese whey wastewater

The studied salty dairy effluent was kindly provided by the cheese industry Bergpracht Milchwerk GmbH & Co, Germany. This industry is specialized in the manufacturing of four types of cheese: Camembert, Feta, Mozzarella and White cheese where the salt addition is made in different steps. The added salt ends up in the final wastewater, which includes, essentially, effluents from the cleaning process, the cheese whey and the cheese salt baths. The company discharges 100 m^3 of wastewater per day that are continuously collected in neutralization tanks before sending it to the wastewater treatment plant. The samples were collected from the neutralization tanks and stored at 2°C before the experiments and analyses. Raw wastewater quality is presented in **Table 3.**

The studied raw effluent is characterized by high electrical conductivity and total organic carbon concentration (TOC). According to previous studies, the selected cheese whey

wastewater has a fluctuating composition that is closely linked to the cheese making and the cleaning processes (**Carvalho and al., 2013**).

2.2 BIOLOGICAL TREATMENTS OF THE SALINE SYNTHETIC WASTEWATER

2.2.1 Aerobic bioreactors

Four aerobic reactors, each having a capacity of 1.3 liters, were fed with the synthetic wastewater as feed solution (pH=7± 0.5) with addition a different NaCl concentration for each reactor: 0%, 0.5%, 1% and 2%. The reactors were inoculated with activated sludge from a municipal wastewater treatment plant (Okhla, New Delhi, India) and the sludge was acclimatized for one week. Coarse air diffusers were used to supply the required oxygen in the reactor. The aerobic reactors were operated in a continuous mode at 24°C ± 1°C with a fixed Hydraulic Retention Time (HRT) of 6 hours (**Figure 6**).

Figure 6: *Aerobic biological reactors*

The Mixed Liquor Suspended Solids (MLSS) of the aerobic reactors was measured every week. Excess sludge was removed, as required, to maintain the MLSS in the reactors between 8 and 9 g/L. After biological treatment, the sludge was allowed to settle for 30 min and the supernatant was subjected to analysis and membrane filtrations. After the supernatant's removal, and before running the next set of experiments, the sludge was washed with distilled water to avoid any salt accumulation from the previous treatment.

2.2.2 Anaerobic bioreactors

In order to obtain an anaerobic media, 450 ml of the synthetic wastewater was put in 1 L incubation bottle which served as an anaerobic reactor, then heated at 60-70°C for 2-3 hours. The oxygen content in the reactors is removed by sparging the bottle with nitrogen for 20 min and the addition of 0.25 g of a reducing agent (L-cysteine) before sealing and autoclaving the bottle (**Figure 7**). After autoclaving, the media was inoculated with 50 ml of anaerobic sludge previously enriched in the same media for two weeks.

Figure 7: *Anaerobic biological reactors during the nitrogen sparging step*

The anaerobic sludge was collected from a 2-stage anaerobic reactor treating food waste located at TERI Gual Pahari Campus, Gurgaon, India. Five identically set-up anaerobic reactors were preparedwith the synthetic feed (pH=7± 0.5), each reactor is containing a constant NaCl concentration: 0%, 0.5%, 1%, 2% and 3%, respectively. The reactors were incubated at 37°C for 14 days.

2.2.3 Microfiltration and ultrafiltration membranes

All filtration experiments were conducted at 24 ± 1°C. The microfiltration tests of the reactors' supernatants were carried out using ceramic membranes made of sugarcane bagasse fly ash in TERI were assembled into a flat-sheet module and were used to filter the biologically treated wastewater. The ceramic membrane filters, (**Figure 9**), have surface porosity of 30% and average pore diameter of 1.6 µm, as determined by image J (NIH, USA) (**Marel et al., 2010**). The filtration setup is composed of a peristaltic pump (Electrolab peristaltic pump PP-VT) operating at 13 rpm corresponding to 0. 6 L/h, linked to a 5.1 cm x 5.1 cm ceramic filter. Two ceramic filters were joined in a polyacrylic support frame, so the effective filtration area was 50 cm^2 and the set was submerged in a 500 ml glass beaker that contains the reactors supernatant. The pressure was determined by a mercury manometer connected to the filter (**Figure 8**).

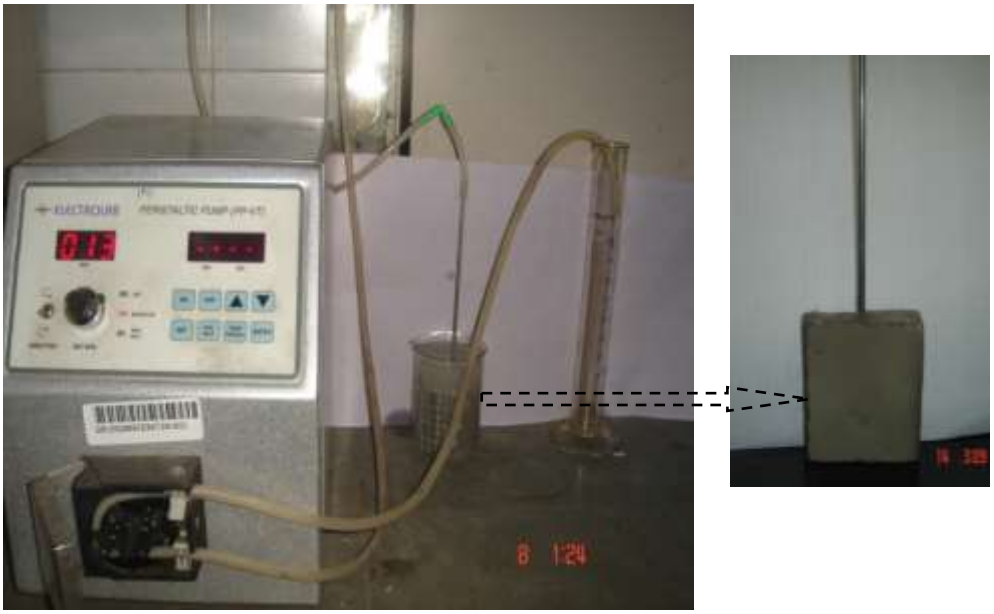

***Figure 8**:microfiltration membrane and set-up*

Sampling was done every 10 min. The conductivity of obtained permeate was measured immediately before the sample was stored at in the refrigerator for further analysis.

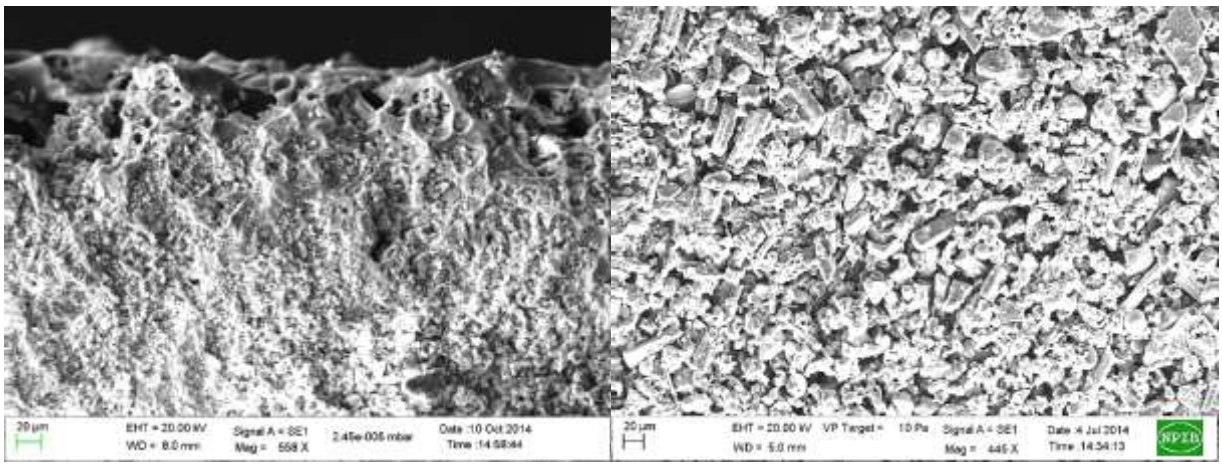

Figure 9: SEM image of the ceramic membrane (left: membrane cross section, right: top view of separation layer)

The ultrafiltration tests were performed by the means of an asymmetric polymeric membrane (Polysuphone PSF 1700), with porous support layer overlain by thin separating layer (**Figure 10**), which was prepared by phase inversion technique with 18% Polysulphone (PSF). The porosity and the pore size of the membrane were 42±1% (determined by gravimetric method) and 0.01-0.0095 µm (determined by filtration velocity method) respectively.

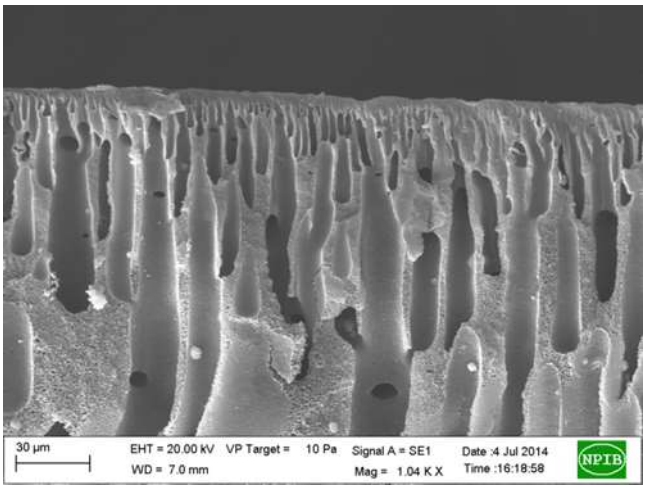

Figure 10: *SEM image of the cross-section of PSF (18%) membrane*

Coupons with 47mm diameter and an effective filtration area of 0.00134 m^2 were used for batch filtration in a stirred cell formed of metal base and cover, in between a glass cylinder maintains the coupon with a plastic ring and the whole set is pressurized using nitrogen gas (**Figure 11**).

***Figure 11**:Ultrafiltration set-up*

Pure water flux was measured before filtration of the biologically treated wastewater. 50 ml wastewater was filtered at 1 bar applied pressure. The filtration was done for 20 minutes before starting to take samples every 10 minutes.

2.3 DIRECT CONTACT MEMBRANE DISTILLATION (DCMD)

2.3.1 Benchscale DCMD setup

DCMD apparatus used in the section (**3.2.**) is composed of a bench scale direct contact membrane distillation set-up composed mainly of one heating and one cooling thermostatic water baths connected to the membrane cell via two peristaltic pumps. The two thermostatic cycles (heating closed loop for feed and cooling closed loop for permeate) are connected to a membrane cell made of Plexiglas that has an effective membrane surface of 0.0032 m^2 (**Figure 12**).

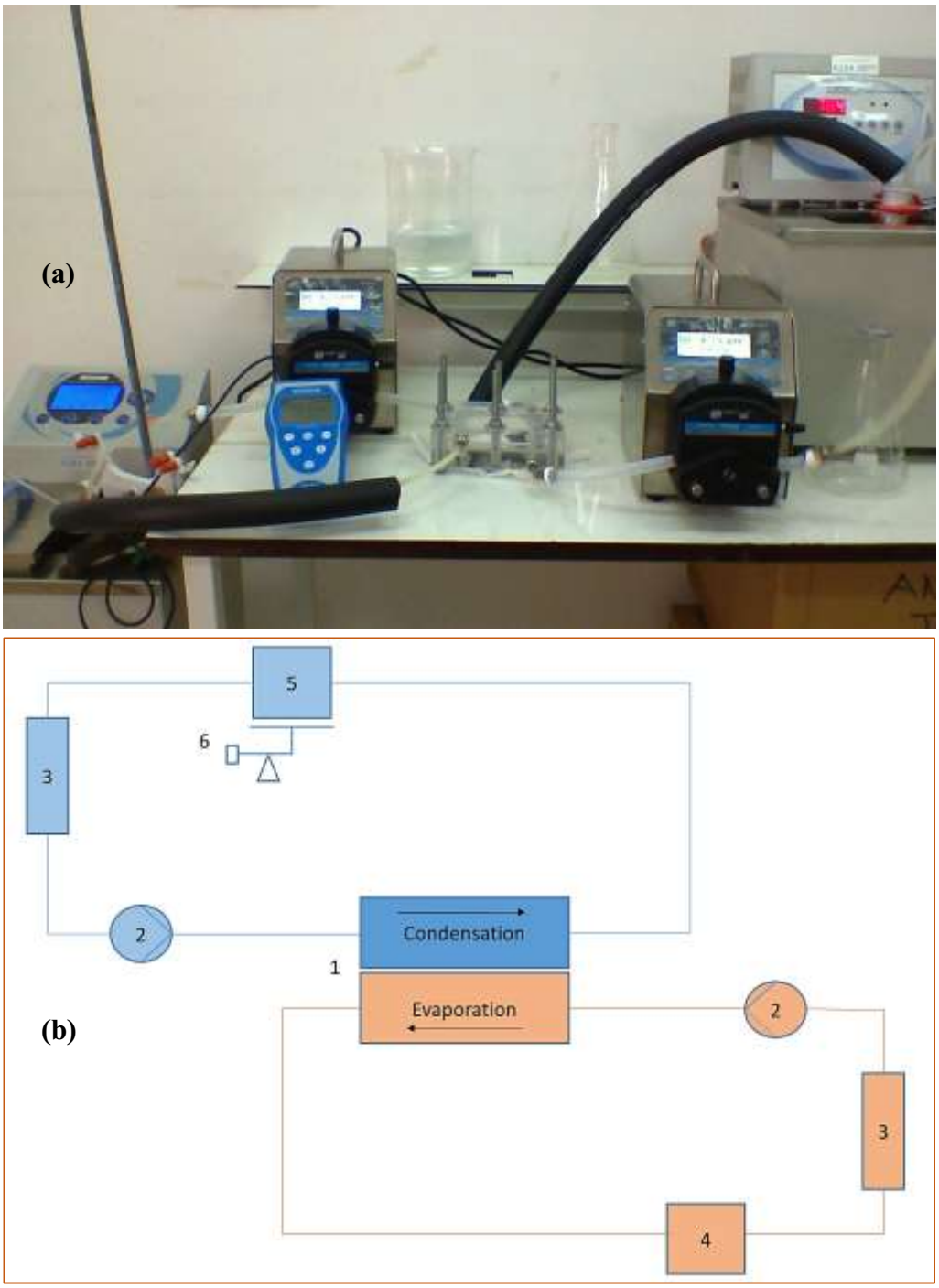

***Figure 12**:**(a)** Bench scale DCMD set-up and **(b)** schematic of the DCMD set-up [**(1)** membrane test cell, **(2)** circulation pump, **(3)** heat exchanger, **(4)** feed water tank **(5)**permeate water tank **(6)**electronic balance].*

New Hydrophobic PTFE membrane sample, with a nominal pore size of 0.45µm (**Table 2**), was placed inside the module for each experiment. Permeate electrical conductivity and temperatures of the feed and permeate solutions were measured continuously during the experiments with variation ranges of [26-80°C] and [18-23°C], respectively.

All experiments were conducted during 90 minutes in a counter-courant configuration to maintain the temperature gradient.

The permeate flux (*Jp*) is by definition the flux of water vapor which is crossing the hydrophobic membrane through its pores and it is proportional to the vapor pressure difference across the membrane following the law of Darcy:

$$Jp = Bm\ (Pf - Pp)$$

Where *Bm* is the membrane coefficient, *Pf* is the vapor pressure (bar) at the feed side water/vapor interface and *Pp* is the vapor pressure at the permeate side water/vapor interface. Besides, it is noteworthy to indicate that the water vapor is an exponential function of the operating temperature according to Antoine equation:

$$P^0 = \exp\left(23.238 - \frac{3.841}{T-45}\right)$$

Such that, P^0 is the pure water vapor (Pa) and T is the water temperature (K).
The volumetric permeate flux (L/m^{2}h) is expressed as follows:

$$Jp = \frac{\Delta V}{S.\Delta t}$$

Such that, ΔV is the permeate volume (L), S is the effective membrane surface (m^2) and Δt is the DCMD operating time (h).

2.3.2 Laboratory scale DCMD setup

Direct Contact Membrane Distillation (DCMD) experiments were performed using a laboratory scale unit developed and built by Fraunhofer ISE, Freiburg, Germany. The experimental setup is formed of a 150*250 mm^2 test cell; a detailed description of the setup (**Figure 13**) is listed in **Winter et al. (2013)**. For each DCMD experiment, a new membrane sample was placed in the test cell. All experiments were run for several hours (at least 5 hours) and the process evaluation was made after 3 hours. The DCMD plant is equipped with sensors and controllers that record multiple parameters in the systems every 5 seconds: inlet and outlet temperatures of both, the feed and permeate (°C), feed and permeate flow rates (L/h), feed inlet pressure (bar) and feed tank weight (kg). The feed inlet and permeate outlet temperatures (Tei and Tco, respectively) were controlled automatically to set a constant temperature difference

(ΔT=Tei-Tco). When varying the temperature difference in the experiments, only the permeate flow temperature was varied (from 25 to 40°C) and the feed flow has had a constant temperature of 55°C through all experiments. The temperature range was set between 25°C and 55°C for two main reasons: to preserve the proteins' quality for possible valorization and recovery of the concentrate, on one hand, and on the other hand, to reduce the energy consumption during the DCMD treatment. Besides, the feed and permeate velocities (Ve and Vc, respectively) were controlled and were maintained at equal values during the experiments. For all experiments, the tests started with a feed tank volume of around 8 liters and ended with 1.5 to 2 liters of concentrated feed.

Reference tests were conducted, using tap water as the feed stream, before each experiment at the same operational conditions to control the setup stability and functioning. The obtained reference flux served as a reference to study the fouling and wetting phenomena.

(a)

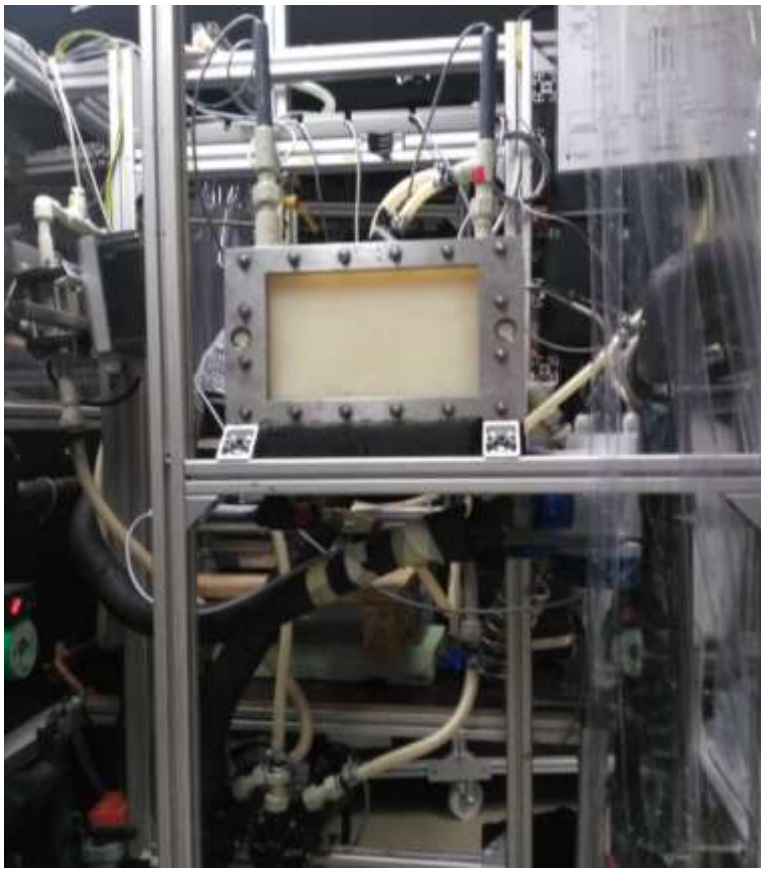

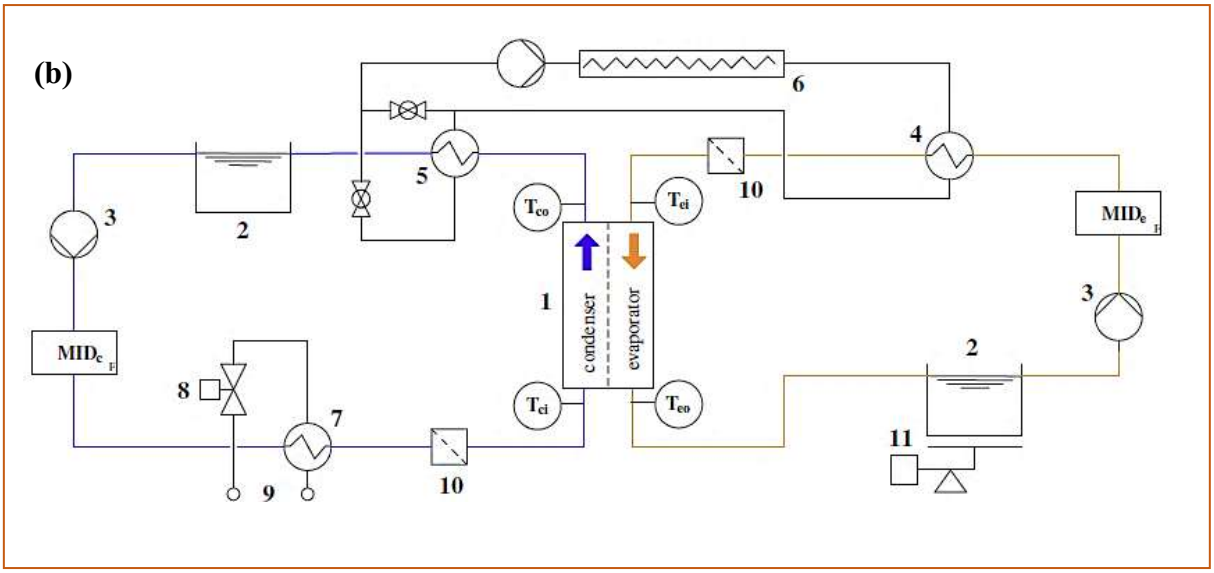

***Figure 13**: **(a)** Laboratory scale DCMD set-up and **(b)** Schematic diagram of experimental laboratory scale DCMD set-up; **(1)** membrane test cell, **(2)** feed water tank, **(3)** feed pump, **(4)** heat exchanger, **(5)** support heat exchanger, **(6)** electric heater, **(7)** heat exchanger, **(8)** motor valve, **(9)** laboratory cooling circuit, **(10)** filter, **(11)** electronic balance (**Winter et al., 2013**).*

Concerning both the membrane and setup cleaning, it was performed using Cleaning in Place (CIP) method by circulating three different aqueous solutions at 70°C for 20 minutes for each one of them: 0.5% Sodium Hydroxide (NaOH) solution followed by water circulation and then 0.5% nitric acid (HNO_3) solution, respectively. One final rinsing step with water at room temperature was performed in the end. The setup cleaning procedure was carried after each DCMD test.

2.3.3 DCMD membranes

Two commercial flat sheet polytetrafluoroethylene (PTFE) membranes were investigated. The utilized membranes were of two different brands (Membrane Solution (M1) GORE membrane (M2)) with two different pore sizes and backing structures (**Table 2**): the first membrane (M1) has a polypropylene (PP) nonwoven backing and the second membrane (M2) has a PP scrim backing. In addition to the difference of the nominal pore sizes between M1 and M2 and the different hydrophobicity (see LEP and contact angle) the backing structure of M2 gives a higher resistance to the membrane which can be identified by its thickness (**Table 2**). During all experiments, the PTFE surface was orientated towards the feed flow.

***Table 2**: DCMD membranes characterization (source: membranes data sheets, *parameters measured in the laboratory)*

Membrane	Material	Nominal Pore Size (µm)	Thickness (µm)	Porosity (%)	Tortuosity	LEP* (bar)	Contact Angle* (°)
M1	PTFE	0.45	160±40	-	-	2.3	123.4
M1 backing	PP	-		-	-	-	-
M2	PTFE	0.2	70	80	1.3	3.9	131.2
M2 backing	PP	-	280	0.5	1.8	-	-

For each experiment, a new membrane was applied which finally was used for further analyses and fouling diagnostic after finishing the test.

2.4 DCMD PRETREATMENTS

In order to study the influence of the dairy effluent pre-treatment on the DCMD performance, two pretreatments were adopted to process the raw cheese whey wastewater, namely microfiltration and ultrafiltration processes.

2.4.1 Macrofiltration (MAF)

The raw effluent was first subjected to a macrofiltration (MAF) step using a 30µm pleated nonwoven Polyester filter cartridge (Pentek Filtration R30). Macrofiltration pretreatment will help to decrease the organic load in the feed, (**Table 3**), by the elimination of all suspended solids, colloids and macromolecules that have bigger size than 30µm.

2.4.2 Ultrafiltration (UF)

For further processing, after the MAF step an ultrafiltration (UF) step is performed using a tubular PES Multibore® membrane 0.9 module (Inge GmbH) with a pore size of approximately 0.02 µm and a molecular weight cut-off (MWCO) = 100 KDa. The UF was applied in cross-flow filtration. And the tubular membrane module has capillaries with an internal diameter = 0.9 mm, external diameter = 4 mm and pores diameter ≈ 0.02 µm.

In this investigation, all traces of casein micelles (large aggregates = 10^5KDa) which are causing the effluent's whitish color are eliminated by the UF step, in addition to the traces of fat globules. However, the UF pretreated feed still contains the majority of the whey proteins (β-lactoglobulin and α-lactalbumin) (**Singh and al., 2014**).

***Table 3**: Characterization of the raw and pretreated effluents*

Parameters	Raw effluent	MAF permeate	MAF-UF permeate
pH (± 0.1)	6.8	6.8	6.8
Conductivity (± 0.4 mS/cm) at 25°C	9.9	9.9	9.9
TOC (mg/L)	1,730 (± 45)	784 (± 27)	293 (± 13)
TC (mg/L)	1,860 (± 45)	851 (± 27)	344 (± 13)
TIC (mg/L)	130 (± 45)	67 (± 27)	51 (± 13)

Both obtained permeates, by MAF and UF pre-treatments, were characterized before being used for further DCMD experiments (**Table 3**). The measures illustrated in **Table 3** are the mean average of the results of three samples characterization.

2.5 ANALYTICAL METHODS

2.5.1 Pollution parameters

2.5.1.1 Mixed Liquor Suspended Solids (MLSS)

The sludge's MLSS was determined according to the "Standard Methods for the Examination of Water and Wastewater".

2.5.1.2 Gas Chromatography analysis (GC)

The composition of the gas formed during anaerobic process was analyzed using gas chromatography (GC). This analysis was performed immediately after taking the anaerobic reactors out of the incubator and before unsealing them for further analysis. Agilent Technologies system number 7890A was used for this analysis. The GC analysis were

conducted at a total flow rate= 6ml/min using a Nucon SS packed column with Argan as reference gas (flow rate=10ml/min) and Nitrogen for the makeup flow (flow rate=3 ml/min).

2.5.1.3 Chemical Oxygen Demand (COD)

The Chemical Oxygen Demand (COD) was measured depending on the samples' salinity: the permeate quality was tested according to the "Standard Methods for the Examination of Water and Wastewater" and for the samples with high electrical conductivity the COD was determined using the modified method described by **Vyrides and Stuckey (2009.a)**.

2.5.1.4 Microbiological observation

The bacterial Gram staining was realized using a Gram stain kit and the followed by a microscopic observation were conducted at 100 times magnification.

2.5.1.5 Turbidity

The turbidity was measured using a "Bionics" digital Nephelometer, model No: BST/DN-341.

2.5.1.6 Total Organic Carbon (TOC)

Permeate samples were analyzed to measure their Total Organic Carbon (TOC) using the difference method by cuvette tests (LCK 380 and LCK 381) purchased from Hach Lange, Germany.

2.5.1.7 Electrical conductivity (EC)

In section 3.1., EC was measured directly by a "Bionics" conductivity meter: Digital conductivity meter model NO: BST/CM-601.

During all DCMD experiments, the permeate quality was monitored by measuring its electrical conductivity in the permeate tank every hour using a digital conductivity meter (Kobold, HND-C) and using an S823 pH/Conductivity meter.

2.5.2 Membrane characterization

2.5.2.1 Liquid Entry Pressure (LEP)

The LEP was measured using 0.5 wt. % NaCl solution to which a gradually increasing pressure perpendicularly to the PTFE membrane surface with a fixed pressure slope (dp/dt= 0.01 bar/s) was applied. Instantly, when the liquid solution breaks through the membrane the corresponding pressure (LEP) is recorded. The LEP setup and experimental procedure are developed and designed at Fraunhofer ISE.

2.5.2.2 Contact Angle (CA)

Contact angle measurements were performed to analyze the membranes hydrophobicity degree using an automated method of the DataPhysics Contact Angle System OCA and the DataPhysics SCA20 software. The contact angle measurements were performed by an automatic generation of water drops using 5 µm dispenser. Pure water was utilized as reference at 22°C.

The measured contact angles in **Table 2** show that the membrane has a good hydrophobic nature that forms a physical barrier in front of the feed water stream (CA > 90°). According to the literature, the utilized membranes has good contact angle values in comparison to other synthesized and modified hydrophobic membranes in which its value varies between 112.7° and 154.2° (**Prince et al., 2012; Prince et al., 2014.b; Efome et al., 2016**). Moreover, according to the aforementioned references, this parameter could contribute in the improvement of the DCMD performance.

2.5.2.3 Scanning Electron Microscopy (SEM)

The SEM analysis was used to determinate the morphology of the fouling layers after DCMD experiments by a scanning electron microscope «Auriga 60" from the company Zeiss and for the detection and quantification of the fouling layer, an Energy Dispersive X-ray (EDX) Detector "XFlash Detector with internal FET" from the company Bruker was used for the detection and quantification of the fouling layer.

For the membrane samples coating, a Cressington Sputter Coater 108 auto was used at 30 mA and 0.06 mbar for 30s to 40s. A gold layer of ~10nm thickness was necessary to get an adequate conductivity to the undercuts of the membranes. For cross-section SEM images, an additional step was added in which the samples were frozen using liquid nitrogen.

2.5.3 Permeate flux and permeability

In section (**3.1.**), the flux was measured volumetrically (permeate volume collected over a known time). Applied pressure was measured using a mercury manometer (mm Hg) for the ceramic membrane filtration. For the polymeric membrane, pressure was measured using a pressure gauge fixed to the nitrogen cylinder used for pressurizing the filtration cell.

The flux (J) is calculated using the following formula where flux is in LMH ($L/m^2.h$):

$$J = Vol/(A \times t)$$

Permeability (P)is expressed in LMH/bar [which is the abbreviation of the permeability unit ($L/m^2.h.bar$)] and it was calculated using the following equation:

$$P = Vol/(A \times t \times \Delta p)$$

Where: Vol = Permeate volume (liter)

A = Membrane filtration area (m^2)

Δp = Transmembrane pressure (bar)

t = Filtration time (hour)

2.6 RESPONSE SURFACE METHODOLOGY (RSM)

Response Surface Methodology is applied in this study to optimize the DCMD process for saline wastewater treatment through one of the most used forms of RSM: The Central Composite Design (CCD). This method, which is fit for a quadratic surface, is generally utilized to optimize the effective parameters of a process and to identify their existing interactions and their extent with a minimum number of experiments. The CCD is a second-order design which is based on adding a number of (2k) axial-points experiments and a number of center-points replications (n_0) to a simple first order design (2^k) where k is the factors number. The added experiments serve in helping to get more information about the response surface and in the optimization of the process through a second-order model (**Khuri & Mukhopadhyay, 2010**).

The CCD model is a mathematical polynomial function expressed as follows, in the case of four independent variables:

$$\boldsymbol{Y} = b_0 + b_1\boldsymbol{X_1} + b_2\boldsymbol{X_2} + b_3\boldsymbol{X_3} + b_4\boldsymbol{X_4} + b_{11}\boldsymbol{X_1^2} + b_{22}\boldsymbol{X_2^2} + b_{33}\boldsymbol{X_3^2} + b_{44}\boldsymbol{X_4^2} + b_{12}\boldsymbol{X_1X_2} + b_{13}\boldsymbol{X_1X_3} + b_{14}\boldsymbol{X_1X_4} + b_{23}\boldsymbol{X_2X_3} + b_{24}\boldsymbol{X_2X_4} + b_{34}\boldsymbol{X_3X_4}$$

In our study, with a factors number k=4, we have carried a total number of 28 experiments that included 2^4 orthogonal design points, 8 axial points ($\alpha=\pm1.682$) and 4 replications of the center-points (**Table 4**).

The analysis of variance (ANOVA) was applied to determine the statistical significance of the obtained model and to study the quality of the model's fit. The statistical and graphical analysis tool used in this work is Minitab® 17 software by Minitab Inc.

In our study, the volumetric permeate flux *Jp* (L/m^2.h) is considered as the main response (Y) to be optimized by CCD through the optimization of four different factors [X_1: temperature difference ΔT (°C), X_2: feed velocity *Vf* (m/s), X_3: NaCl concentration [*NaCl*] (g/L) and X_4: glucose concentration [*Gluc*] (g/L)]. The first step to apply the CCD is to identify the factors and their different levels. **Table 4** illustrates the four chosen independent factors in our study with their respective coded levels and actual values. The choice of the variation ranges of each parameter was made according to preliminary tests with respect to the volumetric permeate flux (*Jp*) as the main response monitored during this study.

***Table 4**: Central Composite Design (CCD) variables levels in their coded and actual values.*

Factors	Symbols	Actual values of the coded levels				
		-α	**-1**	**0**	**+1**	**+α**
Temperature difference ΔT (°C)	X_1	4.77	15	30	45	55.23
Feed velocity V_f (m/s)	X_2	0.027	0.039	0.057	0.075	0.086
Initial salt concentration [NaCl] (g/L)	X_3	10.07	14.1	20	25.9	29.92
Initial glucose concentration [Gluc] (g/L)	X_4	0.49	4.45	10.25	16.05	20

2.7 SINGLE-NODE MODEL SIMULATION

As an evaluation tool for the DCMD process performance, one of the parametric node models developed by **Winter (2015)** was utilized in order to predict the transmembrane vapor flux as well as the thermal efficiency (based on calculations of mass and heat transfers) in the studied laboratory scale DCMD configuration where the operating conditions, materials and channel configuration were taken into consideration. The C programming language was used for the model implementation and the different mass and heat transfer calculations were carried out via an iterative algorithm. Since the model conception is made according to a steady-state scenario and homogeneous conditions, its application in our study could present an interesting indicator of the fouling and wetting phenomena effects and the extent of their influence on the process performance in comparison to the ideal DCMD treatment outcome.

2.8 EXPERIMENTAL PERFORMANCE ANALYSIS

The main purpose of this section is to extend the process performance analysis by incorporating the cost-effectiveness analysis of the saline dairy wastewater DCMD process associated with the two different pretreatments. To this purpose, the set of parameters (i.e. criteria) is first introduced. These parameters have been shown in the literature to affect the applicability and the performance of the DCMD process in the industry. Based on these parameters, a set of indicators is defined that will be used in our cost-effectiveness analysis relying on the utility theory. Then, a mathematical model is presented to assess the performance of the scenarios that have been experimented using our setup. Finally, the results are discussed based on the present case study in order to analyze the cost-effectiveness of the DCMD process with respect to the two pretreatment options. In addition to the indicators used to assess the efficiency of the filtration process, the time needed to reach a specific level of performance is considered as a measurement of the cost-effectiveness of each of our scenarios. In fact, time is strongly correlated to the cost in the context of the DCMD process since the components of the cost (e.g., energy consumption, membrane lifetime) vary according to time.

The criteria as well as their corresponding indicators used to assess the performance of DCMD in the context of the saline diary effluents treatment are displayed in **Table 5**. It is noteworthy that these criteria have been already used in the literature to evaluate the performance of the DCMD process.:

1. Rejection factors: One of the most important advantages of DCMD is its ability to provide a better quality of the output water compared to other technologies. Production of high-quality water is well-established with rejection factors of almost 100% of non-volatile compounds (**Khayat and Matsuura, 2011**). We use in our work the electrical conductivity of the DCMD permeate and its total organic carbon (TOC) to evaluate the performance of the DCMD process with regard to this criterion.

2. Permeate flux: it refers to the ability of the DCMD process to achieve good performance in terms of mass transfer. From the practical point of view, the flux varies following different parameters including the thickness and the morphology of the membrane. Therefore, it is trivial to state that this characteristic is substantially affected by the DCMD process since during the effluent treatment the surface of the membrane, its porosity and its thickness could be affected (**Drioli et al., 2009; Alkhudhiri et al., 2012**).

3. Energy consumption: As for any other distillation process, this technology also requires energy for water evaporation. Henceforth, we consider the amount of energy spent to conduct the water treatment process as a comparison criterion between the implementation scenarios that will be described in the sequel. Mainly, intel cold temperature, intel hot temperature, flow rate and pretreatment energy are the four indicators used to assess the energy consumption. The pretreatment energy is the energy spent to conduct the pretreatment process varies according to the characteristics of the equipment used to this purpose. The interest of considering this parameter stems from the fact that it is one of the fundamental components of the Capital Expenditure (CAPEX) and the Operational Expenditure (OPEX) of the global effluent treatment solution.

4. Void volume: This criterion expresses the void volume fraction of the membrane (defined as the volume of the pores divided by the total volume of the membrane). Higher porosity membranes have a larger evaporation surface area. In our experimental setup, we use the Scanning Electron Microscopy (SEM) as an indicator to estimate the membrane fouling. This indicator is very important since, beyond a low porosity threshold, the performance of the DCMD process becomes unacceptable and the membrane must be either cleaned or changed.

   The void ratio in the SEM images can be estimated if the regions corresponding to the membrane are known. In fact, the void volume fraction of the membrane, defined as the volume of the pores divided by the total volume of the membrane, is proportional to the density of the membrane material (**Khayet and Matsuura, 2001**). In fact, the Smolder-Franken equation provides an expression of the void ratio:

$$\varrho = 1 - \frac{\varrho_m}{\varrho_{pol}},$$

where ϱ_m and ϱ_{pol} refer to the densities of membrane and polymer materials, respectively.

In order to estimate the void ratio, we rely on the following three-step process:

a. The SEM image is segmented in order to identify the regions corresponding to the membrane region.

b. The segmented image is binarized in order to convert the values of the pixels to black (non-membrane regions) and white (membrane regions).

c. The void ratio is computed based on the following equation:

$$VR = \frac{\#W}{\#W + \#B}$$

where $\#W$ and $\#B$ are the number of white pixels and the number of black pixels, respectively. This process is illustrated in **Figure 14**.

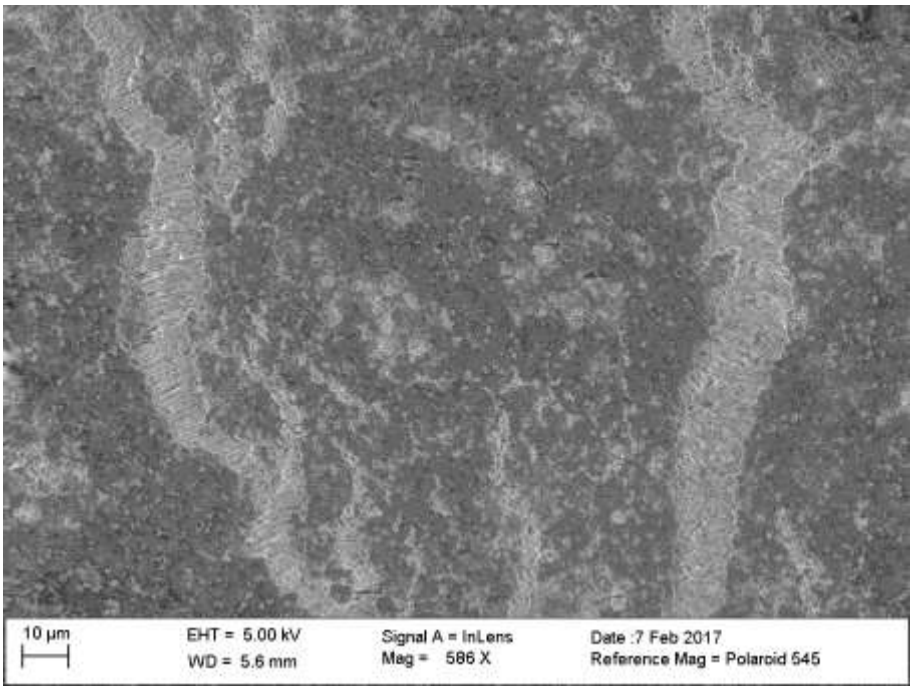

(**a**)

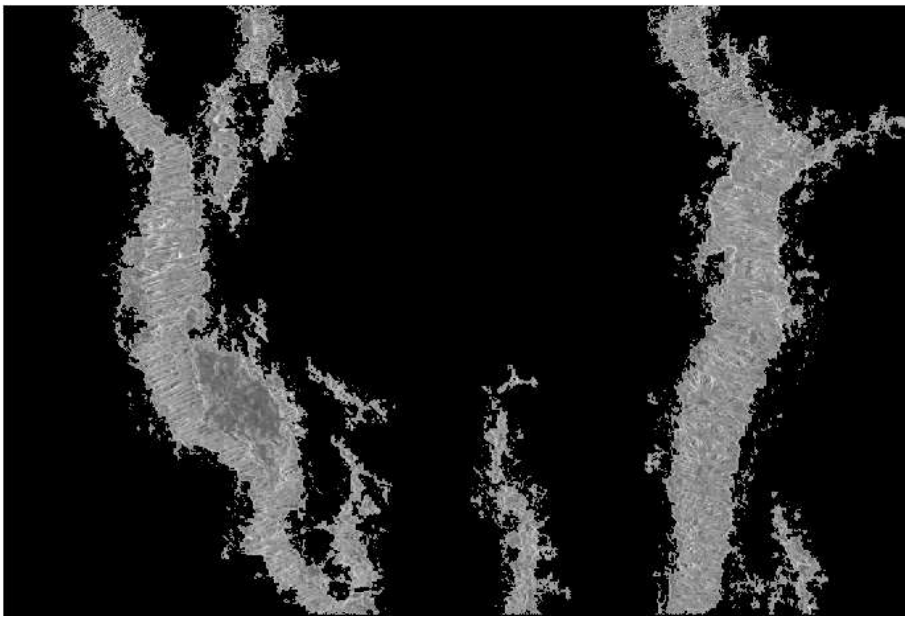

(**b**)

(**c**)

***Figure 14**: Illustration of the steps of the void ratio estimation: original SEM image (**a**), segmented image (**b**), binarized image (**c**).*

In addition to the volume of the void region, the geometric distribution of the pores consistently affects the efficiency of the membrane. Therefore, we consider the entropy of the membrane regions (i.e., white regions provided by the previous segmentation process) as an indicator of the distribution of the pores in this region.

5. Liquid entry pressure: Liquid entry pressure (LEP) is a significant membrane characteristic. The liquid feed must not penetrate the membrane pores in other terms the applied pressure should not exceed the limit (LEP) above which the feed (i.e. aqueous solution) penetrates the hydrophobic membrane. LEP depends on the maximum pore size and the membrane hydrophobicity and it is directly related to the feed concentration and the presence of organic solutes, which usually reduce the LEP (**Gostoli, 1989; Alkhudhiri et al., 2012; Abdelkader et al., 2018)**.

6. Time: The time needed to achieve a level of mass transfer is an important parameter when applying the DCMD process in an industrial environment. In fact, it is inversely proportional to the cost of the process. Therefore, reducing the execution time can be considered as one of the objectives to be reached. The indicators for this criterion are the distillation time (DCMD time) and the pretreatment time. The DCMD time corresponds to the time spent to reach a given mass transfer performance. In our context, we set the termination condition of the experiment to a concentrate weight of 2kg.

***Table 5**: Numerical indicators and criteria*

Criterion	Indicator	Index
Rejection factors	TOC	I_1
	Conductivity	I_2
Flux	Permeate flux	I_3
Energy consumption	Inlet cold temperature	I_4
	Inlet hot temperature	I_5
	Flow rate	I_6
	Pretreatment energy	I_7
Void volume	Void ratio in SEM images	I_8
	Entropy of SEM images	I_9
LEP	LEP	I_{10}
Time	Distillation time	I_{11}
	Pretreatment time	I_{12}

3 RESULTS AND DISCUSSION

3.1 BIOLOGICAL AND MEMBRANE PROCESSES PERFORMANCE FOR SALINE EFFLUENTS TREATMENT

3.1.1 Aerobic bioreactors performance

The microorganism's growth in the aerobic reactors was monitored by measuring the MLSS content. The MLSS profile for all the reactors under different salt mass percentage is shown in **Figure 15**, where for each aerobic reactor, we have the almost the same initial sludge quantity expressed in MLSS (8±0.4 g/L).

Figure 15 depicts also the effect of salt concentration on the aerobic microbial growth. As shown in **Figure 15**, the increase of the salt concentration in the synthetic effluent has leaded to a gradual decrease in the MLSS growth rate to obtain the lowest growth with 2% NaCl bioreactor. In terms of MLSS increase, the growth rates observed after 8 days incubation in the different bioreactors in comparison with the initial one equal to 8 g/L, were as follows: 101%, 62%, 54% and 53% for the NaCl concentration of 0%, 0.5%, 1% and 2%, respectively. The observed MLSS drop could be attributed to the increasing osmotic stress endured by the different microbial communities causing the microorganisms' plasmolysis and/or their activity inhibition which affect significantly the physical and biochemical properties of the activated sludge (**Kargi and Dincer, 1996.a; Dincer and Kargi, 2001; Reid et al., 2006; Luo et al., 2015**).

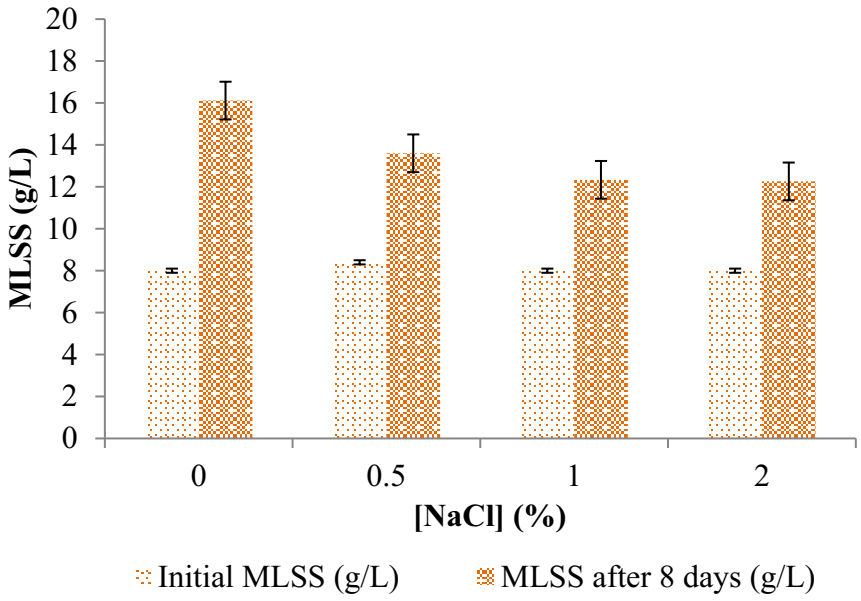

***Figure 15**: MLSS evolution after 8 days in the aerobic bioreactors at different NaCl concentrations (%).*

With respect to the aerobic treatment efficiency and performance, COD removals were measured for each bioreactor after an HRT of 6 hours (**Figure 16**). It is noteworthy that the addition of 0.5% of NaCl didn't affect significantly the COD removal in comparison to the control bioreactor (0% NaCl) where the rates reached 93%. This result could be explained by the adaptation ability of microorganisms at low and moderate salt concentration (<1%) which allows the aerobic process to relatively maintain its good efficiency through the adjustment of the microorganisms' metabolism (**Kargi and Dincer, 1996.a; Dincer and Kargi, 2001; Wang et al., 2005**). In another side, the 40% decrease of microorganism's growth (**Figure 15**) after increasing NaCl concentration to 0.5% did not have any impact on the COD performances of the reactor.

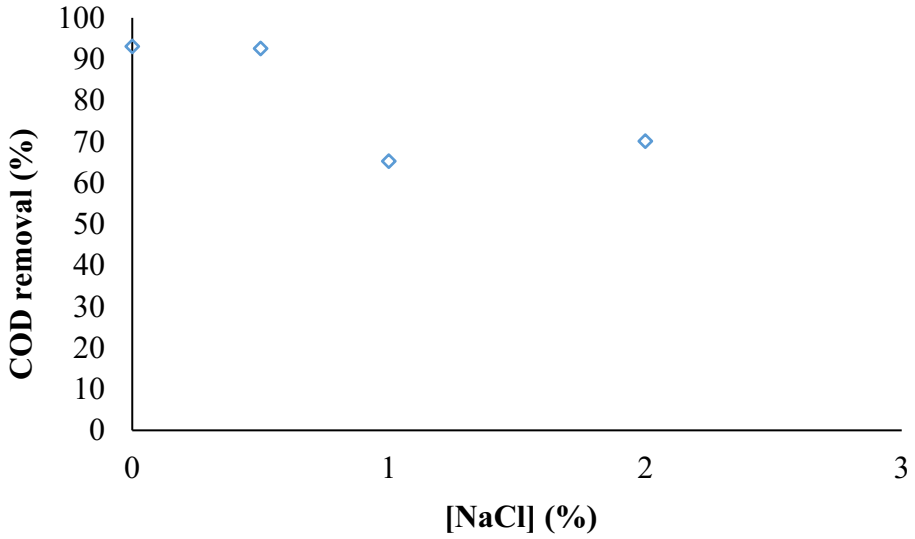

***Figure 16**: COD removal in aerobic bioreactors at different NaCl concentrations (%)*

As shown in **Figure 16**, the aerobic treatment of 1% and 2% NaCl effluents has led to lower process efficiency in terms of COD removal (65% and 70%, respectively). This result confirms the suspected effect of high salt content on the aerobic treatment effectiveness. The recorded performance reduction could be related on one hand to the notable bacteria's growth decrease (**Figure 15**) and on the other hand to the reduction of the effluents biodegradability engendered by its toxic effect on the bacterial community which causes the inhibition of its activity in addition to its limited and slowed down growth since most of halophilic bacteria are moderate or extremely sensitive to oxygen (**Kargi and Dincer, 1996.a; Dincer and Kargi, 2001; Wang et al., 2005**).

3.1.2 Anaerobic bioreactors performance

In order to study the increasing salt concentration effect on the anaerobic process performance, both the methane production and the COD removal after 13 days incubation time were measured in the anaerobic bioreactors with NaCl concentrations up to 3%. The methane production, expressed in ml/l, is shown in **Figure 17**. The illustrated results indicate that though the methane production in all bioreactors is relatively low, there has been a visible reduction of the anaerobic microorganisms' activity in terms of methane production especially when the NaCl concentration is 1%. This observation could be explained by the metabolism changes accompanying the salinity increase. As it was previously reported, under high saline conditions

the anaerobic biomass tries to acclimate to extreme environmental conditions by producing the compatible solutes and consequently there are lower substrates for methane synthesis (**Kempf et al., 1998**; **Vyrides and Stuckey, 2009.b**).

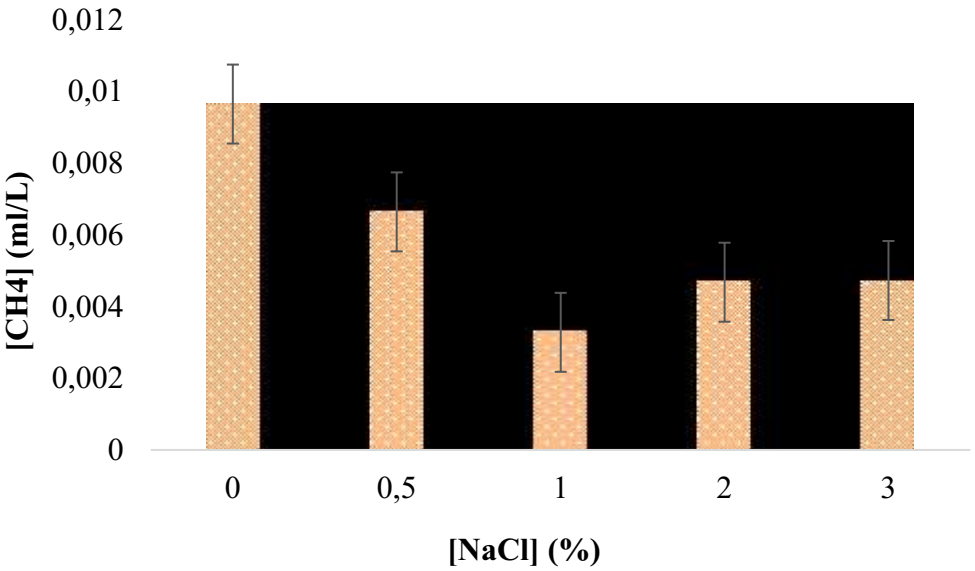

***Figure 17**: Methane production in the anaerobic bioreactors (13 days incubation time)*

Figure 17 shows also an increase in the methane production at 2% and 3% NaCl probably due to the development of moderate halophiles at 2% and 3% NaCl concentrations. It is previously reported that some of the halophiles maintain their osmotic balance in the presence of high salt concentration using intracellular accumulation which is enabled only in this saline medium and this makes the survival of this kind of bacteria not possible in low salt concentration medium (**Vijay et al., 2018**). Moreover, among anaerobic bacteria we find halophilic methanogens which tolerate up to 12% NaCl concentration and which could be responsible of the increase in methane production in the presence of 2% and 3% NaCl concentrations (**Lai et al., 2002**).

With respect to the COD reduction, the anaerobic treatment of saline effluents has shown too lower pollution reduction in terms of COD removal for all the bioreactors. **Figure 18** illustrates the COD reduction for the different salt concentrations after 13 days incubation.

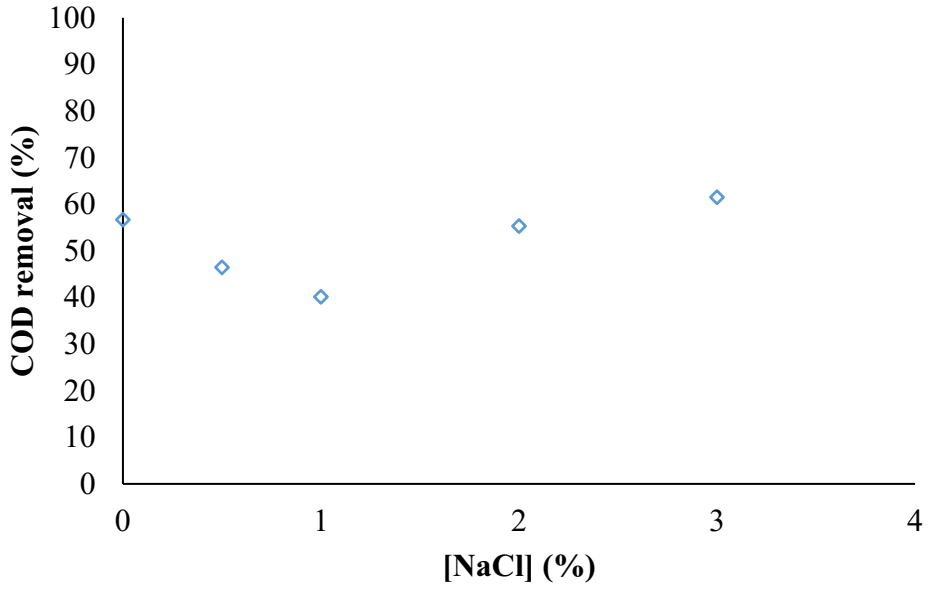

***Figure 18**: COD removal in the different anaerobic bioreactors at different NaCl concentrations (%)*

As shown in **Figure 18**, when no NaCl is added to the medium the COD removal reached 57%. When adding 0.5%, 1%, 2% and 3% of NaCl to the medium the COD removal had shown a relatively small change to reach 46%, 40%, 55% and 62%, respectively. The increase in COD removal in the 2% and 3% NaCl bioreactors could be attributed to a change in the biomass composition through the development of halotolerant and moderately halophilic anaerobic bacteria that decreases the supernatants' COD (**Lai et al., 2002; Vijay et al., 2018**).

Moreover, the observed variations in the COD removal in comparison to the 0% NaCl anaerobic bioreactor is lower than those observed in the aerobic treatment which could be explained by a possible lower sensitivity that anaerobic biomass has towards saline environments (**Vyrides and Stuckey, 2009.c; Ozalp et al., 2003**).

Figure 19 illustrates the microbiological observations of the aerobic and anaerobic sludge samples after Gram staining at different NaCl concentrations mass percentage.

As it could be shown in **Figure 19**, in anaerobiose conditions, fermentative halophilic bacteria could be a Gram (-) or Gram (+) bacteria with a slight difference under 1% and 2 % of NaCl. The increase of the NaCl concentration leaded to the selection of Gram-negative bacteria in the anaerobic sludge especially at 3% NaCl where almost all the bacteria didn't retain crystal violet dye (Gam-negative bacteria). The halophilic fermentative bacteria belong mostly to proteobacteria or actinobacteria (**Kivistö and Karp, 2011**). This observation

confirms the results shown by **Figure 17** and **Figure 18**, where the increase of the methane production and COD removals at 2% and 3% NaCl suggested the development of moderately halophilic Gram-negative anaerobic strains. In addition, it has been previously proved in the literature that the majority of moderate halophiles are Gram-negative rods which confirms the obtained results (**Quesada et al., 1983; Ventosa, 1988; Prado et al., 1991; Kivistö and Karp, 2011**).

However, under aerobic conditions, it is notable that most of bacteria are a Gram (-) bacteria under 1 and 2% NaCl. With respect to the aerobic sludge, The Gram staining in **Figure 19** shows that the NaCl increase from 1% to 2% has led to the reduction of the bacterial population density that could be induced by the increased osmotic stress of the aerobic bacteria at high NaCl concentrations which could have inhibitory or toxic effects and lead to cell plasmolysis (**Reid et al., 2006; Luo et al., 2015**). Besides, most of halophilic bacteria are a moderate or extremely sensitive to oxygen.

The observed population density decrease confirms the observed decrease in the sludge MLSS and the COD removal at 2% and 3% NaCl concentrations (**Figure 15** and **Figure 16**).

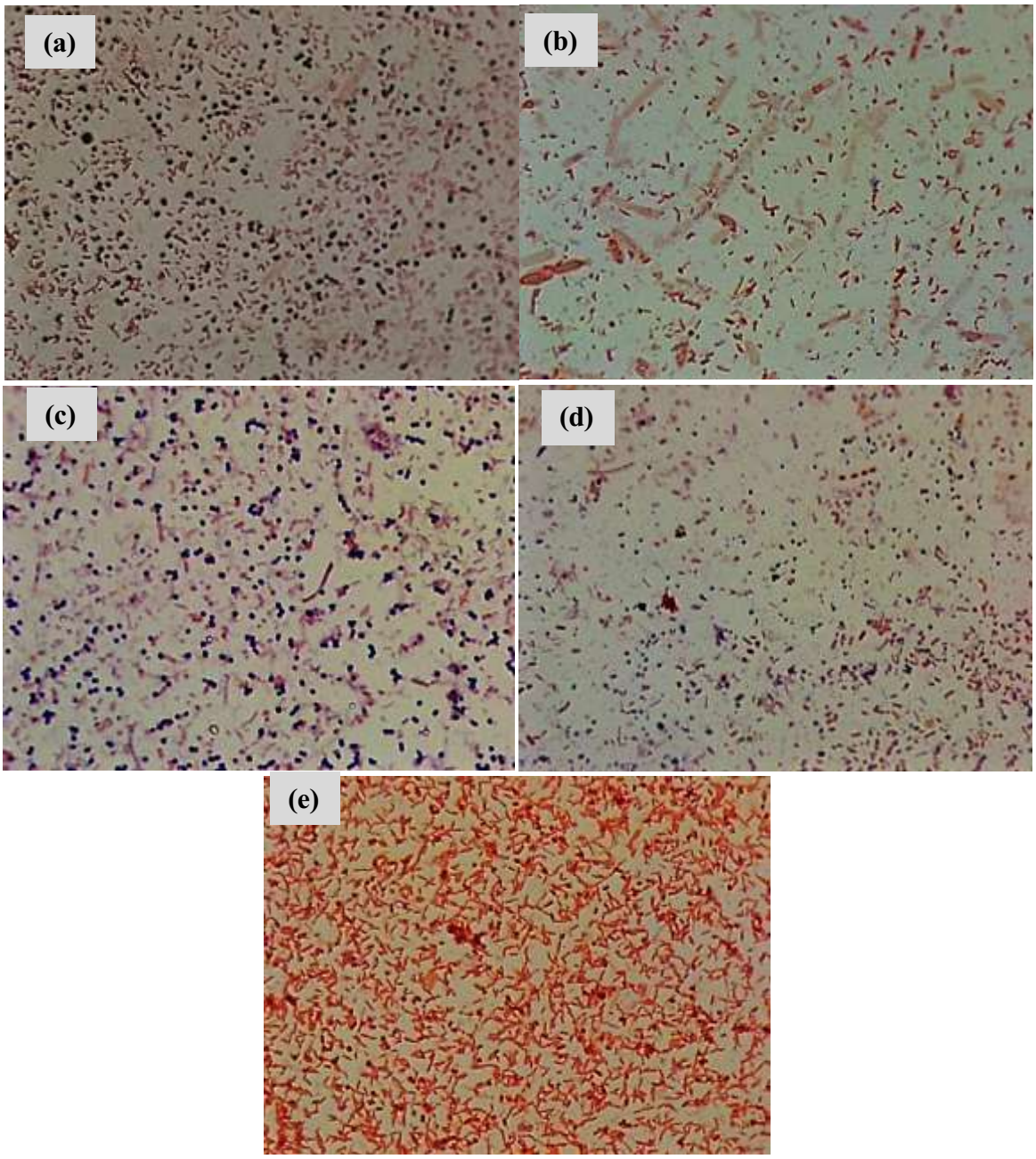

***Figure 19**:Microbiological observations of sludge samples after Gram staining: anaerobic sludge at 1% NaCl (**a**), aerobic sludge at 1% NaCl (**b**), anaerobic sludge at 2% NaCl (**c**), aerobic sludge at 2% NaCl (**d**) and anaerobic sludge at 3% NaCl (**e**)*

3.1.3 Membrane microfiltration and ultrafiltration

3.1.3.1 Biological treatments coupled with Microfiltration

Following the synthetic saline wastewater biological treatments, further filtration tests were performed as an additional step to improve the effluents' quality. First, microfiltration treatment was applied on the obtained aerobic bioreactors supernatants and the permeability was calculated and plotted as a function of the filtration time (**Figure 20**).

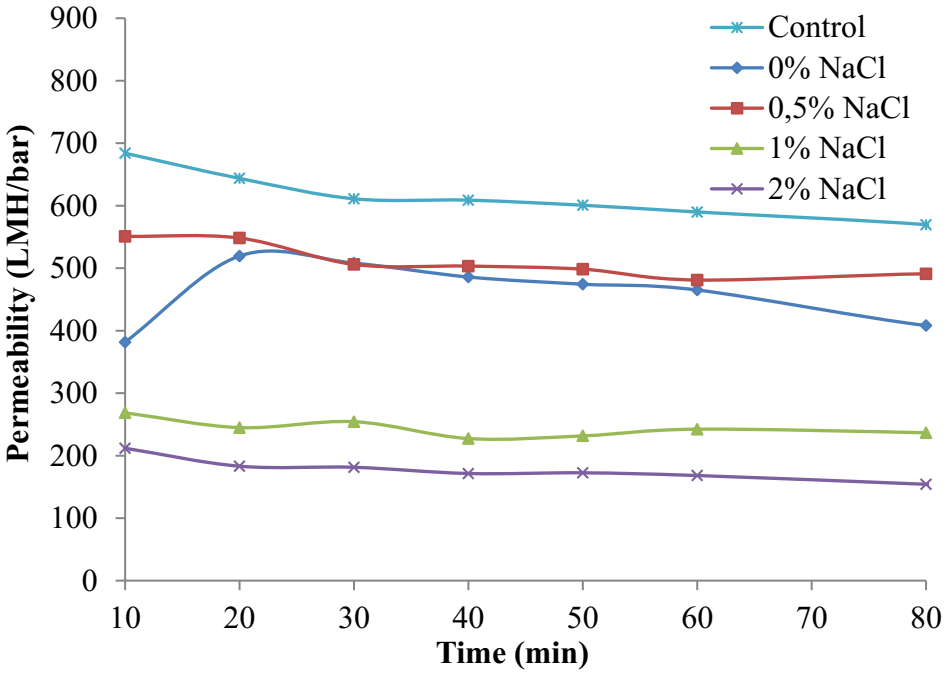

Figure 20: *Microfiltration membrane permeability of the different aerobic bioreactors' supernatants (control is reverse osmosis water)*

As shown in **Figure 20**, the membrane permeability has maintained comparable values for the supernatants of the 0% and 0.5% NaCl aerobic bioreactors. However, a notable reduction in membrane permeability values in the case of the 1% and 2% NaCl supernatants was observed. This is accompanied with a relatively stationary phase over the operation time.

The aforementioned permeability drop reached 50% and 64%, respectively for 1% and 2% NaCl, in comparison to the 0% NaCl microfiltration which could be related to the cells' metabolism changes occurring under high salinity conditions. The obtained results are confirmed by the observations of **She et al. (2017)** which found that the increase of NaCl to 1% and 2% led to a significant increase of the total extracellular polymeric substances (EPS) contents in the sludge, especially humic substances. The production of the EPS becomes

remarkably higher due to the cells' plasmolysis and the secretion of polymers and intracellular constituents which effects significantly the filtration process and induces more severe membrane fouling (**Reid et al., 2006; Vyrides and Stuckey, 2011; Jang et al., 2013**). Moreover, the sludge properties and its settlement ability are significantly affected by the treated effluents salinity since the produced EPS can influence the hydrophobicity of the biomass aggregates and the flocs formation in the bioreactors (**Guo et al., 2012**).

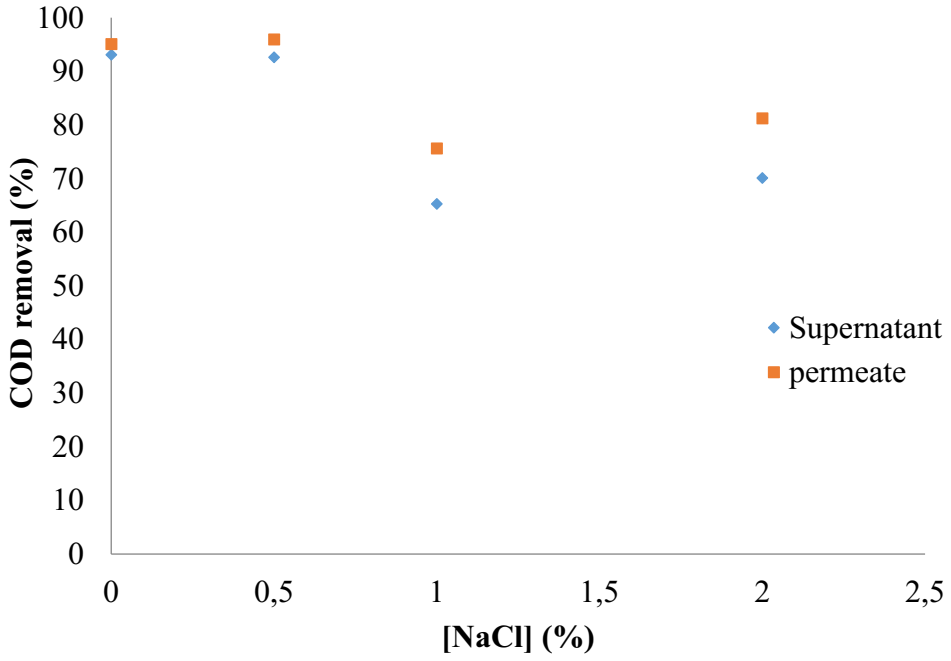

***Figure 21**: COD removal after microfiltration of the aerobic bioreactors' supernatants and permeate.*

Following the microfiltration of the aerobic bioreactors' supernatants, COD removal in permeates was measured as illustrated in **Figure 21**. The improvement of the COD removal was insignificant after filtration of the 0% and 0.5% NaCl supernatants which has led to removal of 95% and 96% COD, respectively. Meanwhile, after the microfiltration of the 1% and 2% NaCl supernatants, the COD removal showed higher difference with a decrease to reach 76% and 81%, respectively.

Regarding the anaerobic treatment, the microfiltration of the bioreactors supernatants has shown lower permeability values for all treated effluents in comparison to the aerobic bioreactors' supernatants microfiltration (**Figure 22**).

When comparing the membrane permeability levels depicted by **Figure 22**, we can see that the best permeability was obtained when treating the 0% NaCl supernatant followed by the 0.5%,

1%, 2% and 3% NaCl as the lowest obtained permeability level, the permeability reduction in comparison to the 0% NaCl was as follows: about 28%, 54%, 62% and 77%, respectively. The observed results could be explained by the fouling layer formation due to the released anaerobic biomass' EPS which increase gradually with the increasing effluent salinity and builds up the membrane resistance during the filtration process due to biofilm formation over operation time (**Vyrides and Stuckey, 2011**). Moreover, the salinity increase contributes in the change of the EPS characteristics including their compositions and contents (**Zhao and al., 2016**).

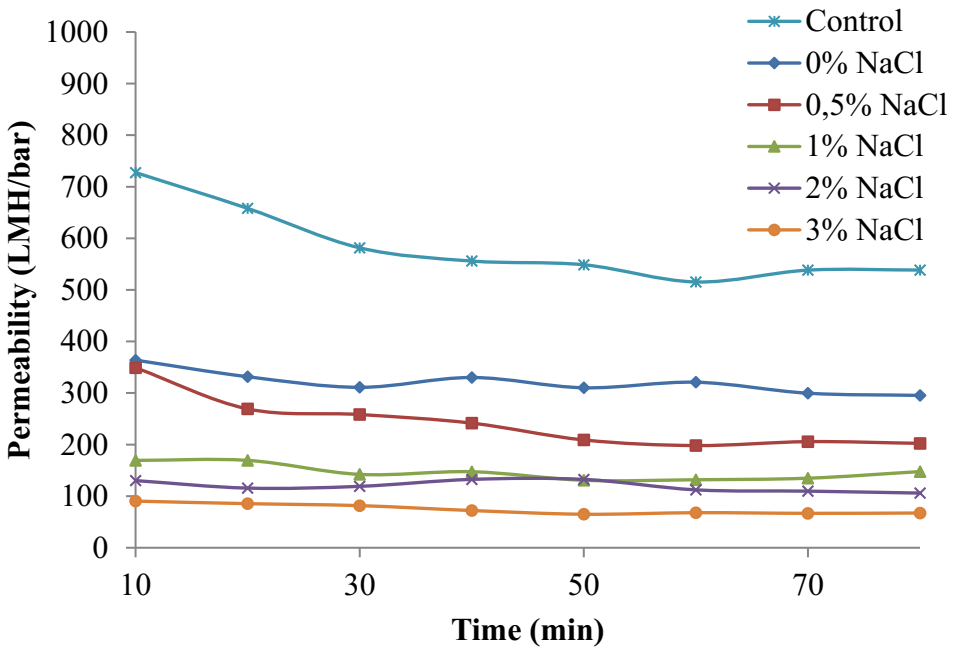

***Figure 22**: Microfiltration membrane permeability of the different anaerobic bioreactors' supernatants (control is reverse osmosis water)*

Figure 23 illustrates the COD removal measured after both anaerobic treatment and microfiltration process at different NaCl concentrations. The microfiltration process has enhanced the effluents quality and had led to final COD removal of 77%, 59%, 51%, 72% and 77% which correspond to the 0%, 0.5%, 1%, 2%, and 3%NaCl concentrations, respectively.

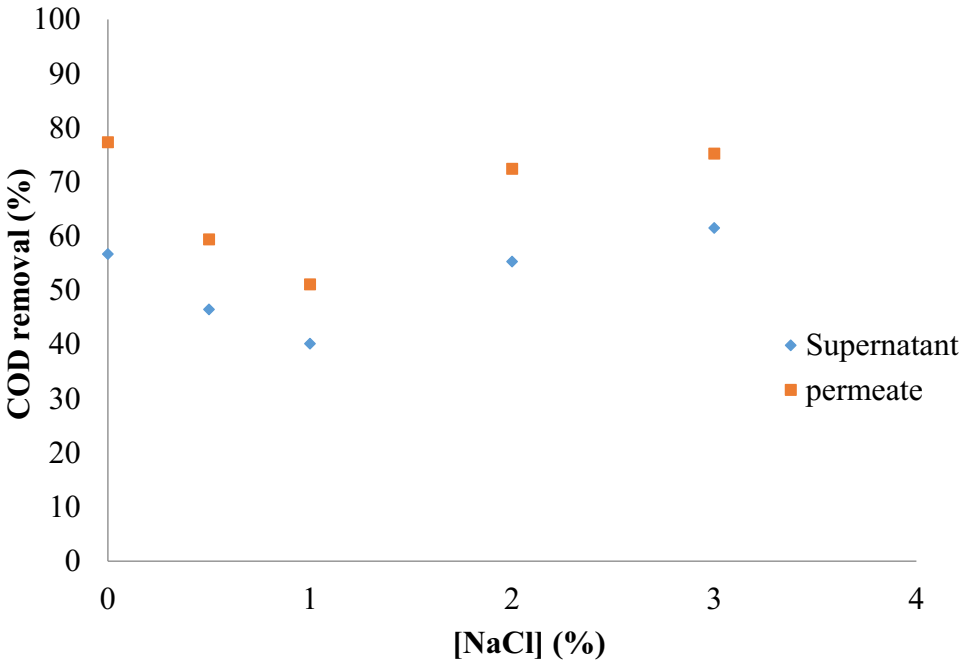

***Figure 23**: COD removal after microfiltration of the anaerobic bioreactors' supernatants*

The turbidity removals measured following microfiltration of the aerobic and anaerobic supernatants has shown relatively good rates with slight variation between the different salt concentrations (**Table 6**). It is important to mention that the supernatant turbidity is affected by the increase of the NaCl concentration since it could induce more production of extracellular polymeric substances and the mean floc size is relatively bigger which influence the sludge settlement ability (**Vyrides and Stuckey, 2009.b**). Nevertheless, the turbidity removals by microfiltration did not drop significantly during the operation time when increasing the salt concentration (**Table 6**).

***Table 6:** Turbidity removals following microfiltration of aerobic and anaerobic supernatants at different salinities*

	Aerobic supernatant	**Anaerobic supernatant**
0% NaCl	78%	68%
0.5% NaCl	96%	74%
1% NaCl	79%	88%
2% NaCl	86%	79%
3% NaCl	-	72%

Even though the microfiltration process has improved the final COD removal in the anaerobic process, the observed increase didn't exceed the results obtained after the aerobic/microfiltration treatment. Consequently, we can conclude that, in our study, when the aerobic digestion is coupled with microfiltration process higher treatment performance and effluent quality could be reached for all the studied NaCl concentrations.

3.1.3.2 Biological treatments coupled with Ultrafiltration

Ultrafiltration tests were performed to treat the biological aerobic bioreactors' supernatants at different NaCl concentrations. The measured permeability has shown similar behavior with a relatively stable evolution over the studied filtration time and permeability reduction rates that are lower than the ones obtained during the microfiltration process when compared to the 0% NaCl supernatant (**Figure 24**).

The membrane permeability levels reduced by around 25% with 0.5% NaCl supernatant and by 25% and 19% with 1% and 2% NaCl supernatants, respectively. As shown previously, the increasing NaCl concentration could lead to more membrane fouling due to the released biomass' EPS which becomes remarkably higher due to cell plasmolysis at high NaCl concentration in addition to the secretion of polymers and intracellular constituents which participate in the biofilm formation over filtration time (**Reid et al., 2006; Vyrides and Stuckey, 2011; Jang et al., 2013**). This influences directly the permeability which decreases gradually with the increasing salt content. In the case of ultrafiltration tests, the fouling layer formation could have higher impact on the treatment performance due to the smaller pore size (0.01 μm) in comparison to the microfiltration's membrane (1.6 μm).

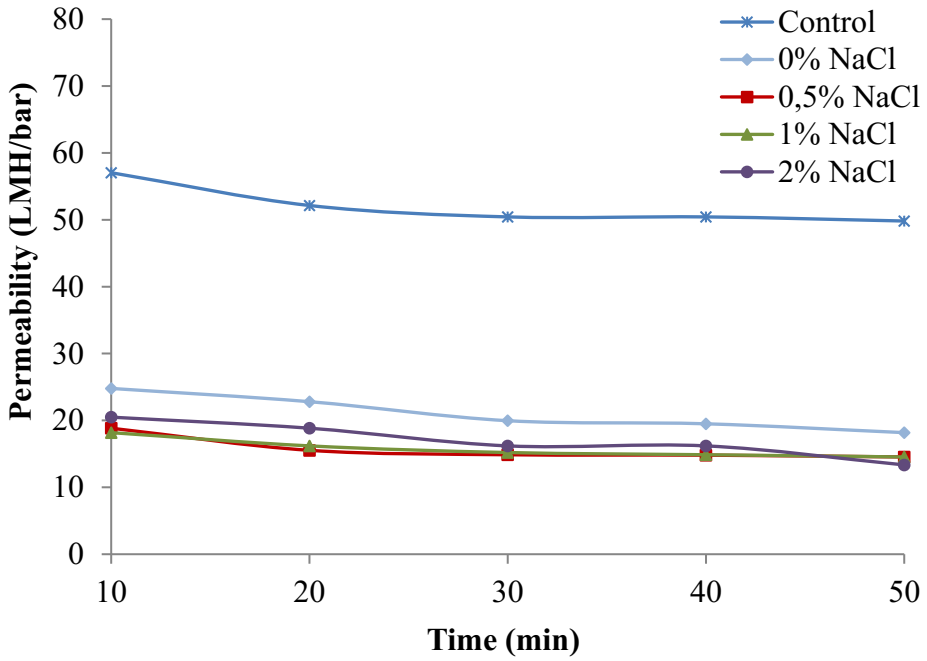

***Figure 24**: Membrane permeability during ultrafiltration of the aerobic bioreactors' supernatants (control is reverse osmosis water)*

In terms of COD removal, the ultrafiltration treatment has improved the effluent quality especially for the 2% and 3% NaCl supernatants where the improvement is of 11% and 18%, respectively (**Figure 25**).

The COD removal have reached the following percentages: 97%, 96%, 74% and 85% in the 0%, 0.5%, 1% and 2% NaCl ultrafiltration permeates, respectively. The obtained results are comparable to the ones illustrated in **Figure 23** after microfiltration process, with a slight increase in the COD reduction after ultrafiltration treatment.

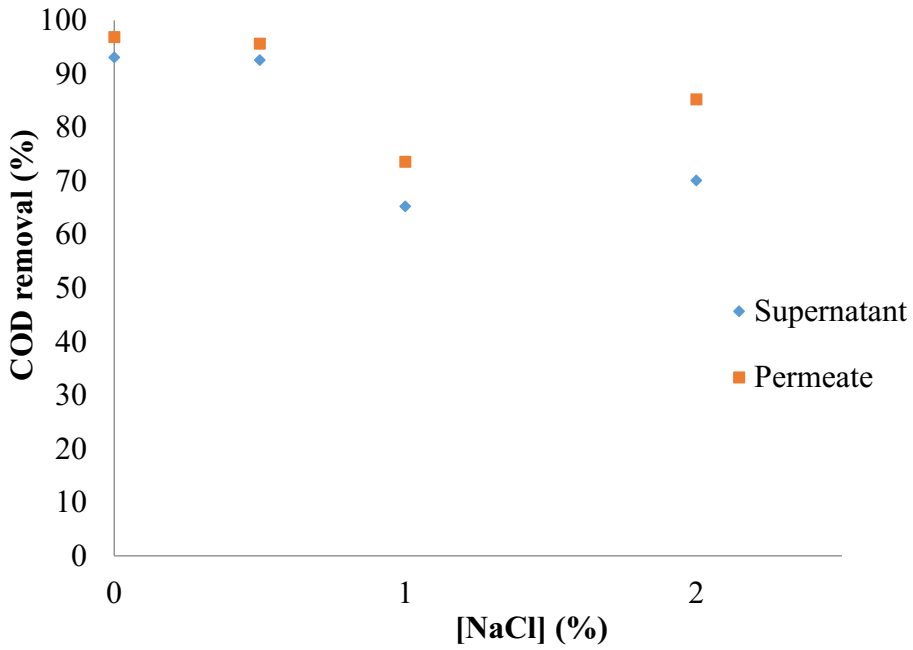

Figure 25: *COD removal after ultrafiltration of the aerobic bioreactors' supernatants*

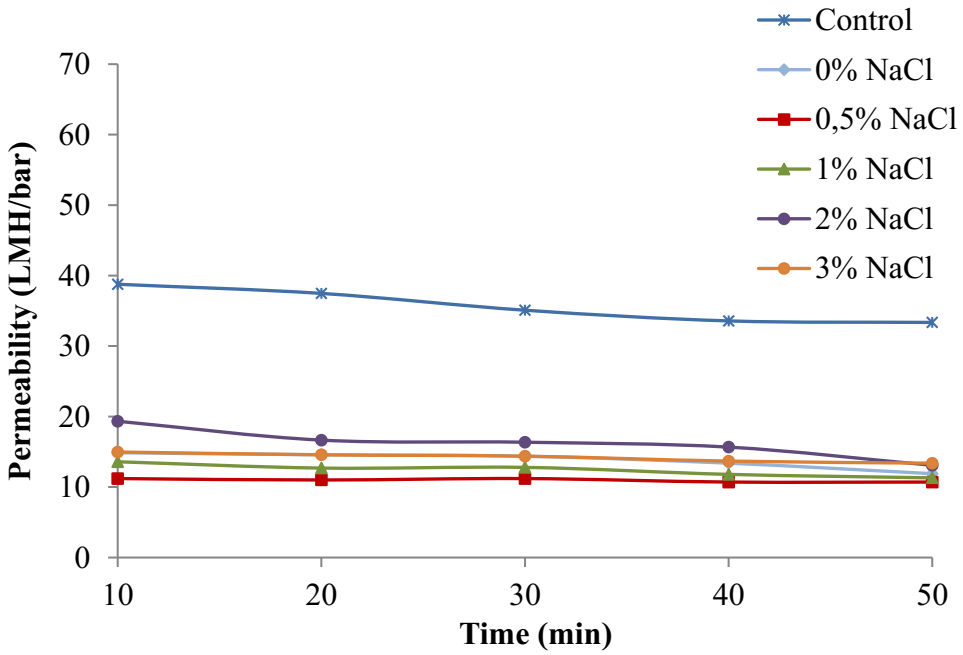

Figure 26*: Membrane permeability during ultrafiltration of the anaerobic bioreactors' supernatants (control is reverse osmosis water)*

The ultrafiltration of anaerobic bioreactors' supernatants led to similar membrane permeability behavior and lower permeability levels which ranged between 10 and 20 LMH/bar for all salt concentrations (**Figure 26**). The illustrated membrane permeability levels didn't show a marked variation between the different treated NaCl concentrations which is similar to the results obtained by the ultrafiltration of the aerobic bioreactors' supernatants.

***Table** 7: Turbidity removals following ultrafiltration of aerobic and anaerobic supernatants at different salinities*

	Aerobic supernatant	**Anaerobic supernatant**
0% NaCl	84%	-
0.5% NaCl	85%	82%
1% NaCl	83%	84%
2% NaCl	81%	86%
3% NaCl	-	87%

Table 7 shows the turbidity removals measured following ultrafiltration of the aerobic and anaerobic supernatants. The ultrafiltration at the different NaCl concentrations has led to good removal rates that are comparable to the ones obtained by microfiltration in the case of the aerobic reactors supernatants (**Table 6**). Concerning the anaerobic reactors supernatants, the turbidity removals obtained by ultrafiltration are slightly higher and this could be explained by the tight pore size of the utilized membrane in addition to possible differences between the supernatants composition (EPS, flocs settlement, etc...) that contribute in the fouling layer formation.

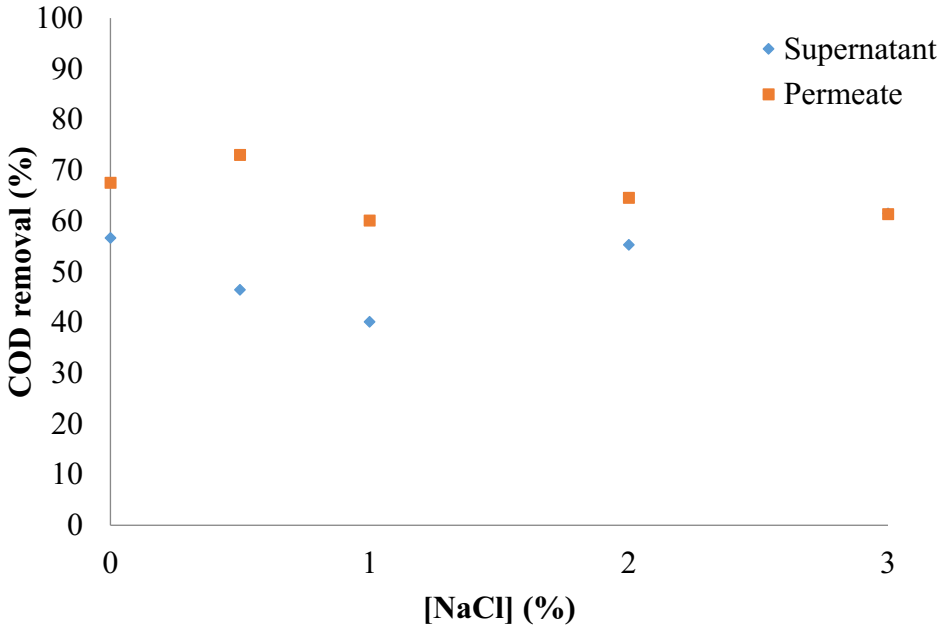

Figure 27: *COD removal after ultrafiltration of the anaerobic bioreactors' supernatants*

The COD removal obtained after the anaerobic supernatants' ultrafiltration are shown in **Figure 27** which depicts the increase of the 0%, 0.5%, 1% and 2% NaCl permeate qualities which reached 68%, 73%, 60% and 65% of COD reduction, respectively. For the 3% NaCl ultrafiltration permeate, the COD removal didn't show significant difference in comparison to the anaerobic digestion supernatant.

3.1.4 Conclusions

In this first section, different treatment processes and wastewater qualities were analyzed and investigated to show the effect of the NaCl mass percentage and the treatment characteristics on the final water quality and the processes performances.

According to this investigation, the aerobic treatment was more efficient when combined to the ceramic membrane microfiltration since we have obtained higher water quality with good overall performance: the microfiltration led to COD removal of 96%, 76% and 81% for aerobically treated feed of 0.5%, 1% and 2% NaCl, respectively. Concerning the ultrafiltration, the COD removal reached 96 %, 74%, 85% for saline feed concentrations of 0.5%, 1% and 2% NaCl, respectively. In our study, the anaerobic biological treatment didn't lead to sufficiently good COD removal when compared to the aerobic process which didn't improve significantly after the filtration processes.

Regarding the studied membranes, the ceramic microfiltration membrane was more cost-effective since it was regenerated during the study and required only a peristaltic pump to run the different tests. However, the polymeric membrane required higher pressure and its study could be developed into investigating the membrane regeneration and use for longer periods.

In all the studied processes, the conductivity and the salt concentration were not affected by the filtration procedures and the main COD was removed mainly by the biological treatments. Besides, the final water qualities were very similar in the case of low salt concentrations (0% NaCl and 0.5% NaCl) in comparison to the higher concentrations (1%, 2% and 3% NaCl).

In order to solve the treated effluents salinity issue, good performance desalination process has to be considered for this purpose. Direct Contact Membrane Distillation (DCMD) as emerging process and one of the promising desalination technologies will be investigated and discussed in the next sections of this research work.

3.2 DCMD OPTIMIZATION FOR SALINE SYNTHETIC EFFLUENT TREATMENT

3.2.1 Permeate flux stability

The stability of the DCMD process during operation time for synthetic saline wastewater treatment is checked through preliminary tests to evaluate the permeate flux evolution and the obtained permeate quality (**Figure28**). The volumetric permeate flux maintained an almost constant level with an average value of 9.5 L/m^2.h during 5 hours treatment under the following operating conditions: ΔT= 30°C, *Vf* = 0.051 m/s, *[NaCl]*= 10g/L and *[Gluc]*= 5 g/L.

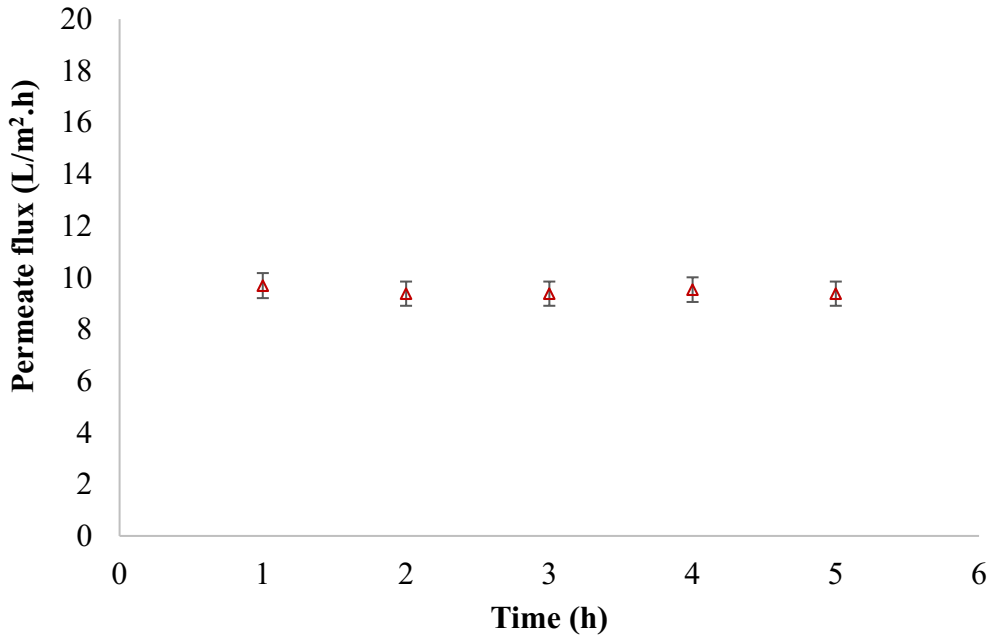

Figure 28: *Permeate flux evolution during operation time.*

Concerning the permeate quality, the electrical conductivity reduction from the feed side to the permeate side is 99.9% and in terms of COD the reduction was higher than 99.9 %. These reduction rates confirm the ability of the DCMD process with the PTFE membrane (pore size= 0.45 µm) to treat and desalinate the synthetic saline wastewater with a stable performance over time (5 hours treatment).

Following this observation, an operation time of one hour has been selected for all optimization experiments via response surface methodology. Following each experiment performed in this study, both COD and permeate conductivity were measured and the removal rates have been

all higher than 99.9% with very low variations. Therefore, only the permeate flux was considered as the main response in our work.

3.2.2 Response Surface Methodology (RSM) application in DCMD

The results of CCD experiments in terms of experimental and predicted permeate flux values are shown in **Table 8**.

As it could be observed in this table, the predicted response values are highly comparable to the experimental set of data which indicates that the developed regression model provides a good fit to the experimental results.

The predicted flux is calculated by the means of the following regression equation that presents the empirical model written in terms of actual variables. As illustrated in **Table 8**, the predicted permeate flux values have a large range of variation following the changes in the studied parameters from 3 to 23 L/m^2.h which indicates the important effect of the chosen parameters on the DCMD process. In the following, the regression model written with the coded symbols:

$$\boldsymbol{Jp} = 11.38 + 5.706\boldsymbol{X_1} + 2.21\boldsymbol{X_2} - 0.549\boldsymbol{X_3} + 1.209\boldsymbol{X_4} + 0.313\boldsymbol{X_1^2} - 0.321\boldsymbol{X_2^2} - 0.405\boldsymbol{X_3^2} - 0.127\boldsymbol{X_4^2} + 0.646\boldsymbol{X_1X_2} - 0.417\boldsymbol{X_1X_3} - 0.098\boldsymbol{X_1X_4} - 0.074\boldsymbol{X_2X_3} + 1.292\boldsymbol{X_2X_4} - 0.503\boldsymbol{X_3X_4}$$

The regression model could be also written in terms of actual variables as follows:

$$\boldsymbol{Jp} = 11.38 + 5.706\boldsymbol{\Delta T} + 2.21\boldsymbol{Vf} - 0.549[\boldsymbol{NaCl}] + 1.209[\boldsymbol{Gluc}] + 0.313\boldsymbol{\Delta T}^2 - 0.321\mathbf{Vf^2} - 0.405[\boldsymbol{NaCl}]^2 - 0.127[\mathbf{Gluc}]^2 + 0.646\boldsymbol{\Delta TVf} - 0.417\boldsymbol{\Delta T}[\boldsymbol{NaCl}] - 0.098\boldsymbol{\Delta T}[\boldsymbol{Gluc}] - 0.074\boldsymbol{Vf}[\boldsymbol{NaCl}] + 1.292\boldsymbol{Vf}[\boldsymbol{Gluc}] - 0.503[\boldsymbol{NaCl}][\boldsymbol{Gluc}]$$

When studying the coefficients given in the previous equation, we can conclude that the temperature difference *ΔT* has the most significant influence on the mass transfer in DCMD followed by the feed velocity with coefficient values of b_1=5.706 and b_2=2.21, respectively. Both studied variables did affect positively the permeate flux (*Jp*) since when increasing one or both of them we did get an increase in the permeate flux.

Previously, it was proven the significant effect of both temperature difference and feed flow rate, and consequently the feed velocity, as part of the major parameters on which DCMD process performance is depending. Following the temperature difference and feed flow rate variations, significant high or low permeate fluxes could be reached and this could be attributed to the nature of the process driving force (**Hou et al., 2010; He et al., 2011; Singh et al., 2013 Ashoor et al., 2016;**).

The summarized main effects of the investigated operating conditions, which are illustrated in **Figure 29**, confirm the previously revealed results which indicate that the water vapor, and consequently the permeate flux, are an exponential function of the temperature.

Moreover, **Figure 29** shows that the temperature difference (ΔT) has the greatest effect on DCMD treatment of the saline synthetic wastewater in comparison to the rest of the considered and studied variables, followed by the feed velocity (*Vf*) as proven previously. Meanwhile, the NaCl and glucose concentrations are showing lower influence on the permeate flux in the respective ranges of variation.

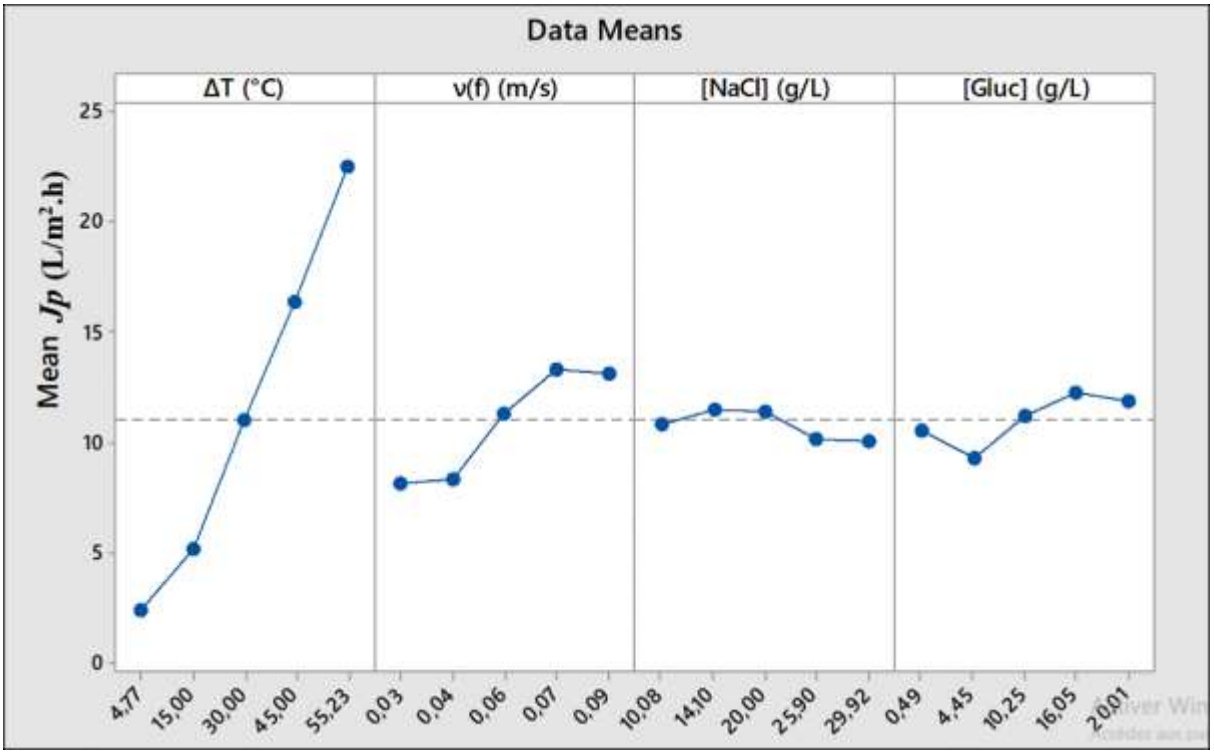

***Figure 29**: Main effects plot for the permeate flux (Jp).*

However, the NaCl concentration has a low negative influence (b_3=-0.549) on the response value (*Jp*). Regarding its influence on the DCMD performance, the NaCl concentration increase affects slightly the water activity in the feed side and consequently, the driving force

which leads to a small decrease in the permeate flux (**Martinez & Rodriguez-Maroto, 2007; Boubakri et al., 2014**).

The glucose concentration has shown low influence on the studied response with a coefficient value of b_4=1.209. In previous studies on DCMD with sucrose aqueous solutions, the increase of the feed concentration has led to a small drop of the permeate flux that is linked to change in the feed water activity. However, this influence was lower than the one obtained with salt feed solutions at the same concentration.

It is important to indicate the close link between the feed viscosity and its water activity since when adding sucrose as a solute to the feed stream viscosity increases. More precisely when the feed solution temperature is relatively low: ≤35°C and at high glucose concentrations (from 100 g/L to 500 g/L) (**Schofield et al., 1990; Izquierdo-Gil et al., 1999; Martinez & Rodriguez-Marot, 2007**).

However, in our case of study the glucose concentration didn't exceed 20 g/L as a maximum value which is much lower than the concentrations used in the aforementioned investigations realized on sucrose aqueous solutions that started with 100 g/L as the lowest sucrose concentration. This difference in glucose concentration could be the reason behind the different observed impact on the permeate flux. According to our model, at high temperature differences the positive effect of glucose concentration gets lower.

Table 8: *CCD with predicted and experimental DCMD results.*

Experiment number	X_1	X_2	X_3	X_4	Predicted flux (L/m².h)	Experimental flux (L/m².h)
1	-1	-1	-1	-1	3.1	3.1 ±0.4
2	1	-1	-1	-1	14.3	12.8±0.3
3	-1	1	-1	-1	3.8	4.4±0.7
4	1	1	-1	-1	17.6	17.5±0.1
5	-1	-1	1	-1	4.0	2.8±0.2
6	1	-1	1	-1	13.5	14.1±0.4
7	-1	1	1	-1	4.4	4.1±0.1
8	1	1	1	-1	16.5	15.9±0.4
9	-1	-1	-1	1	4.2	5.6±0.8
10	1	-1	-1	1	14.9	14.1±0.5
11	-1	1	-1	1	10	6.6±0.9
12	1	1	-1	1	23.6	27.5±0.3
13	-1	-1	1	1	3.0	1.9±0.2
14	1	-1	1	1	12.1	12.5±0.3
15	-1	1	1	1	8.6	13.0±0.5
16	1	1	1	1	20.3	19.1±0.4
17	-α	0	0	0	2.7	2.3±0.2
18	α	0	0	0	21.9	22.5±0.2
19	0	- α	0	0	6.8	8.1±0.3
20	0	α	0	0	14.2	13.1±0.2
21	0	0	-α	0	11.2	10.8±0.3
22	0	0	α	0	9.3	10.0±0.2
23	0	0	0	-α	9.0	10.5±0.1
24	0	0	0	α	13.1	11.9±0.4
25	0	0	0	0	11.4	11.3±0.1
26	0	0	0	0	11.4	11.4±0.1
27	0	0	0	0	11.4	11.3±0.1
28	0	0	0	0	11.4	11.3±0.1

3.2.3 Analysis of Variance

Variance analysis (ANOVA) was applied to investigate the statistical significance of the created regression model as well the effects significance of the various studied parameters and their interactions. The statistical significance is mainly reflected by both the p-value that has usually a significance level of 0.05 (p-value <0.05 for significant influence) and the R^2 which indicates the proportion of variation in the regression model response with a value close to 1 for a model having good effectiveness and well predictive ability (**Boubakri et al., 2014**).

With respect to the different operating variables and their interactions, the results of ANOVA showed that the temperature difference and the feed velocity had most significant positive influence on the DCMD response with a low probability values for both of them (p-value= 0.000). Concerning the NaCl concentration, the variance analysis indicated that it has an insignificant effect on the permeate flux response (p-value= 0.119). However, the glucose concentration has a relatively significant influence on the process response with p-value= 0.003. According to the ANOVA results, the only significant variables interaction in this case is the one between the feed velocity and the glucose concentration (p-value= 0.005). The increase of the feed flow rate, and consequently its velocity, decreases the temperature difference between the inlet and outlet of the DCMD module. This decrease leads to higher ΔT which affects the feed stream viscosity and consequently causes the increase of the permeate flux (**Schofield et al. 1990; Gryta, 2012**).

In our study, the developed model has a high R^2 level of 0.967, which indicates that the empirical model could explain more than 96.7% of the data deviation and therefore has a good statistical significance. This observation is strengthened by the obtained R^2_{Adj} value: 0.932 which means that, significant terms have been included in the empirical model (**Khayet et al., 2007**). In addition, the regression model has a very low p-value (0.000) which reflects its high significance and its ability to provide a good prediction of the response permeate flux (*Jp*). All the results obtained by the statistical estimators of ANOVA lead to confirm the effectiveness and significance of the model.

By considering both the good effectiveness of the developed model and its high fit to the experimental data by the comparison between the predicted and the experimental responses, we can conclude that its statistical validation is well established. The regression model could be applied for the description and optimization of the DCMD permeate flux response through

the optimization of the chosen variables (*ΔT* (°C), *Vf* (m/s), *[NaCl]* (g/L) and *[Gluc]* (g/L)) in their aforementioned respective ranges of variation.

3.2.4 Response surface and contour-line plots

In order to study the interactions between the different studied variables, response surface and contour-line plots are presented in **Figure 30.** These graphics and plots will lead to the identification of the variables optimum levels which help to achieve the higher possible permeate flux value. For each plot, two of the four variables are maintained constant and the regression model is used to calculate the permeate flux and follow its evolution as a function of the two other variables.

Figure 30 ***(a)*** and ***(b)*** show the simultaneous effect of *ΔT* and *Vf* on *Jp* at constant glucose and NaCl concentrations (maintained at their center points). As both variables have the most significant effects with a more pronounced influence of *ΔT* (b_1=5.706 > b_2=2.21), high permeate fluxes (>25 L/m^2.h) are obtained at their highest levels (*ΔT* ≥ 50°C and *Vf* ≥ 0.081 m/s). At low temperature difference the increase of the feed velocity does not improve significantly the permeate flux which shows the importance of providing higher driving force through increasing *ΔT* (**Nakoa et al., 2014**). It is important to indicate that there is no significant interaction between the temperature difference and the feed velocity (p-value> 0.05).

The effect of the temperature difference and the glucose concentration is illustrated by **Figure 30** ***(c)*** and ***(d)*** where the feed velocity and the NaCl concentration have constant values (0.057 m/s and 20 g/L, respectively). As expected, the temperature difference has the greater influence on the flux response which achieves the highest values (> 15 L/m^2.h) at *ΔT* > 40°C for all glucose concentrations varying from 0 to 20 g/L. The pronounced effect of ΔT in comparison to [*Gluc*] is confirmed by both their coefficients in the regression model (b1=5.706 > b4=1.209) and their calculated p-values (0.000 and 0.003, respectively). In addition, the plotted curve presents a parallel aspect that could lead to the assumption that there is no significant interaction between the two studied variables.

At constant feed velocity (0.057 m/s) and glucose concentration (10.25 g/L), the permeate flux in **Figure 30** (**e**) and (**f**) increases significantly when increasing the temperature difference. A slight decrease could be identified when increasing the NaCl concentration. The observed results could be attributed to the induced reduction of the partial vapor pressure over the membrane surface as it was proven previously (**Schofield et al., 1990; Kamrani et al., 2014**). The plotted response surface suggests that the interaction between *ΔT* and [*NaCl*] is negligible.

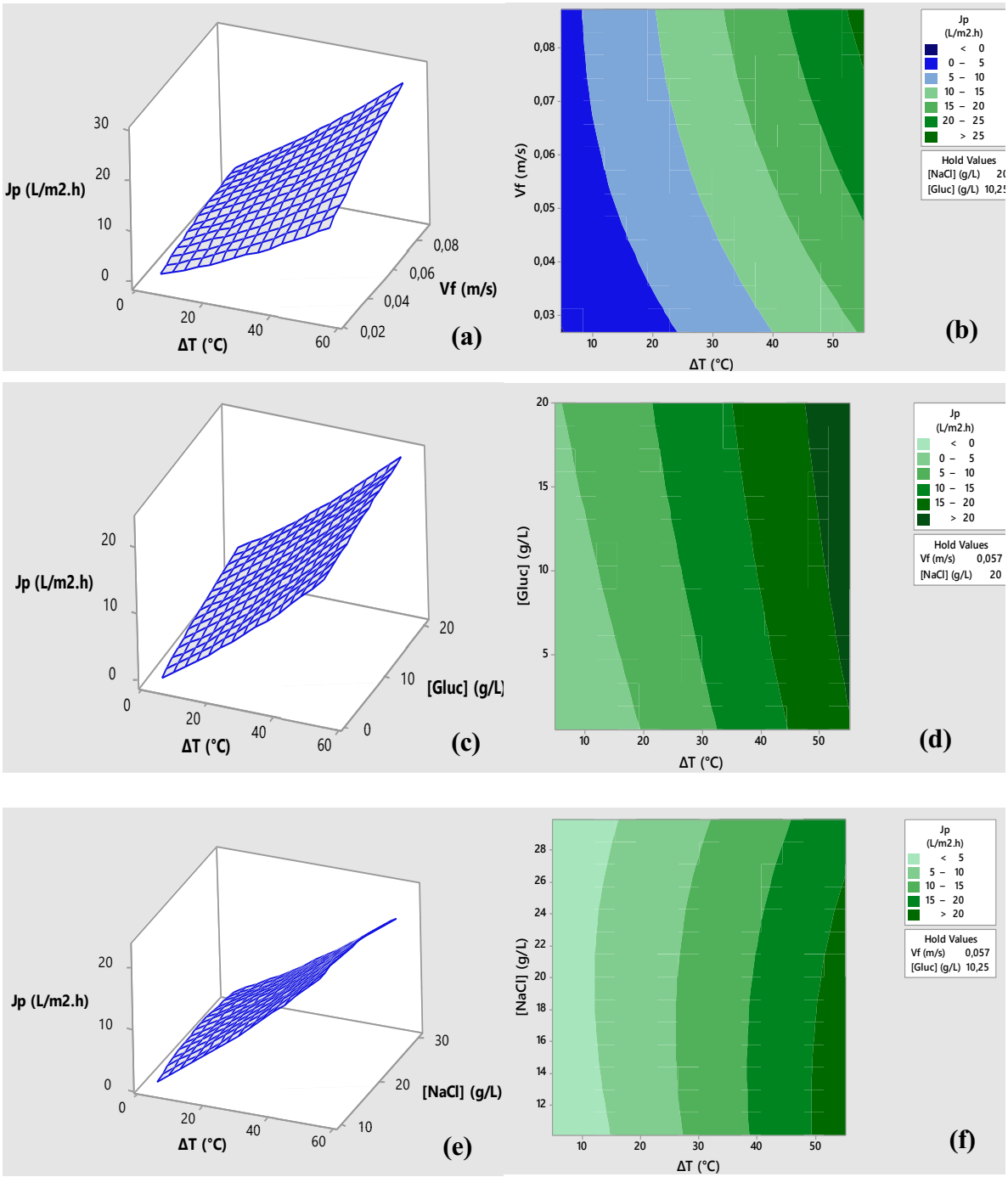
Jp (L/m2.h)
ΔT (°C)
Vf (m/s)
(a)
Vf (m/s)
ΔT (°C)
Jp (L/m2.h)
< 0
0 – 5
5 – 10
10 – 15
15 – 20
20 – 25
> 25
Hold Values
[NaCl] (g/L) 20
[Gluc] (g/L) 10,25
(b)
Jp (L/m2.h)
ΔT (°C)
[Gluc] (g/L)
(c)
[Gluc] (g/L)
ΔT (°C)
Jp (L/m2.h)
< 0
0 – 5
5 – 10
10 – 15
15 – 20
> 20
Hold Values
Vf (m/s) 0,057
[NaCl] (g/L) 20
(d)
Jp (L/m2.h)
ΔT (°C)
[NaCl] (g/L)
(e)
[NaCl] (g/L)
ΔT (°C)
Jp (L/m2.h)
< 5
5 – 10
10 – 15
15 – 20
> 20
Hold Values
Vf (m/s) 0,057
[Gluc] (g/L) 10,25
(f)

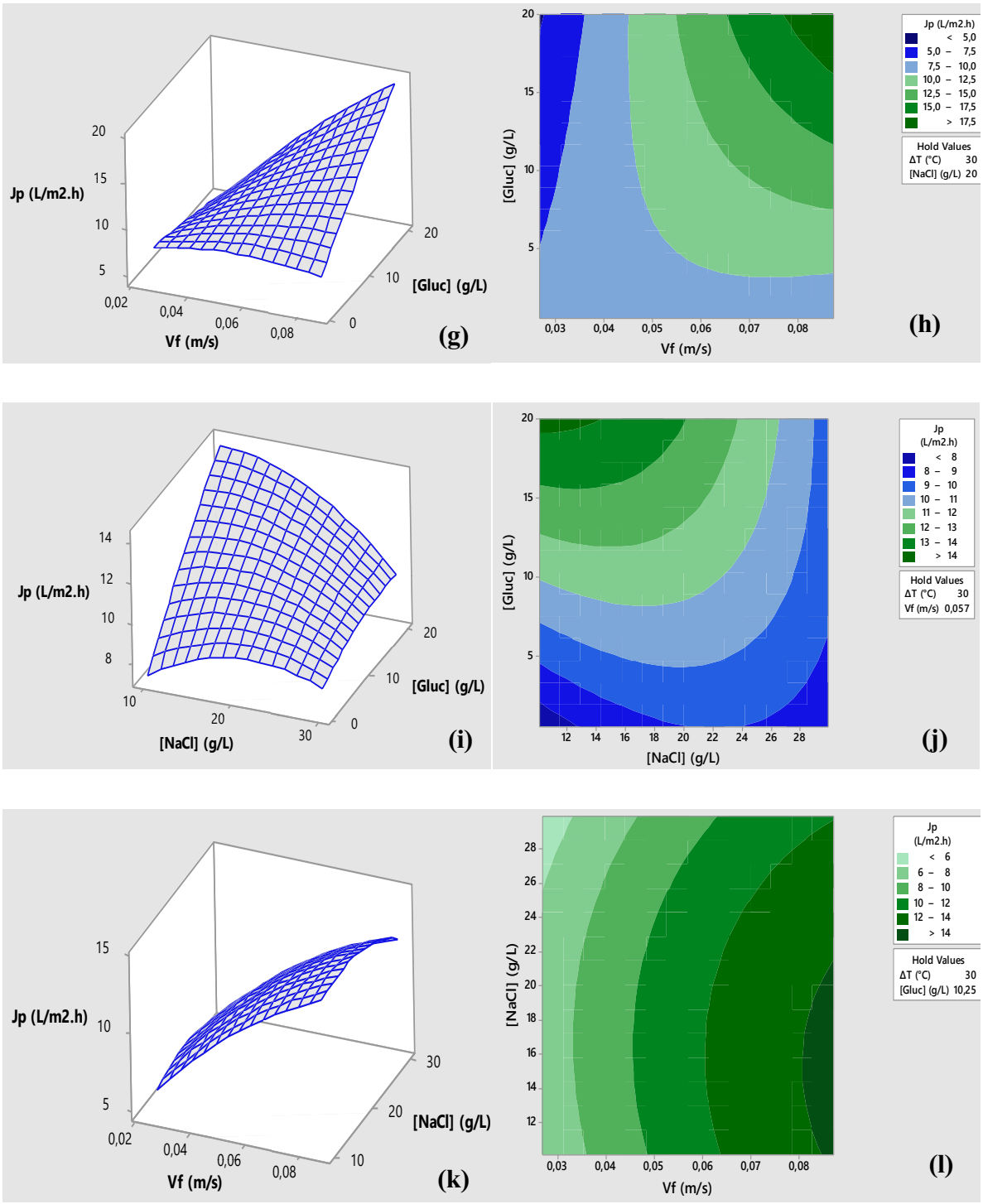

***Figure 30**: Response surface plots (**a**, **c**, **e**, **g**, **i** and **k**) and contour-line plots (**b**, **d**, **f**, **h**, **g** and **l**) of the predicted DCMD permeate flux (Jp) as function of: temperature difference and feed velocity [(**a**) and (**b**)], temperature difference and glucose concentration [(**c**) and (**d**)], temperature difference and NaCl concentration [(**e**) and (**f**)], feed velocity and glucose concentration [(**g**) and (**h**)], NaCl concentration and glucose concentration [(**i**) and (**j**)] and feed velocity and NaCl concentration [(**k**) and (**l**)]*

As illustrated in **Figure 30** ***(g)*** and ***(h)***, the plotted responses show the variation of the DCMD studied response *Jp* when varying both the feed velocity and glucose concentration with constant ΔT and [*NaCl*] of 30°C and 20 g/L, respectively. At low feed velocities (*Vf* <0.046 m/s) the permeate flux doesn't exceed 10 L/m^2.h for all glucose concentrations. A simultaneous increase of both variables leads to *Jp* augmentation that could exceed 17.5 L/m^{2}h. This increase might be induced by the decrease of the temperature polarization effect caused by the increase in the heat transfer on the membrane surface that is led by the feed flow rate increase (**Al-Asheha et al., 2006**). The interaction surface plot between *Vf* and glucose concentration could indicate a significant interaction between these variables which is confirmed with the probability p-value obtained by ANOVA (<0.05).

The combined variation effect of [*NaCl*] and [*Gluc*] on the permeate flux at constant ΔT (30°C) and feed velocity (0.057 m/s) is shown in **Figure 30** ***(i)*** and ***(j)***. At low levels of both studied variables, the permeate flux has a minimum of 8 L/m^2.h and it increases gradually with the glucose concentration to reach 14 L/m^2.h at low NaCl concentration and it ranges between 10 L/m^2.h and 11 L/m^2.h for the highest [*NaCl*]. We could assume from the response plot that there is no significant interaction between the two variables.

Figure 30 ***(k)*** and ***(l)*** illustrate the influence of feed velocity and salt concentration on the permeate flux variation when maintaining the rest of the variables constant (ΔT= 30°C and [*Gluc*] = 10.25 g/L). The plotted response reveals the effect of *Vf* increase which leads to the augmentation of the *Jp* that exceeds 14 L/m^2.h when *Vf* is around 0.081 m/s and [*NaCl*] < 21g/L. At low feed velocities (<0.035 m/s) the calculated flux is under 8 L/m^2.h for all salt concentrations in the studied range. As it could be seen in the plotted responses, the interaction between *Vf* and [*NaCl*] is negligible.

3.2.5 DCMD response optimization and model verification

As a result of the response surface methodology application on the studied saline synthetic wastewater, a maximum response (*Jp*) should be predicted. In order to identify the optimum operating conditions leading to achieve the aforementioned response, all the studied effects and interactions are taken into consideration using Minitab software (**Table 9**).

A maximum permeate flux of 34.14 L/m^2.h is predicted to be achieved at the following optimum operating conditions: temperature difference ΔT= 55.23°C, feed velocity *Vf*= 0.086 m/s, NaCl concentration [*NaCl*]=10.08 g/L and glucose concentration [*Gluc*]= 20.01 g/L.

The composite desirability is calculated to assess how good the combination of the defined optimum variables does meet the desired goal (maximizing the permeate flux Jp). In this study we have a good desirability value of 0.975 (1 is the maximum).

Table 9: *Optimum operating conditions and their correspondent predicted and experimental responses.*

Variable	***ΔT*** **(°C)**	***Vf*** **(m/s)**	***[NaCl*** **(g/L)**	***[Gluc]*** **(g/L)**	***Jp*** **(L/m².h) predicted**	***Jp*** **(L/m².h) experimental**	**Composite Desirability**
Value	55.23	0.086	10.08	20.01	34.14	35.69	0.975

In order to verify the optimization procedure and results, experiments were conducted at the obtained optimum conditions and the responses were compared to the predicted maximum response.

Table 9 illustrates both the experimental permeate flux mean value after three repeated experiments at optimum operating conditions: 35.69± 0.6 L/m^2.h and the maximum permeate flux predicted by the developed regression model at the same conditions: 34.14 L/m^2.h. The deviation of 4.3 % indicates and confirms the validity of the optimization procedure and the developed DCMD optimization model in addition to high performance in terms of COD removal and conductivity rejection.

3.2.6 Conclusions

In this second section, the response surface methodology was applied for the optimization of synthetic saline wastewater DCMD treatment and desalination via the optimization of the permeate flux (*Jp*) with a remarkable high permeate quality in terms of electrical conductivity reduction (99.9%) and COD removal rate (>99.9%). In this study, four different variables were considered to create the optimization model, namely: temperature difference ΔT, feed velocity *Vf*, NaCl concentration [*NaCl*] and glucose concentration [*Gluc*]. The developed regression model demonstrated a good level of effectiveness and ability to predict the process response with $R^2 = 0.967$ and $R^2_{Adj} = 0.932$. The statistical evaluation and analysis of the model showed that it has a high significance and that the most influencing variable in the studied ranges are the temperature difference and the feed flow rate followed by the glucose concentration with lower significant effect. The optimization procedure has led to the prediction of the maximum permeate flux (34.14 $L/m^2.h$) that could be achieved under the following optimum experimental conditions: $\Delta T = 55.23°C$, *Vf* = 0.086 m/s, *[NaCl]* = 10.08 g/L and *[Gluc]* = 20.01 g/L. As a final step, the experimental verification of the developed regression model showed its validity and suitability within the studied range of variables.

3.3 DCMD APPLICATION FOR CHEESE WHEY WASTEWATER TREATMENT

3.3.1 Raw dairy effluent DCMD treatment

The first step in testing DCMD process on the raw saline dairy effluent (R-WW) was using M1 for the treatment. The feed inlet temperature and the permeate outlet temperature were controlled at 55 and 25°C, respectively. Both feed and permeate velocities were maintained at 0.08 m/s.

Figure 31 shows the fast decline of the permeate flux during 7 hours operation that is characterized by a drop from 11 kg/m^2.h to around 4 kg/m^2.h. Simultaneously, the permeate electrical conductivity continuously increased and reached 1.95 mS/cm after only two hours of treatment which corresponds to the pores breakthrough. This increase reached 5.28 mS/cm at the end of the treatment with a TOC value that is higher than 100 mg/L. This observation shows that M1 had lost its hydrophobicity by letting salts and other organic components crossing through to the permeate stream (**Kezia et al., 2015**).

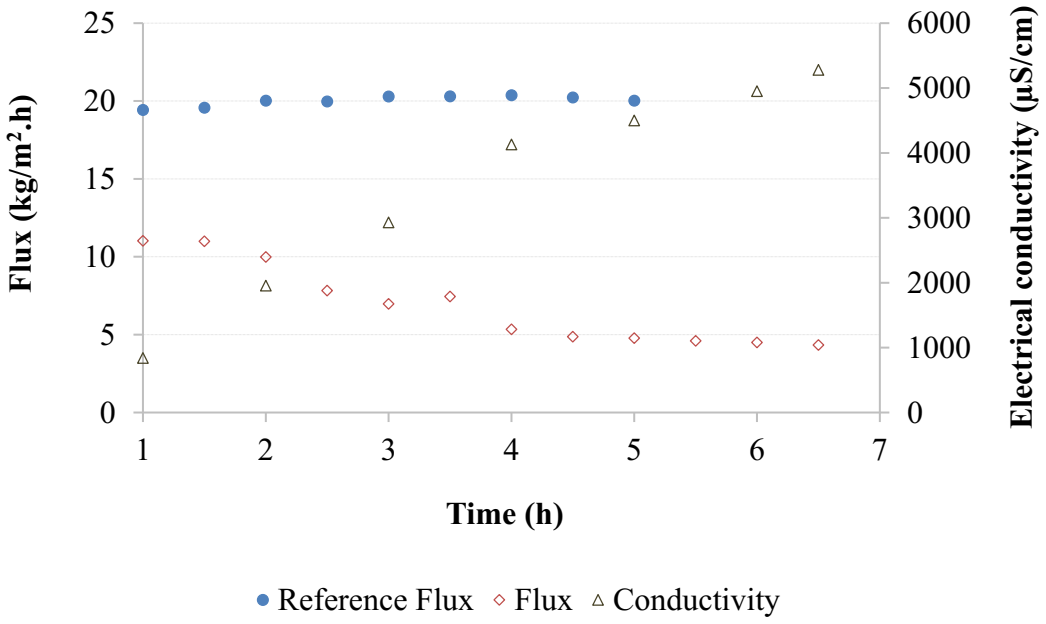

***Figure 31**: Permeate flux and electrical conductivity of raw effluent (R-WW), DCMD treatment with M1, Tei=55°C, Tco=25°C and Ve=Vc=0.08 m/s*

Consequently, the other membrane (M2), with lower pore size (0.2 µm) and higher thickness and resistance was tested with raw saline effluent.

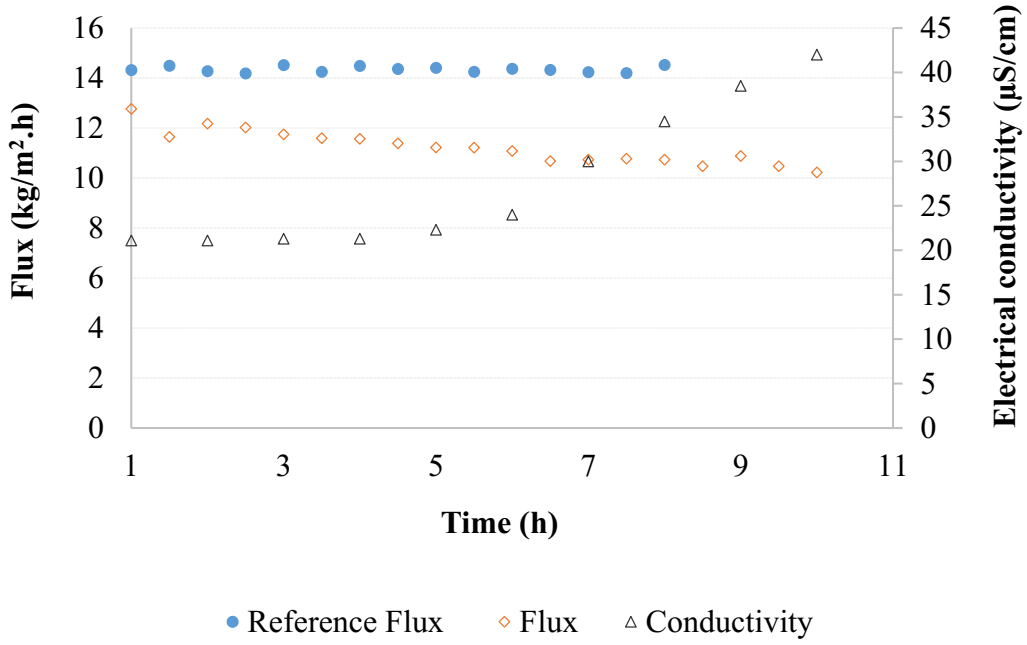

Figure 32: *Permeate flux and electrical conductivity of raw effluent (R-WW), DCMD treatment with M2, Tei=55°C, Tco=25°C and Ve=Vc=0.08 m/s*

Figure 32 shows the evolution of the permeate flux and conductivity when operating with M2. The permeate flux is showing a slower decrease in comparison to M1. Nevertheless, it is decreasing during 10 hours to a value of 10.2 kg/m^{2}h. The electrical conductivity remains stable during 5 hours and starts increasing afterwards to 44 µS/cm after 10 hours. According to **Ge et al. (2014),** this increase in the case of R-WW is related to the initiation of membrane wetting since the feed stream contains a significant quantity of organic substances (**Table 3**) which interact with the membrane surface and change its properties (**De La Fuente and al., 2002**). It is important to note that the permeate TOC did not exceed 2 mg/L until the end of the treatment. This shows that M2 has a higher heat transfer resistance than M1 at the same operating conditions and feed quality in addition to its lower pore size. This can be explained by the fact that it is characterized, in addition to the lower pore size, by a higher thickness, which indicates longer diffusion distance and higher heat transfer resistance. Therefore, as it was proven previously, with higher isolation against heat transfer through the membrane higher temperature difference could be maintained leading to relative flux increase (**Winter, 2015**).The SEM observation of the membranes surfaces, M1 (7 hours) and M2 (10 hours), at the same operating conditions show that the fouling layers cover the majority of the surfaces in both cases with the presence of more cracks in M2 that could possibly be formed following the membrane drying (**Figure 33**).

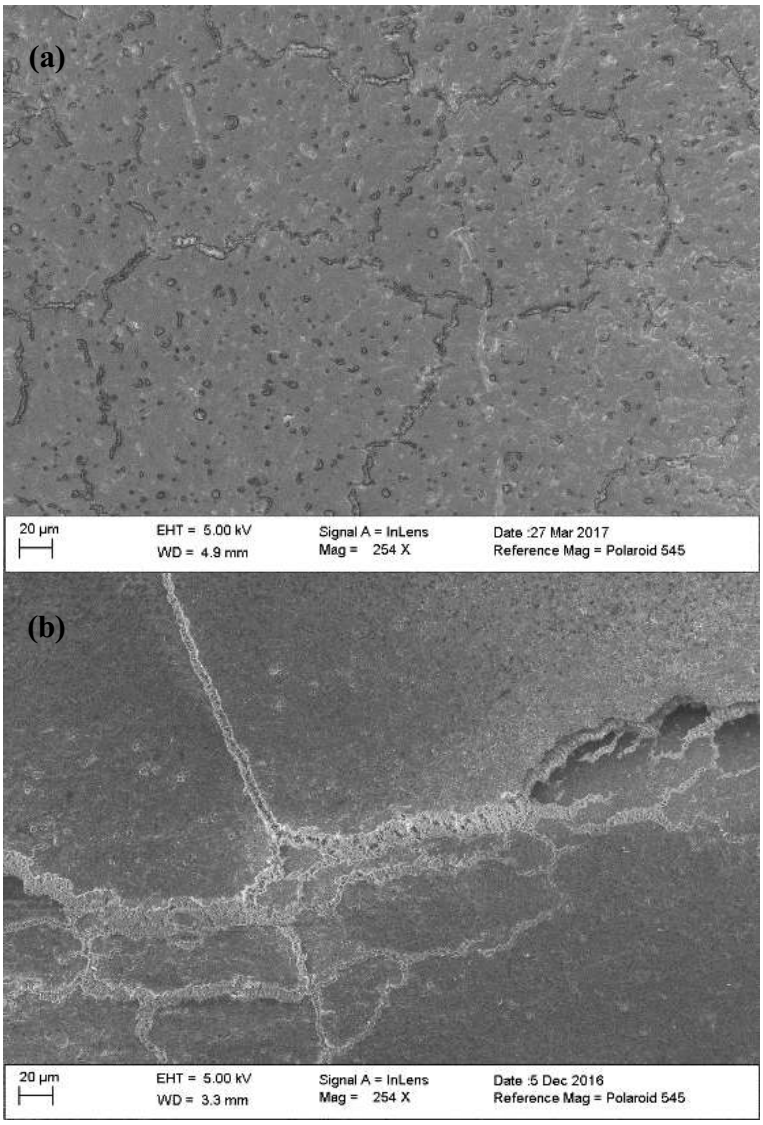

Figure 33: *SEM pictures of membrane samples: fouling layers after raw effluent DCMD treatment with M1 after 7 hours* ***(a)*** *and M2 after 10 hours* ***(b)****. Operating conditions: ΔT= 30 °C and V=0.08m/s*

3.3.2 Pretreated dairy effluents treatment

The feed inlet temperature and the permeate outlet temperature were controlled at 55 and 25°C, respectively during the treatment of MAF and MAF-UF permeates as feed streams. Both feed and permeate velocities were controlled to maintain a constant value of 0.08 m/s. **Figure 34** shows the flux variation obtained by the treatment of: tap water as reference and two pretreated dairy streams by MAF and MAF-UF (MAF-WW and MAF-UF-WW, respectively). The permeate fluxes are illustrated starting from DCMD process stabilization after one hour. The difference in the flux levels at the starting point could be linked to the quick formation of the fouling layer during the first hour.

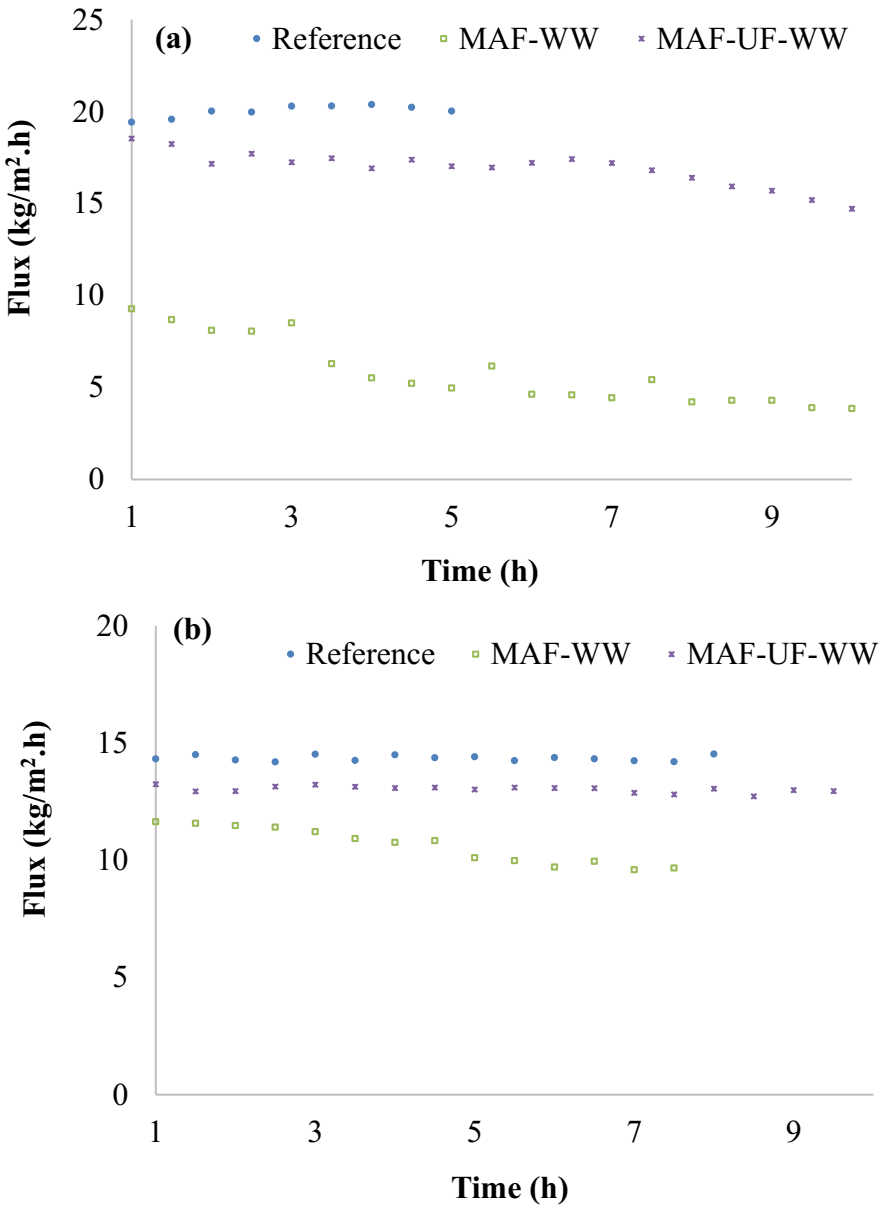

***Figure 34**: Permeate flux variation during MAF-WW and MAF-UF-WW DCMD treatment with: **(a)** 0.45µm pore size membrane (M1) and **(b)** 0.2µm pore size membrane (M2). Operating conditions: Tei=55°C, Tco=25°C and Ve=Vc=0.08 m/s*

Figure 34 shows differences in the permeate flux during the operation time between the two PTFE membranes M1 and M2 for the MAF pretreated effluent (MAF-WW) and the additionally UF pretreated effluent (MAF-UF-WW). At the beginning, the permeate fluxes of M1 of MAF-UF-WW were significantly higher than those of M2 which could be attributed to the larger pore size of M1. For the experiments using MAF-WW as feed solutions with M1, the flux dropped rapidly during the first 5 hours. This fast decline was accompanied by a fast increase in permeate electrical conductivity, equivalent to a pore breakthrough (**Figure 35**).

Additionally, the permeate TOC exceeded 100 mg/L. These findings are similar to previous results where it was found that there is higher decrease in the permeate flux when using a hydrophobic membrane with a pore size of 0.45 µm than with 0.2 µm during DCMD process of dairy effluents which is comparable to the results of this study (**Kezia et al., 2015**). However, when processing the UF permeate with M1, the flux remains stable at 17 kg/m^2.h but decreases slightly after 7 hours to reach 15 kg/m^2.h after 10 hours (**Figure 34**). This flux decrease will induce the reduction of the process productivity. The permeate maintained good quality after the same time with a conductivity of 60 µS/cm and a TOC below 2 mg/L (**Figure 35**).

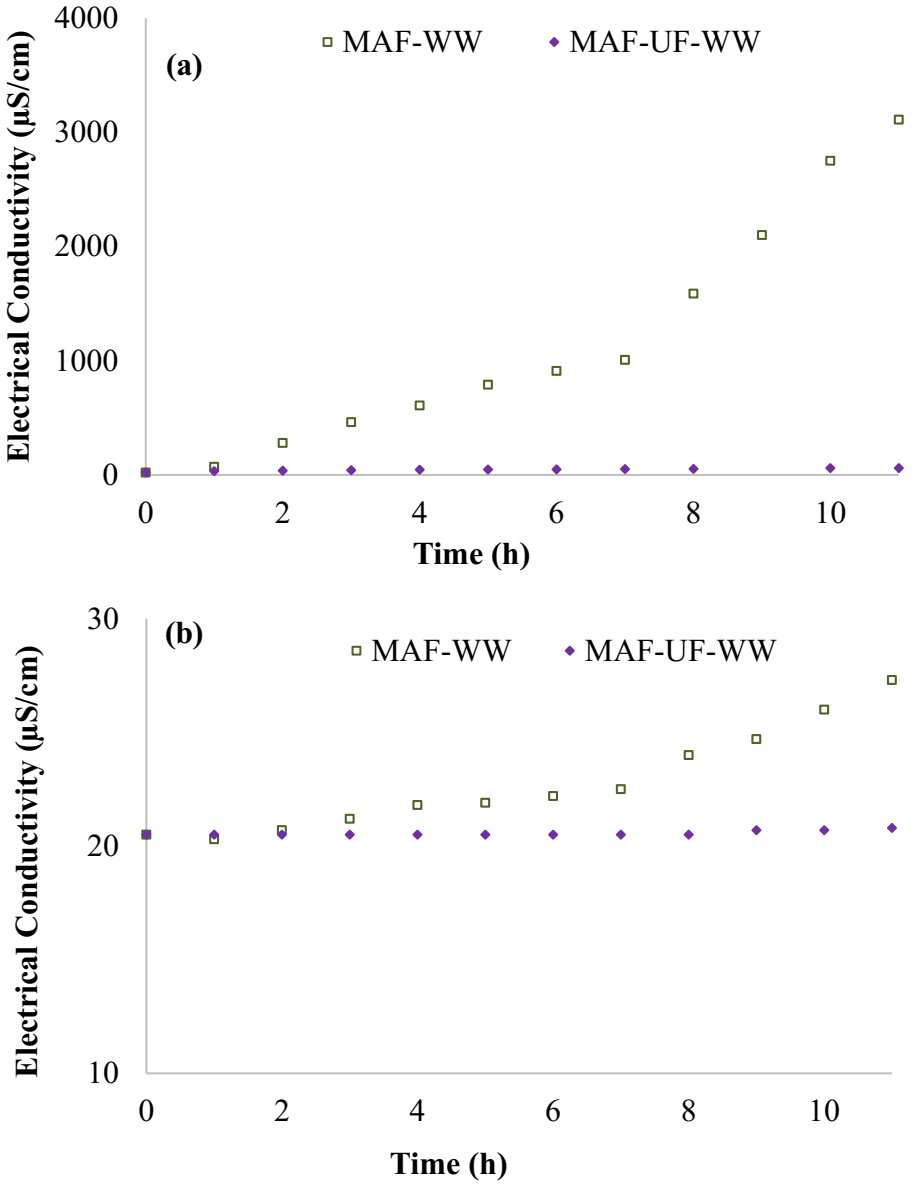

***Figure 35**: Permeate electric conductivity during DCMD treatment with: **(a)** 0.45µm pore size membrane (M1) and **(b)** 0.2µm pore size membrane (M2) of different saline dairy streams. Operating conditions: Tei=55°C, Tco=25°C and Ve=Vc=0.08 m/s*

With respect to the DCMD process using the second membrane (M2) with a pore size of 0.2µm, **Figure 34** shows that the permeate flux remains relatively stable during the first hours of treatment for both effluents. This follows the typical flux variation in the membrane distillation (MD) process (**Laganà et al., 2000**). The feed quality appears to have an influence on the flux behavior even for M2, since for MAF-WW, the flux started to decline gradually after almost 5 hours of treatment. Additionally, the permeate electrical conductivity showed an increase after the same duration from 20 to 27 µS/cm after 10 hours for MAF-WW (**Figure 35**). The observed electrical conductivity increase corresponds to the start of the membrane wetting phenomena, though the measured permeate TOC is lower than 2 mg/L (**Ge et al., 2014**).

The observed difference between the reference flux and the evolution of the permeate fluxes obtained by MAF-WW and MAF-UF-WW confirm that the flux decrease over time is linked to the formation of a fouling layer on the membrane surface.

The previous experiments showed that the DCMD treatment with M2 can lead to higher permeate quality and more stable flux values and variations. The initial flux values are lower in comparison to M1 but the sensitivity against fouling is smaller. Therefore, the following investigations were performed with M2 and MAF/UF permeates as a feed solution.

3.3.3 Parameters affecting the permeate flux

Since the DCMD process could be affected by multiple operating parameters such as the feed velocity and the temperature difference (**Schofield et al., 1990**). Therefore, the influence of these two parameters and the dairy effluent quality on the formation of the fouling layer, the permeate flux and quality was carried out. The thermal efficiency (η_{th}) calculation is based on the single Node simulation developed by **Winter** (**2015**). The thermal efficiency, which is the ratio of the latent heat to the total heat transferring through the membrane is calculated using the monitored mean temperature and permeate flux during the DCMD process. This parameter serves as an indicator of the undesirable heat transfer in the system (heat transferred by conduction).

3.3.3.1 Feed velocity

The thermal efficiency calculated after 5 hours treatment of MAF-WW and MAF-UF-WW at ΔT= 30°C and two different feed flow rates), showed that the treatment of MAF-UF-WW had led to higher thermal efficiencies at both studied velocities (η_{th} = 56% and 52%, at 0.08 m/s and 0.04 m/s respectively). The permeate fluxes reached also higher values of 14 kg/m^2.h and 10 kg/m^2.h at 0.08 m/s and 0.04 m/s, respectively after 5 hours DCMD treatment of MAF-UF-WW. In comparison, after 5 hours MAF-WW treatment, the thermal efficiency did not exceed 50% at 0.08 m/s and 0.04 m/s (η_{th} = 47% and 35%, respectively) and the obtained permeate fluxes were lower (12 kg/m^2.h and 6 kg/m^2.h, respectively) (**Figure 36**). In terms of permeate flux, applying higher feed flow rates, and consequently higher feed velocity, increases the heat transfer coefficient in the fluid boundary layer which declines the temperature polarization effect and consequently increases the permeate flux (**Gryta, 2012**).

The difference between MAF-WW and MAF-UF-WW treatment in terms thermal efficiency could be explained by the presence of higher organic matter concentration in MAF-WW. More precisely, the higher proteins concentration in MAF-WW contributes to the formation of the fouling layer since the beginning of the experiments (**Table 3**). The growth of the fouling layer thickness over time is directly linked to the presence of more proteins and organic matter in the MAF-WW feed stream (in comparison to MAF-UF-WW) that are known to deposit and adsorb on hydrophobic materials and consequently, form a higher resistance in front of the mass and heat transfer phenomena (**Bottino et al., 2000**; **Hausmann et al., 2013.a**).

Figure 36 shows also that the treatment of MAF-UF-WW had led to results that are close to the reference tests in terms of thermal efficiency and permeate flux. This confirms that an ultrafiltration pretreatment improves the feed quality in such a way that the DCMD efficiency is enhanced significantly.

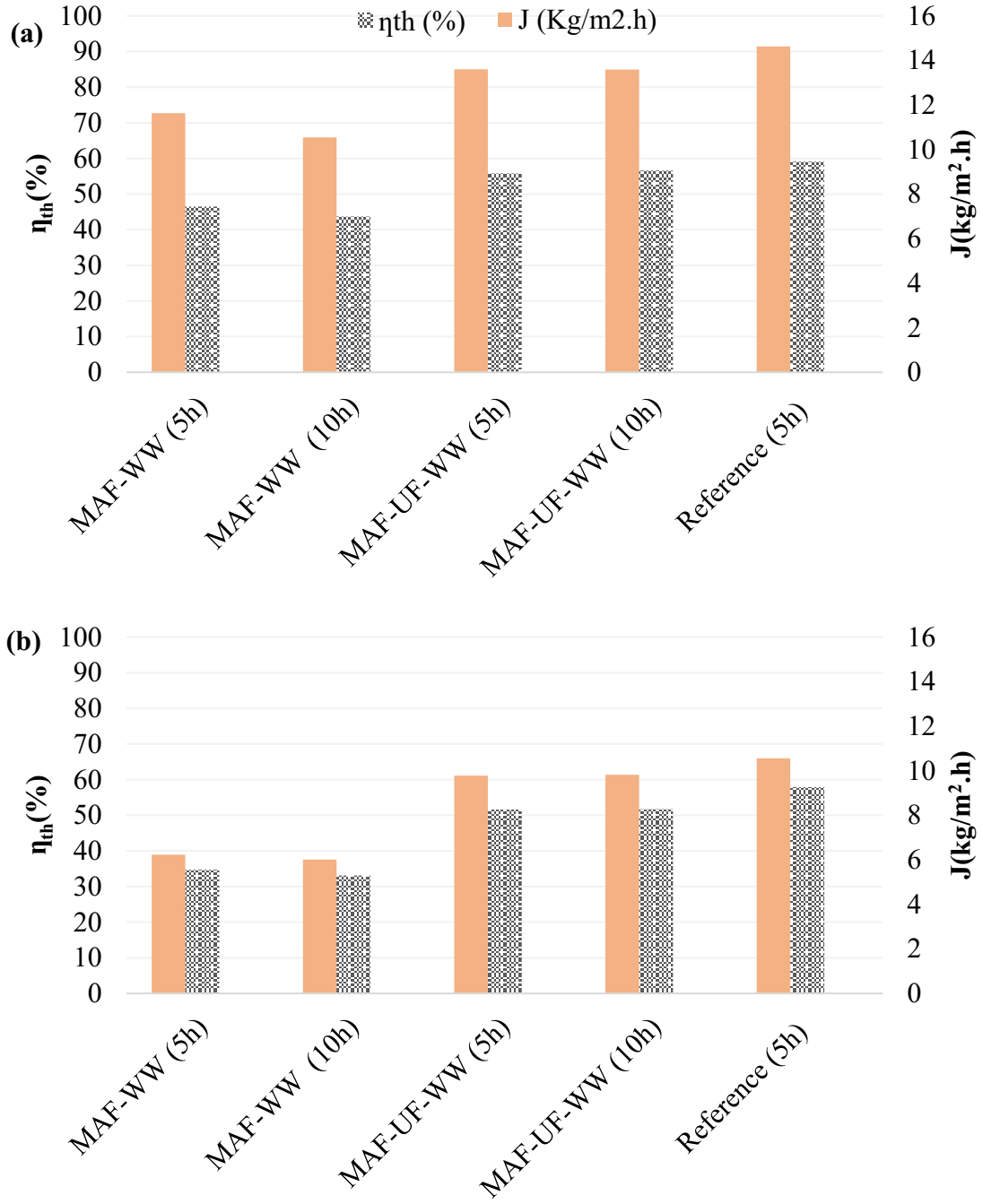

***Figure 36**: Thermal efficiency η_{th} and flux J of MAF-WW and MAF-UF-WW DCMD treatment in comparison to normal tap water test (Reference). Operating conditions: ΔT= 30°C and **(a)** V= 0.08 m/s and **(b)** V=0.04 m/s*

A comparison of the results illustrated by **Figure 36** shows that both the thermal efficiency and the permeate flux diminished after 10 hours treatment of MAF-WW slightly (flux reduction of 3.5% at V=0.04 m/s and 9.3% at V=0.08 m/s). In contrast to the UF-pretreated effluent which resulted in almost stable values of η_{th} and the flux.

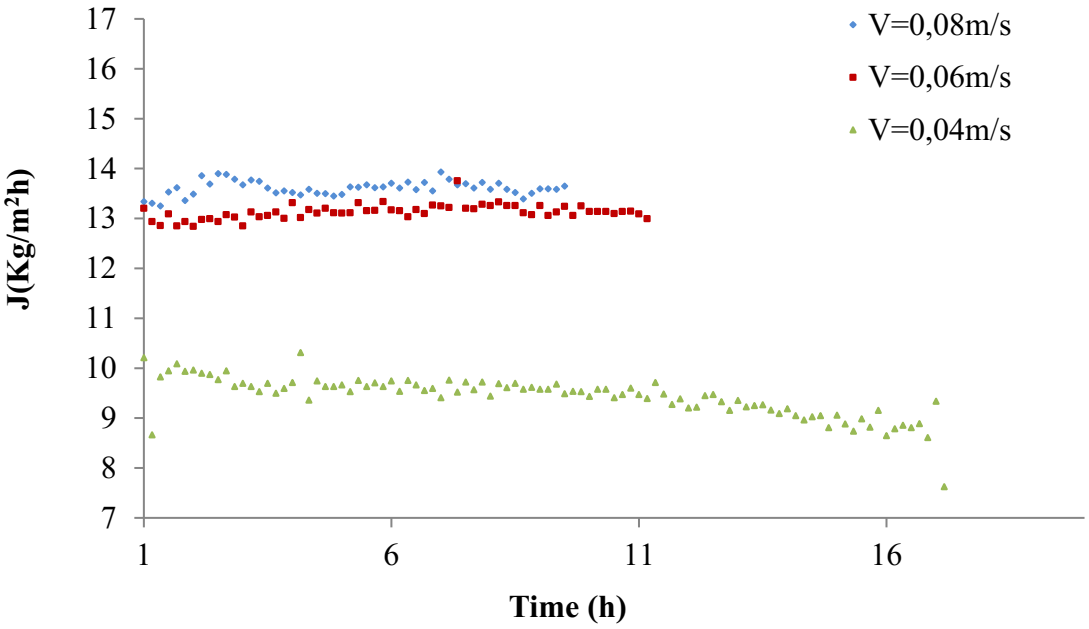

***Figure 37**: Flux behavior during operation time of DCMD treatment with MAF-UF-WW at ΔT=30°C and three velocities (0.08 m/s, 0.06 m/s and 0.04 m/s)*

A study of the permeate flux during MAF-UF-WW treatment at a constant temperature difference and multiple velocities (0.08 m/s, 0.06 m/s and 0.04 m/s) shows an interesting difference between the flux profiles at the two higher velocities and the lowest velocity (V=0.04 m/s) (**Figure 37**). At 0.08 and 0.06 m/s feed velocities, the flux kept stable in the range of 13 kg/m^{2}h. However, at a feed velocity of 0.04 m/s, the permeate flux did not exceed 10 kg/m^2.h and it started to decrease slightly after 10 hours to 9 kg/m^{2}h.

Following the different tests, the liquid entry pressure analyses of the used membranes showed also that at 0.08 m/s and 0.06 m/s the LEP had very close values (1.54 bar and 1.53 bar, respectively) in comparison to 0.87 bar at 0.04 m/s which indicates a stronger wetting under the latter operating conditions. In despite of the LEP drop at 0.04 m/s, the permeate conductivity at the end of the experiment was 68.2 µS/cm and the TOC <2 mg/L. At 0.08 m/s and 0.06 m/s, the electrical conductivity was 25 and 45.3 µS/cm, respectively. These results confirm that a relatively low feed flow rate and consequently low feed velocity declines the

shear stress that influences the fouling layer deposition. The fouling layer alters both the membrane and the permeate quality due to the wetting phenomenon.

3.3.3.2 Temperature difference

Researchers have found that when the permeate temperature is constant the flux increases monotonically with the increase of the bulk temperature difference. However, when the feed temperature is maintained constant and temperature difference is increased by decreasing the permeate stream temperature, as it is the case in this study, the flux tends to follow an asymptotic behavior at high ΔT (**Lawson and Lloyd 1996**; **Laganà et al. 2000**; **El-Bourawi et al. 2006**).

DCMD experiments with MAF-WW and MAF-UF-WW as feed solutions were carried at 0.08 m/s and at two temperature differences, ΔT=30°C and ΔT=15°C (**Figure 38**). ΔT was changed by keeping the feed stream temperature constant and varying the permeate stream temperature which changes also the mean temperature. After 5 hours treatment, a significant decrease in the permeate flux was observed for both experiments: MAF-WW (from 11.63 kg/m^2.h to 7.2 kg/m^2.h at ΔT=30°C and 15°C, respectively) and MAF-UF-WW (from 13.6 kg/m^2.h to 7.96 kg/m^2.h at ΔT=30°C and 15°C, respectively). This observation is in line with the general finding that permeate flux rises with increasing temperature difference. This increase is due to the growing driving force by the increase of vapor pressure difference that has an exponential effect on the permeate flux (**Schofield et al., 1987**).

Figure 38 depicts also the influence of the operating time on the flux evolution. It is interesting to note that for MAF-UF-WW, permeate flux reached almost stable values after 10 hours treatment at ΔT=30°C and ΔT=15°C. This could be due to the lower organic content in MAF-UF-WW which influences the fouling layer composition and deposition and contributes in the stability of water vapor diffusion over time. In the case of MAF-WW, a decline in the flux after 10 hours was observed that could be attributed to the buildup of the fouling layer. This decrease was more important at ΔT=30°C than at the lower temperature difference: from 11.63 kg/m^2.h to 10.55 kg/m^2.h at ΔT=30°C and from 7.2 kg/m^2.h to 6.84 kg/m^2.h at ΔT=15°C, respectively.

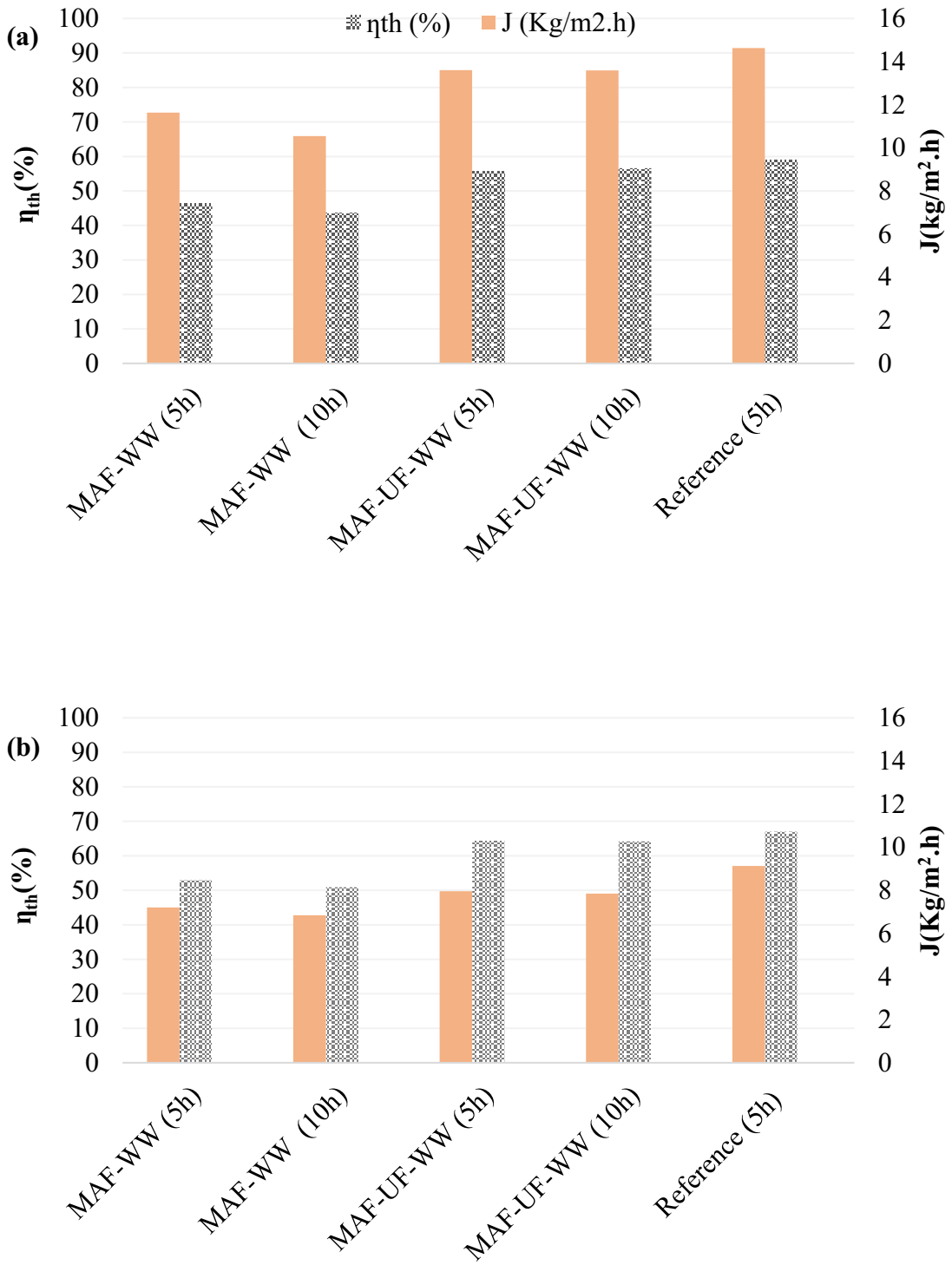

***Figure 38**: Thermal efficiency η_{th} and flux J of MAF-WW and MAF-UF-WW DCMD treatment in comparison to normal tap water test (Reference). Operating conditions: V=0.08 m/s and **(a)** ΔT= 30°C and **(b)** ΔT= 15°C*

The thermal efficiency (η_{th}), decreased by increasing ΔT as shown in **Figure 38.** This could be explained by a possible difference in the fouling layer thickness formed at the two studied

temperature differences. The presence of the fouling layer on the membrane surface adds to its thickness and forms an additional separation layer that increases the thermal resistance of the system (membrane/fouling layer) and thereby, decreases the thermal efficiency. This observation is supported by previous results which prove that the thermal efficiency gets higher when the membrane wall is thinner (**Gryta, 2012**). It is important to note that at both studied temperature differences the thermal efficiencies of MAF-UF-WW maintained more or less stable and were close to the ones calculated from the reference tests with tap water at the same operating conditions. Concerning MAF-WW, lower η_{th} values were recorded at both temperature differences in comparison to MAF-UF-WW and during operation time (after 10 hours) the thermal efficiency decreased by 6% at ΔT=30°C and by 3.8% at ΔT=15°C.

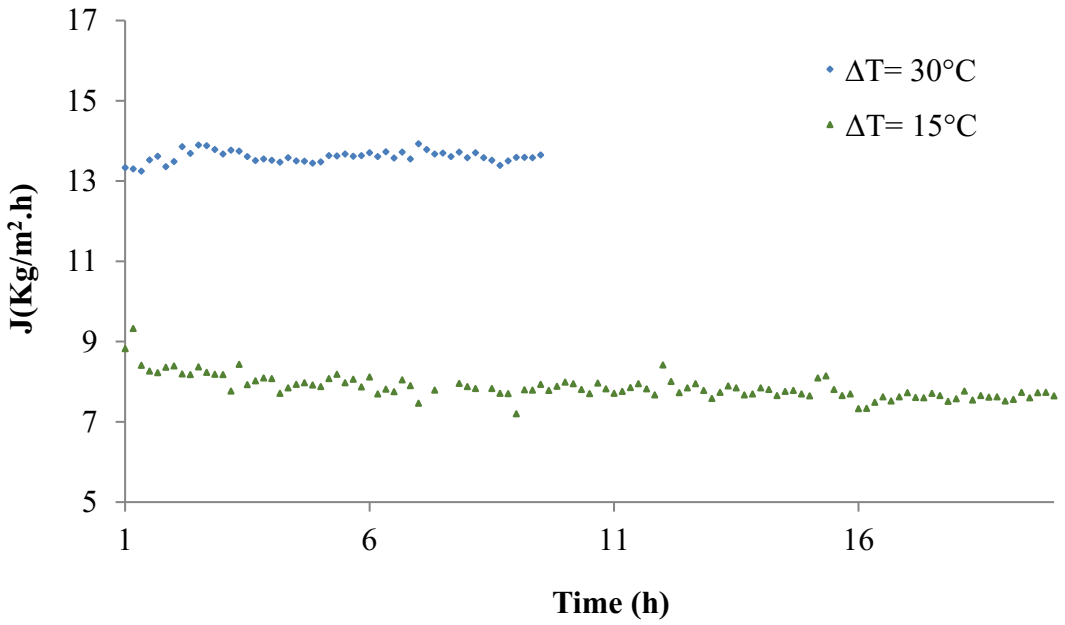

***Figure 39**: Flux behavior during operation time of DCMD treatment with MAF-UF-WW at V=0.08 m/s and two temperature differences (ΔT=30°C and 15°C)*

With respect to the influence of temperature difference variation on the permeate flux during MAF-UF-WW treatment, **Figure 39** illustrates the flux over operating time at two temperature differences. The flux is characterized by relatively stable behavior during operation time at both temperature differences (ΔT=30°C and 15°C).

The flux level difference observed in **Figure 39** could be induced by both the variation of ΔT and the way how this variation was conducted.

3.3.3.3 Process evaluation with Single-Node simulation model

In order to evaluate the saline effluents DCMD treatment, calculations with the single-node simulation model were carried to predict the process thermal efficiency and permeate flux in the steady-state conditions (**Figure 40**). The predicted flux thermal efficiency at V= 0.04 m/s (ΔT=30°C) was 17.92 kg/m^2.h and 65.8%, respectively, whereas at 0.08 m/s and at the same temperature difference the predicted flux increased to reach 23.72 kg/m^2.h with no change in the thermal efficiency. As expected, both predicted parameters had higher values in comparison to the ones obtained after MAF-WW and MAF-UF-WW permeates treatment at multiple velocities (0.08 m/s and 0.04 m/s) (ΔT=30°C). The lower thermal efficiency and permeate flux values could be attributed to the formation of fouling layers in both cases, with higher performance at the highest studied flow rate (0.08 m/s) which confirms our previous findings (**Gryta, 2012**).

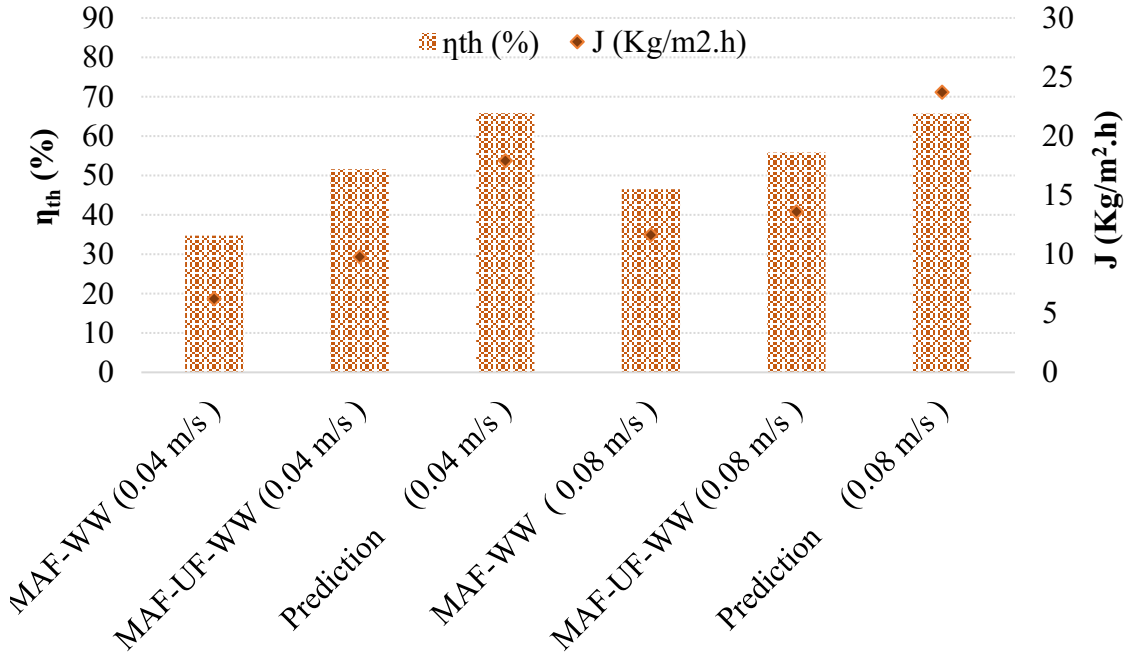

***Figure 40**: Permeate flux and thermal efficiency of treated effluents (MAF-WW and MAF-UF-WW) compared to theoretical prediction at V= 0.04 m/s and 0.08 m/s (ΔT=30°C).*

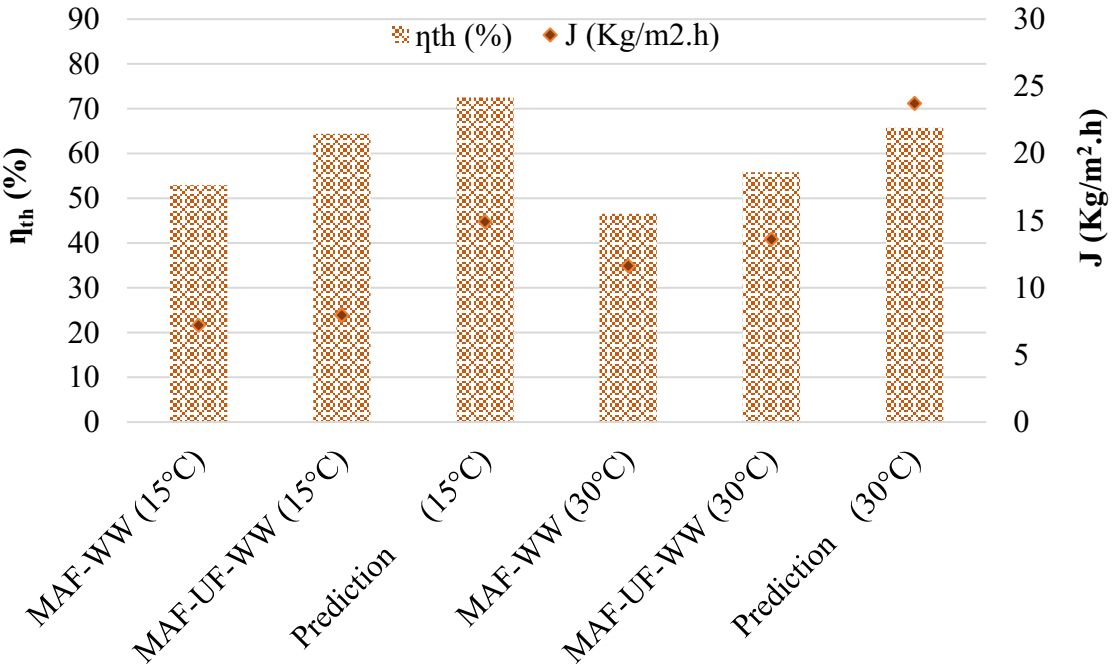

***Figure 41**: Permeate flux and thermal efficiency of treated effluents (MAF-WW and MAF-UF-WW) compared to theoretical prediction at ΔT=15°C and 30°C (V= 0.08 m/s).*

At the same flow rate (V= 0.08 m/s), the predicted permeate fluxes and thermal efficiencies at ΔT=15°C were as follows: 72.7% and 14.92 kg/m^2.h while the predicted values at ΔT=30°C were: 65.7% and 23.21 kg/m^2.h, respectively (**Figure 41**). These calculated values are, as well, higher than the ones calculated after MAF-WW and MAF-UF-WW treatments where permeates fluxes were lower by 51.7% and 46.7% at ΔT=15°C, respectively. Besides, at ΔT=30°C, the difference between the predicted permeate flux and the ones obtained by S2 and S3 was about 51% and 42.7%, respectively. The highlighted performance difference confirms the aforementioned influence of the feed quality on the DCMD performance and the significant affect that fouling has on this process.

3.3.4 Membrane fouling and wetting

3.3.4.1 SEM analysis

SEM pictures of the fouling layers of the tested PTFE membrane samples as well as the new membrane sample (Reference) are shown in **Figure 42.** The SEM pictures of the membrane samples showed that the fouling layer (observed after the same operation time and at the same operating conditions) had different aspects.

It can be seen that the membrane surface is increasingly covered by the fouling layer with increasing organic content of the treated feed solutions. The fouling layer formed after treating

R-WW is characterized by a relative uniformity and a more or less compact aspect that shows less membrane cracks formed after the drying process (in comparison to the other samples).

This observation indicates that the fouling layer in R-WW membrane sample could be denser due to the presence of higher organic content in the raw effluent. EDX analysis of the membrane sample (R-WW) at 10 kV showed the levels of chloride (Cl), sodium (Na) and potassium (K) which were around the following values: 13.06 %, 10.64 % and 1.58 %, respectively (**Table 10**).

The results obtained from **Figure 42** and **Table 10** are supported by the literature. In their study of PTFE membrane fouling during DCMD treatment of synthetic whey solutions, **Hausmann et al. (2013.a)** showed that during 6 hours, the formation of the fouling layer is mainly depending on the proteins' deposition on the membrane surface. This has a direct influence on the flux due the increased diffusion resistance. Since proteins tend to aggregate usually at a high concentration (present on the membrane surface), the formation of the fouling layer appears to involve proteins aggregation. This is on one hand via their interaction with the membrane material (PTFE) and on the other hand via the presence of salts that promote with their ionic strength the reduction of intermolecular repulsions to create the interaction between the proteins causing their aggregation (**De La Fuente et al., 2002**).

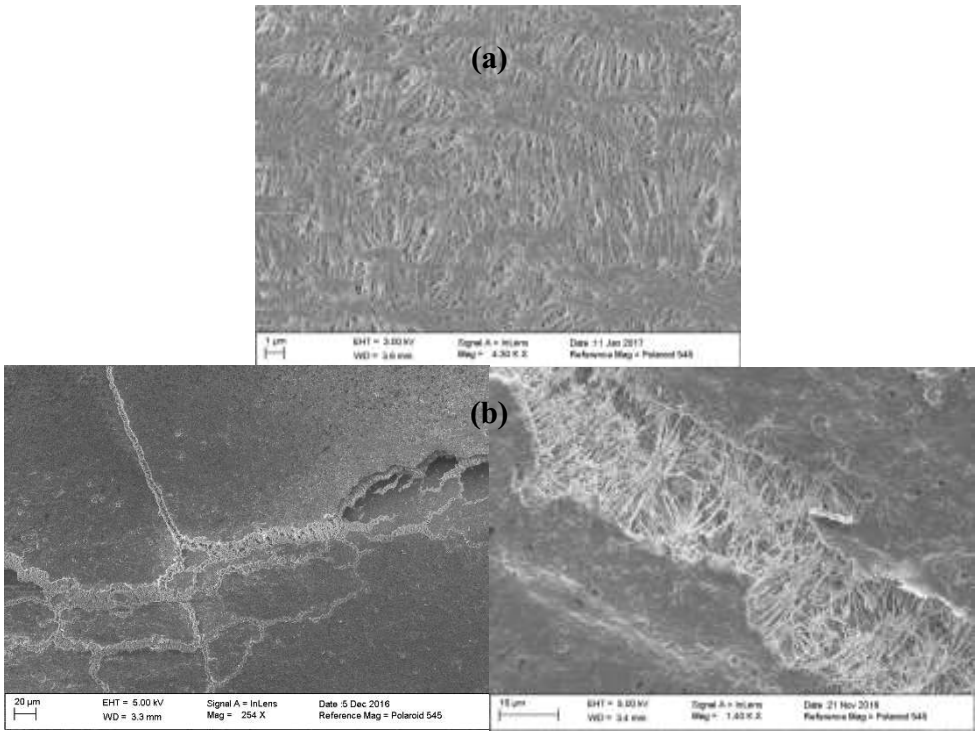

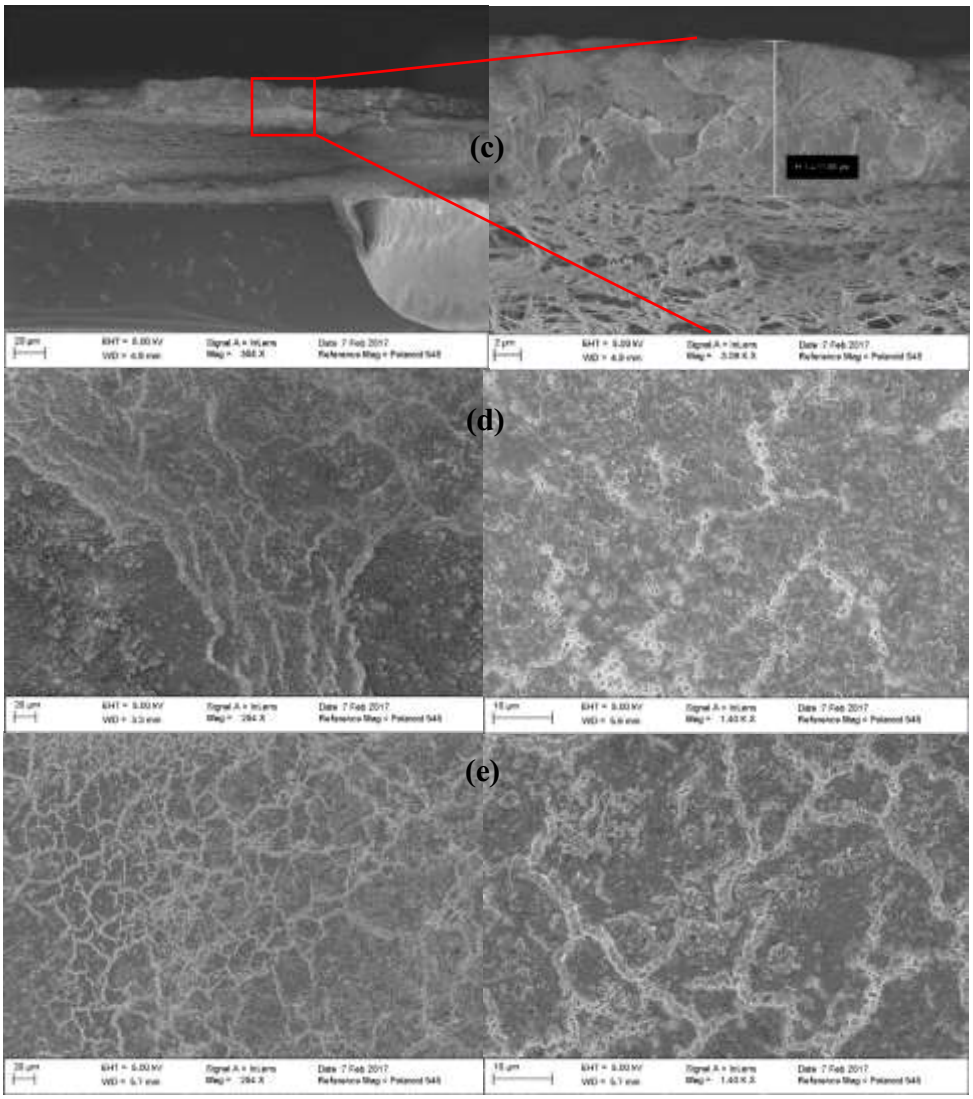

Figure 42: *SEM pictures of membrane samples: Reference (**a**) and fouling layers after 10h DCMD process of different feed solutions: raw effluent R-WW (**b**), cross section with R-WW (**c**), macrofiltration permeate MAF-WW (**d**) and macrofiltration-ultrafiltration permeate MAF-UF-WW (**e**). Operating conditions: ΔT= 30°C and V= 0.8 m/s, during 10 hours treatment*

A close observation of the SEM pictures of both membrane samples MAF-WW and MAF-UF-WW (**Figure 42)** shows that at the same operating conditions and time, the formed layers are uneven and that their density is less when the feed is pretreated by macrofiltration (MAF-WW) and even less after an ultrafiltration step (MAF-UF-WW). The reduced density is shown by the increasing visibility of the membrane surface through the fouling layer which is confirmed by the presence of fluorine (F), since F is one of the most important components of the PTFE membrane material (**Table 10**). This observation could be related to the removal of any traces of lipids by UF. Such lipids interact by adsorption with whey proteins to form a film that is adsorbed on the hydrophobic membrane surface since the early stages of the DCMD process

and grows thicker and more stable with time and this result is consistent with previous observations (**Waninge et al., 2005**).

The observed low fouling layer density in S3 confirms the higher flux values that we obtained by DCMD and this shows that the fouling layer is playing an important role in the decrease of mass transfer resistance through the membrane.

Table 10 shows that the ultrafiltration step that removed all traces of whey proteins and other whey components larger than 100 kDa had led to a less dense fouling layer (**Figure 42**). This layer is mainly characterized by the presence of the highest content of calcium (Ca) and phosphorus (P) and the lowest of sodium (Na) and chloride (Cl) among the samples analyzed by EDX. This result is consistent with a previous work (**Hausmann and al., 2013.a**) with DCMD process of synthetic whey solution in which it was found that those ions were dominant in the fouling layer. However, in our study this finding is not applicable in the case of R-WW and MAF-WW, where the predominant ions present in the fouling layers were sodium and chloride. This result could be linked back to the presence of micellar casein in both R-WW and MAF-WW (which is only removed by a 0.2 µm pore size filtration). It was showed in previous researches that the existence of micellar casein in solution with whey proteins and salts (NaCl) could affect the proteins aggregation process through the enhancement of the attractive forces between proteins in high ionic strength solutions (**Kehoe and Foegeding, 2011; Mounsey and O'Kennedy, 2009; Pierre et al., 1992**).

Table 10: *Chemical elements mass percentage by EDX analysis at 10Kv of multiple membrane samples: without any treatment (Reference) and with 10 hours DCMD treatment of R-WW, MAF-WW and MAF-UF-WW at the following operating conditions: ΔT= 30°C and V= 0.08 m/s*

Mass percentage (%)	C	N	F	Na	P	Cl	K	Ca
Reference	10.64	-	20.54	-	-	-	-	-
R-WW 10kV	23.21	2.44	-	10.64	-	13.06	1.58	3.61
MAF-WW 10kv	42.43	3.31	3,38	3.07	-	6.20	-	2.47
MAF-UF-WW 10kv	10.51	-	4.36	1.31	13,33	1.09	-	12.76

According to **Rice et al. (2009)**, calcium and phosphorus salts solubility is highly influenced by the solution acidity (through an inversely proportional relationship) and it decreases at high temperature values. Therefore, since the treated feed solutions had a neutral pH (pH=7), the presence of both calcium and phosphorus salt in the fouling layer will contribute both to the organic fouling and the mineral scaling. This could explain the strong presence of those salts in the fouling layer treating the MAF-UF-WW. Nevertheless, the effluent acidity could affect the mineral scaling. It has an insignificant influence on the final flux and on the membrane wetting (**Kezia et al., 2015**).

3.3.4.2 Liquid entry pressure and membrane resistance

Liquid entry pressure tests have shown that the pre-treatment of the salty wastewater by MAF-UF improved significantly the membrane quality in comparison to the raw and the MAF pretreated effluent (**Figure 43**). However, since the LEP indicates directly the degree of membrane wettability, it is important to note that the measured LEP of a new membrane is more than the double of that achieved by MAF-UF pre-treatment (3.88 bar and 1.54 bar, respectively).

The effluent organic load and the composition have a great influence on the pores' wettability. Since the raw saline whey effluent is mainly composed of whey proteins, minerals and sugars, all these components contribute in the fouling layer formation which alters the membrane resistance, especially with the presence of casein micelles and fat traces (**Hausmann et al., 2013.b**).

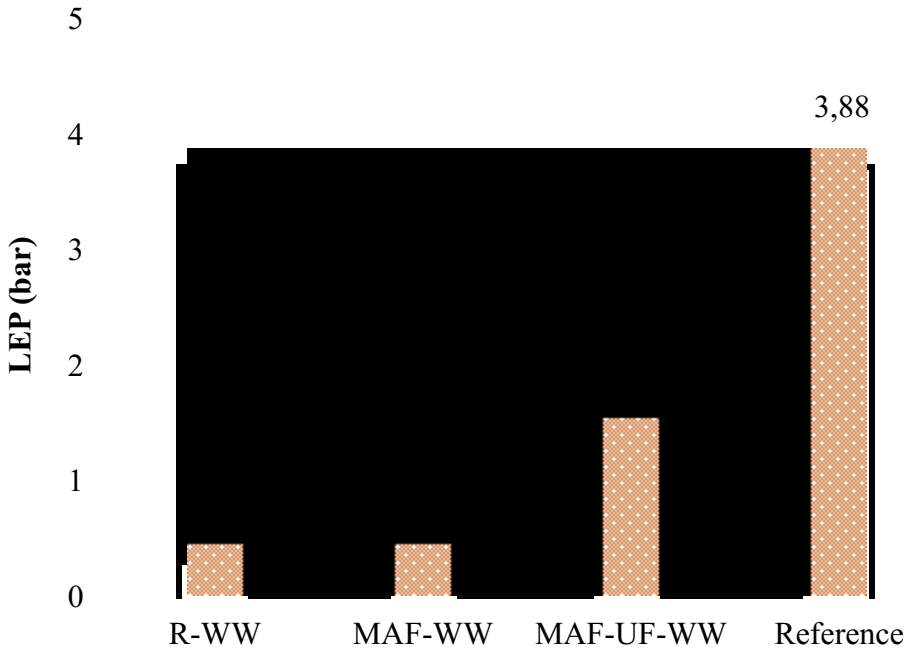

***Figure 43**: Liquid entry pressure (LEP) of membrane samples after 10h DCMD process of different feed solutions: R-WW, MAF-WW and MAF-UF-WW. Operating conditions: ΔT= 30°C and V= 0.08 m/s*

Kezia et al. (2015), found that the presence of a protein concentration superior to 2 g/L in the salty whey effluent could have an influence on the membrane hydrophobicity along with the presence of minerals which enhances the pores wetting. Besides, they found that for 0.2 µm PTFE membrane and for an effluent pretreated by MAF-UF, the LEP values decreased by almost the same rate as those in this study.

The change of the operating conditions (feed velocity and temperature difference) for R-WW and MAF-UF-WW had an influence on the membrane's LEP. At a feed velocity of 0.04 m/s, the LEP dropped to 0.24 bar and to 0.28 bar for R-WW and MAF-WW, respectively, which indicates a lower membrane hydrophobicity in comparison to a velocity of 0.08 m/s. Similar LEP reduction was observed for MAF-UF-WW (section **3.3.3.1**). These results show that low feed velocity induces changes in the fouling layer and reduces the membrane hydrophobicity. However, when decreasing the temperature difference to 15°C an increase in the LEP values was observed (0.55 bar and 0.58 bar for R-WW and MAF-WW, respectively). This could be linked to the influence of the temperature on the interactions between proteins with the hydrophobic membrane via the salts' presence (**De La Fuente et al., 2002**).

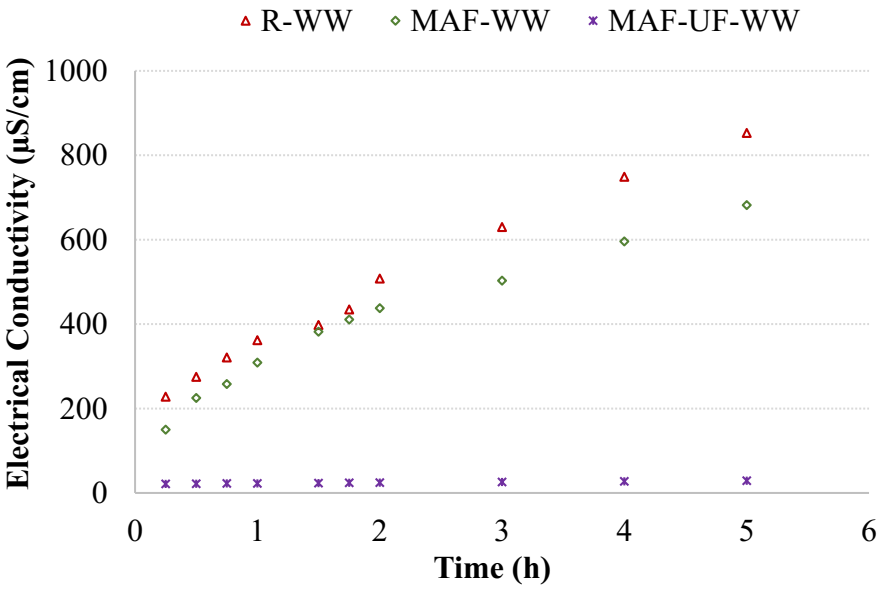

***Figure 44**: Electrical conductivity (µS/cm) at p=0.3 bar during DCMD process of different feed solutions: R-WW, MAF-WW and MAF-UF-WW. Operating conditions: ΔT= 30°C and V= 0.08 m/s*

In order to investigate the influence of the feed pressure on the membrane resistance and wetting, DCMD experiments at $\Delta p = (p_{evaporator} - p_{condensor}) = 0.3$ bar were conducted during 5 hours with the three different salty dairy effluents (**Figure 44**). By monitoring the electrical conductivity during the experiments, it could be confirmed that the raised feed pressure which was close to the LEP of R-WW and MAF-WW, the permeate conductivity increased until it reached after 5 hours 853 µS/cm and 682 µS/cm, respectively. This result confirms that at a pressure close to the LEP, the liquid breaks through the pores to the permeate side. As expected, the rise in the feed pressure didn't influence the permeate quality in the case of MAF-UF-WW where the conductivity didn't exceed 29 µS/cm.

3.3.4.3 Contact angle and membrane cleaning effect

Another parameter that reveals the membrane hydrophobicity in DCMD is the contact angle which is inverse to the wettability. It is known that for membranes with hydrophobic character the contact angle formed by a water drop on the membrane surface has to be higher than 90° (**Zisman, 1964**). The results illustrated in **Figure 45** confirm the previous findings and show that by pretreating the raw salty dairy effluent first by MAF-UF, higher membrane

hydrophobicity can be achieved. As shown above, this influences directly the permeate quality and its stability over operating time. It is important to mention that the contact angle decreases at higher temperatures since the PTFE membrane evolves with temperature variation and the mean pore size get larger with increasing the temperature (**Saffarini et al., 2013**; **Ge et al., 2014**).

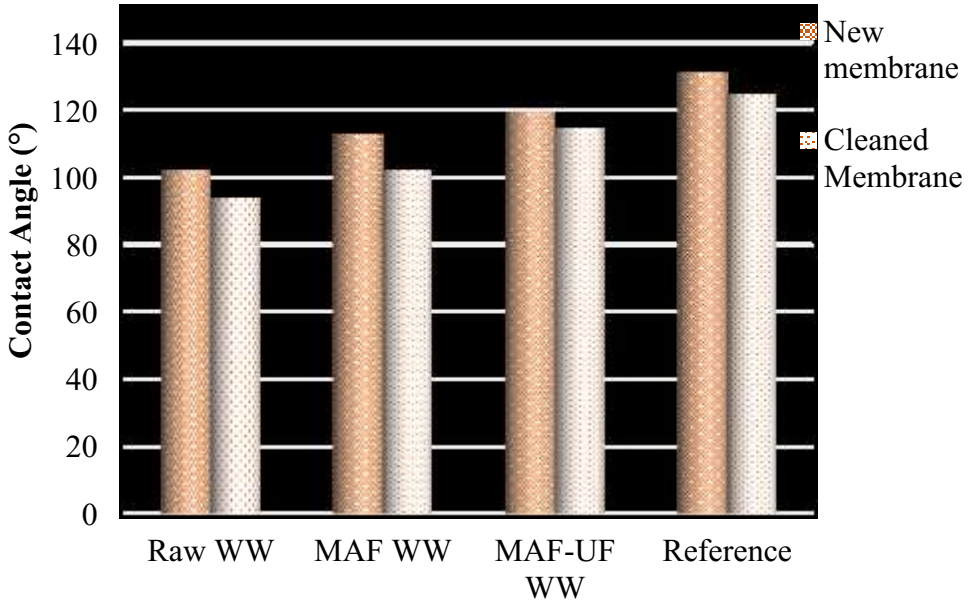

***Figure 45**: Contact angle of new and cleaned membrane samples with different feed solutions: R-WW, MAF-WW, MAF-UF-WW at T= 22°C. Operating conditions: ΔT= 30°C and V= 0.08 m/s*

By cleaning the membrane with basic and acid solutions the membrane loses part of its hydrophobicity measured by a lower contact angle in all the experiments (**Figure 45**). This could be explained by the effect of acidic solution during the removal of the fouling layer which induced the irreversible wetting of a fraction of the membrane pores (**Gryta, 2008**).

The lowest hydrophobicity loss was measured in MAF-UF-WW where the contact angle decreased by 3.9% in comparison to R-WW and MAF-WW where the reduction was of 8.1% and 9.5%, respectively.

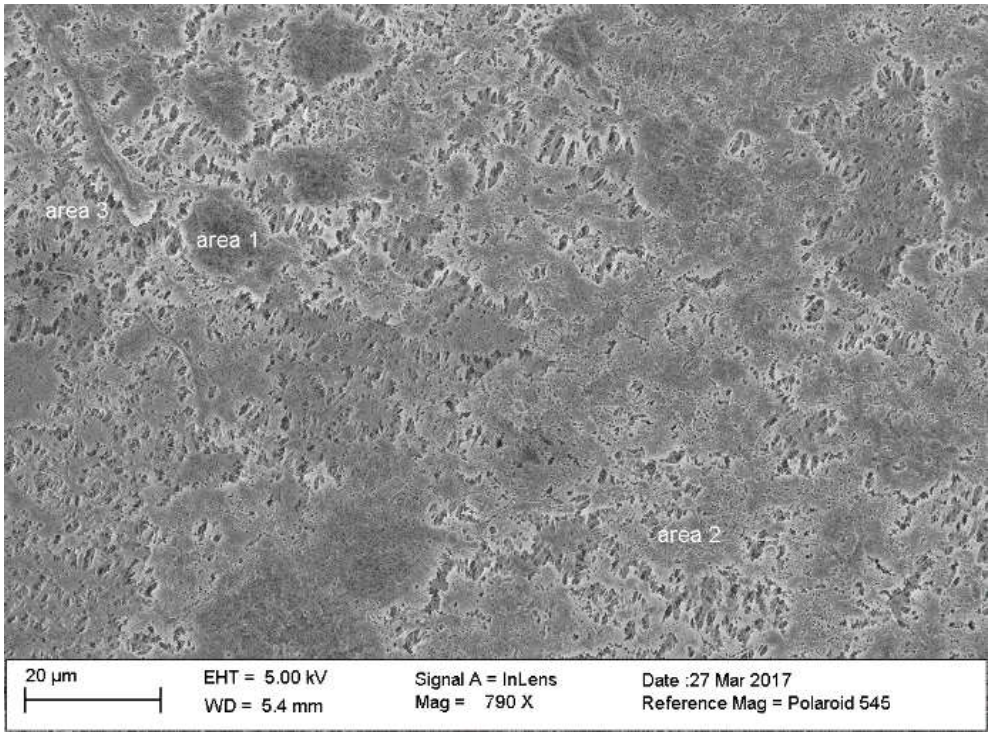

***Figure 46**: SEM picture of a cleaned membrane sample (following the DCMD process of MAF-UF-WW). Operating conditions: ΔT= 30°C and V= 0.08 m/s*

SEM picture of the cleaned membrane sample shows that the membrane is still covered partly by the fouling layer (**Figure 46**). In order to identify the general composition of the different observed zones, an EDX analysis was performed on three different areas of the membrane at 20 kV.

***Table 11**: Chemical elements' mass percentage obtained by EDX analysis at 20kV (the marked areas in **Figure 46**). ND: Not Detectable*

Mass percentage (%)	C	N	F	Na	Ca
Area1 20kV	28,95	3,63	46,66	0,56	0,76
Area2 20kV	20,05	ND	60,56	ND	ND
Area3 20kV	18,35	ND	55,72	ND	0,50

The main chemical elements found in the darkest shaded area 1 on the membrane surface were nitrogen (N) 3.63%, sodium (Na) 0.56% and calcium (Ca) 0.76% which shows that some remaining parts of the fouling layer containing proteins and salts are still deposited and adhered to the membrane which could contribute in the recorded hydrophobicity decrease (**Table 11**). Concerning the other analyzed areas only membrane material, mainly fluorine (F), was found in addition to small mass percentage of calcium (0.5%).

3.3.5 Experimental performance and cost-effectiveness analysis

3.3.5.1 Analytical model

In this section, we study the cost-effectiveness of the DCMD process with respect to the two pretreatment options, namely the MAF and the UF-MAF processes. Based on the results reached in the foregoing sections, we analyze the performance of the DCMD process not only from the perspective of water quality, but also based on the various investments needed to conduct the process. To this end, we represent the DCMD process using a set of inputs and outputs for which the cost and the benefit are assessed using the indicators introduced in **Table 5**. From the practical point of view, this allows an industry to design a cost-effective DCMD process based on a convenient choice of the options available for the pretreatment process. The cost and the benefit of the pretreatment process depend of the following indicators:

- The cost is impacted by the energy consumption, void volume, LEP and time (indicators *I4-I12*). The energy consumption and time correspond to direct costs that are relatively easy to evaluate. Nonetheless, the void volume and LEP affect the lifetime of the membranes. Hence, the budget spent to acquire the membranes varies accordingly;

- The benefit varies according to the rejection factors and the permeate flux (indicators *I1-I3*). These indicators are considered as the benefit variables because they affect the volume of water collected posteriori, which is the main objective of the membrane filtration process.

Since the respective expressions of the cost and benefit functions with regard to the underlying indictors are not straightforward, we use the utility theory (**Cohon, 1978**) to evaluate the two pretreatment scenarios with respect to the options (experimental setup) considered in the treatment phase. Utility theory has been applied in different fields for decision-making purposes through the analyses of an individual's preference-indifference relation (**Kaplinski, 2013**).

In the sequel, we define the demand function *x* as a mapping between a cost value, denoted by *c*, and the indicators defined in **Table 5**. In other terms, for a cost value *c*, the output of the demand function is represented as follows:

$$x(c) = \{I_1^c, I_2^c, \dots, I_{12}^c\}$$

In order to apply utility theory to our context, we define the utility function, denoted by $u(x, c)$, as the projection of x on the subspace corresponding to the indicators that affect the benefit. Hence, the expression of $u(x)$ is defined below.

$$u(x, c) = \{I_1^c, I_2^c, I_3^c\}$$

We use this function in order to express the indifference between the alternatives to implement the MAF and UF-MAF processes. It is noteworthy that, in our experiments, we only consider the indicators $\{I_3, I_8\}$. This choice is motivated by the fact that these indicators strongly affect the cost of the process and the unavailability of data regarding the evolution of other indicators (e.g., I_7 and I_9).

We use the Slutsky equation to model the substitution relationship between the MAF and the UF-MAF pretreatment processes**.** For a demand *x*, the Slutsky equation is expressed as:

$$\left(\frac{\Delta x}{\Delta c}\right)_{\text{MAF}} = \left(\frac{\Delta x}{\Delta c}\right)_{\text{UF-MAF}} - x \times \frac{\Delta x}{\Delta b_i}$$

where b_i stands for one of the benefit indicators (i.e., $\{I_1^c, I_2^c, I_3^c\}$) , $\left(\frac{\Delta x}{\Delta c}\right)_{\text{UF-MAF}}$ denotes the substitution effect (which must be negative as long as the indifference curve between MAF and UF-MAF exhibits a diminishing marginal rate of substitution) and $(-x_1 \times \frac{\Delta x}{\Delta b})$ denotes the compensating effect.

The indifference corresponds to a situation in which the demand functions of the MAF and the UF-MAF processes satisfy the following condition:

$$c_1 x_{\text{MAF}}(c_1) + c_2 x_{\text{UF-MAF}}(c_2) - b_{\text{MAF}} - b_{\text{UF-MAF}} = 0$$

where $b_{\text{MAF}} = u(x_{\text{MAF}}, c_1)$ and $b_{\text{UF-MAF}} = u(x_{\text{UF-MAF}}, c_2)$

Since the time dimension is important in the DCMD process, we express the utility function as $u(x, c, t)$, where *x* expresses the demand function, *c* expresses the corresponding cost, and *t* expresses the time to conduct the process satisfying the demand *x*. Under these assumptions, the indirect utility function, denoted by $V(c_1, c_2, t_1, t_2)$ is given by:

$$V(c_1, c_2, t_1, t_2) = \max\{u(x_{\mathrm{MAF}}, c_1, t_1), u(x_{\mathrm{UF-MAF}}, c_2, t_2)\}$$

We also define the parameters *z* and *l* such as that:

$$z + c_1 x_{\mathrm{MAF}} = x_{\mathrm{UF-MAF}} \quad and \quad l + c_2 t_1 = t_2$$

The utility function is assumed to be differentiable and quasi-concave in x, and the constraints are differentiable and linear in x and in both budget, cost and time (**Cohon, 1978**).

The Lagrangian function of *V* is represented by:

$$V(c_1, c_2, t_1, t_2)\max\{u(x_{\mathrm{MAF}}, c_1, t_1), u(x_{\mathrm{UF-MAF}}, c_2, t_2)\} + \lambda(x_{\mathrm{UF-MAF}} - z - c_1 x_{\mathrm{MAF}}) + \mu(t_2 - l - t_1 c_2)$$

The Lagrange multipliers λ and μ represent the shadow values of cost/budget and time, respectively. Intuitively, λ is the marginal utility of benefit (i.e., optimization of the indicators) and μ is the marginal utility of time.

Through the application of the envelope theorem (**Cohon, 1978**), we define the Value of Time (VoT) as the marginal substitution rate for utility between the cost parameter *c* and the duration time *t*. The value of time can be expressed as:

$$VoT = \frac{-dc}{dt}\Big|_{V=const} = \frac{\mu}{\lambda}.$$

Therefore, it follows from the previous equation that VoT as a resource can be expressed in terms of observable demand *x* as:

$$VoT = \frac{dV/dt_2}{dV/dy} = \frac{dx_{\mathrm{MAF}}/dt_1 + x\, dx_{\mathrm{UF-MAF}}/dt_2}{dx_{\mathrm{MAF}}/dc + x\, dx_{\mathrm{UF-MAF}}/dy}.$$

This equation establishes a link between the marginal rate of substitution of the demand functions (relative to the MAF and UF-MAF pretreatment processes) in terms of time and cost/budget, respectively.

In the following section, we illustrate our analytical model through the analysis of a set of experimental results. Through the indifference curves, we show how a relation can be found between the cost/benefit/time triple for specific executions of the MAF and the UF-MAF processes. In concrete industrial situations, this relation is useful as a decision-support mechanism based on the comparison of the costs needed for each of the pretreatment techniques to achieve the same time performance or, in general, the same benefit.

3.3.5.1 Cost-effectiveness analysis

As it has been stated in the previous subsection, the comparison criterion used in this simulation is the DCMD operation time. In other terms, we generate (from the experimental data sets) the indifference curves allowing the assessment of the amount of time that is gained/lost if one pretreatment technology is utilized rather than the other, for the same output parameter. To this end, we apply the mathematical model detailed previously to estimate the overhead in terms of time for a fixed value of one of the two output parameters (permeate flux and membrane void ratio). Our experiments encompass six scenarios (three scenarios for MAF and three scenarios for UF-MAF) as illustrated in the following table (**Table 12**).

***Table 12**: Experimental scenarios.*

Scenario	Pretreatment	Q (L/h)	ΔT (°C)
1	MAF	100	15
2	MAF	100	30
3	MAF	50	30
4	UF-MAF	100	15
5	UF-MAF	100	30
6	UF-MAF	50	30

To illustrate the potential brought by the utility theory, and more precisely indifference curves, to evaluate the two pretreatment scenarios in terms of cost-effectiveness, we first consider the evolution of the flux with respect to time as a parameter to discuss an illustrative case study of the approach. **Figure 47** illustrates the evolution of the flux with respect to time for each of the scenarios specified in **Table 12**.

It is worthy to underline that the termination criterion corresponds to a mass of 2 kg of the concentrated feed tank. From this figure, it can be deduced that, as a DCMD pretreatment, the UF-MAF technique outperforms the MAF technique in terms of amount of collected water per unit of time and DCMD membrane surface.

A comparison of the performances of the two pretreatment techniques in the same experimental conditions is performed by associating each scenario in which MAF is used to its homologous in which UF- MAF is used.

To this purpose, and using **Table 12**, the scenarios are grouped into three couples (1,4), (2,5), and (3,6). From **Figure 47**, it comes that the average improvement reached by UF- MAF with regard to MAF in terms of permeate flux is 20%.

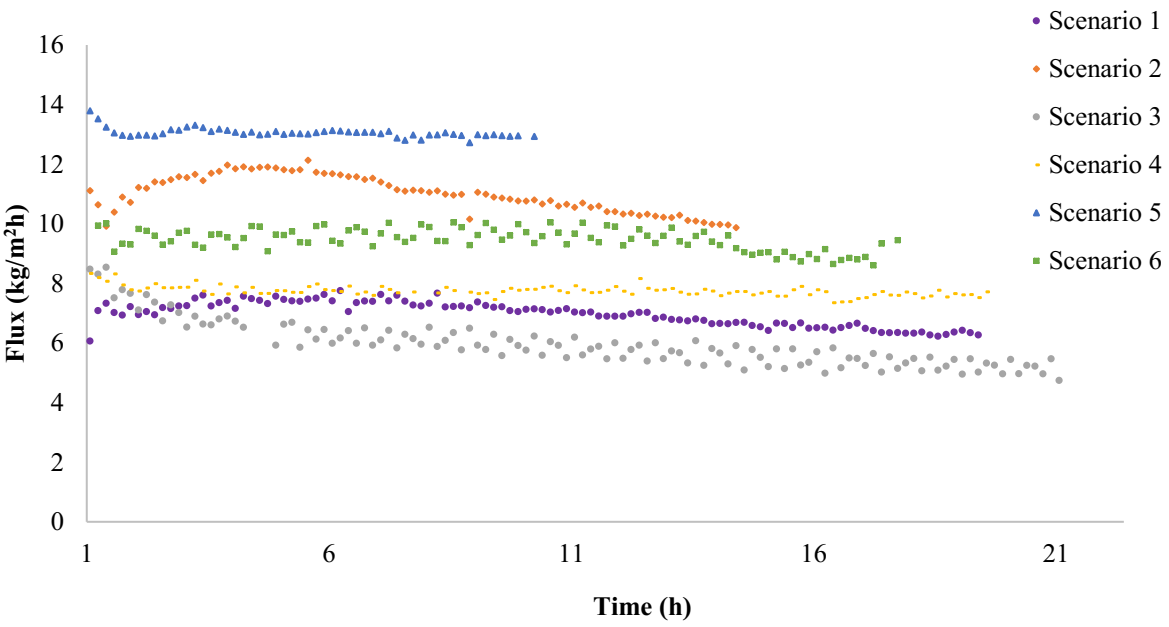

Figure 47: *Flux evolution during time for the 6 studied scenarios.*

Such statement provides a view on the performances of the MAF and UF-MAF pretreatment techniques of the DCMD process from the experimental perspective but it obfuscates the issues related to the overhead that would affect the use of these techniques in concrete industrial environments. For instance, an important parameter that would be interesting to investigate using the results depicted in **Figure 47** is the time overhead, which is the additional amount of time spent for one technique to reach the same performance using the other technique. This parameter is important from the practical point of view since most of the components of the Operational Expenditure (OpEx) are connected to time, such as energy and manpower.

To cope with this issue, we apply the utility theory formalism described above to the functions representing the evolution of flux with respect to time for each of the six scenarios of **Table 12**. Three main steps are followed:

1. Draw the indifference curve in which the two axes represent the DCMD permeate flux obtained following MAF and UF pretreatment techniques, respectively. Such curve is used to model the hypothetic situation in which a user would have access to both pretreatment techniques and expresses his preference (in terms of permeate flux for this case) between them.
2. The equation of the indifference curve elaborated in Step 1 is used to find a mapping between specific values of flux reached through the MAF technique and their

corresponding values reached through the UF-MAF technique and leading to the same preference.

3. We identify, using the Splines interpolation technique applied to the values of **Figure 47**, the amount of time corresponding to the values of flux identified in Step 2.

Throughout this process, it is possible to model the evolution of time with respect to the flux (the dual behavior of **Figure 47**) by considering some values of flux that were not reached experimentally but reconstructed using the indifference curves used in Steps 1 and 2. In the following, we illustrate the execution of this process in the case where the flux is used to draw the indifference. Then, we extend this reasoning to the case where the void percentage is used to this purpose. Obviously, the process is generic enough to encompass all the indicators considered in **Table 12**. However, more experiments must be performed to address the rest of the indicators.

Based on the values expressing the evolution of the flux with respect to time (**Figure 47**), we obtain the indifference curve represented in **Figure 48** where the two axes represent the DCMD permeate flux expressed in ($kg/m^2.h$) following the UF-MAF (X axis) and MAF (Y axis) application. In other terms, this figure illustrates the relationship between the performances, in terms of permeate flux, of the two pretreatment scenarios. It is obtained through the following process:

a. The average permeate flux is computed with respect to time for each of the six scenarios considered above.
b. The averages obtained in step (a) are mapped so as to plot 3 points (plotted in red in **Figure 48**) so as to represent the equivalence (in terms of percentage of flux allocated to each technique) of the pretreatment techniques in terms of flux. From the experimental point of view, this mapping is performed by associating the couple of flux values that result in the least variation of the sum of fluxes. This extends the analogy between baskets (customarily used in utility theory) and our context.
c. The plots are interpolated for the values identifying the aforementioned scenarios using the cubic Spline interpolation to draw a hyperbola which represents the indifference curve. This curve is constituted by the set of points for which we suppose that the performance of the DCMD process for which a user would be indifferent in terms of permeate flux.

The indifference curve plotted in **Figure 48** has the following hyperbolic equation:

$$-1.29\,x^2 + 23.63\,xy + 4.64\,y^2 - 102.05\,x - 247.28\,y = -1022.57$$

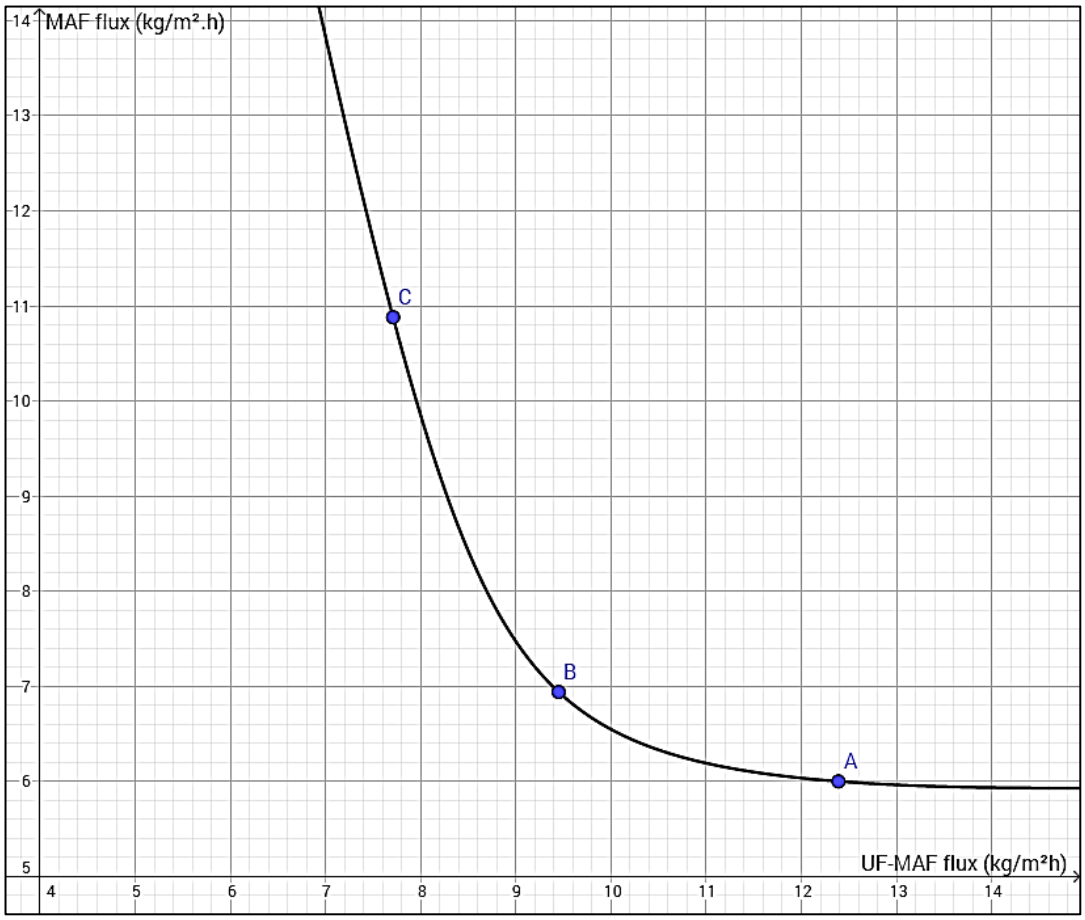

Figure 48: *Indifference curve between the MAF and UF-MAF pretreatment technologies in terms of DCMD permeate flux.*

The plotted indifference curve allows the calculation of the global improvement, in terms of permeate flux, which can be reached through the use of the UF-MAF technique as a DCMD pretreatment. This is, by definition, the average of the different local improvements computed through the mapping between unitary decrease in the MAF axis and the corresponding increase in the UF axis in terms of permeate flux (**Figure 49**).

According to **Figure 49,** we can conclude that the average global improvement (taking both positive and negative performances of UF-MAF with respect to MAF into consideration) is 1.5%. In terms of neat improvement (taking only the positive performances into consideration), the permeate flux improvement ratio that we can obtain by UF-MAF pretreatment have a minimum of 25% and a maximum of 71%.

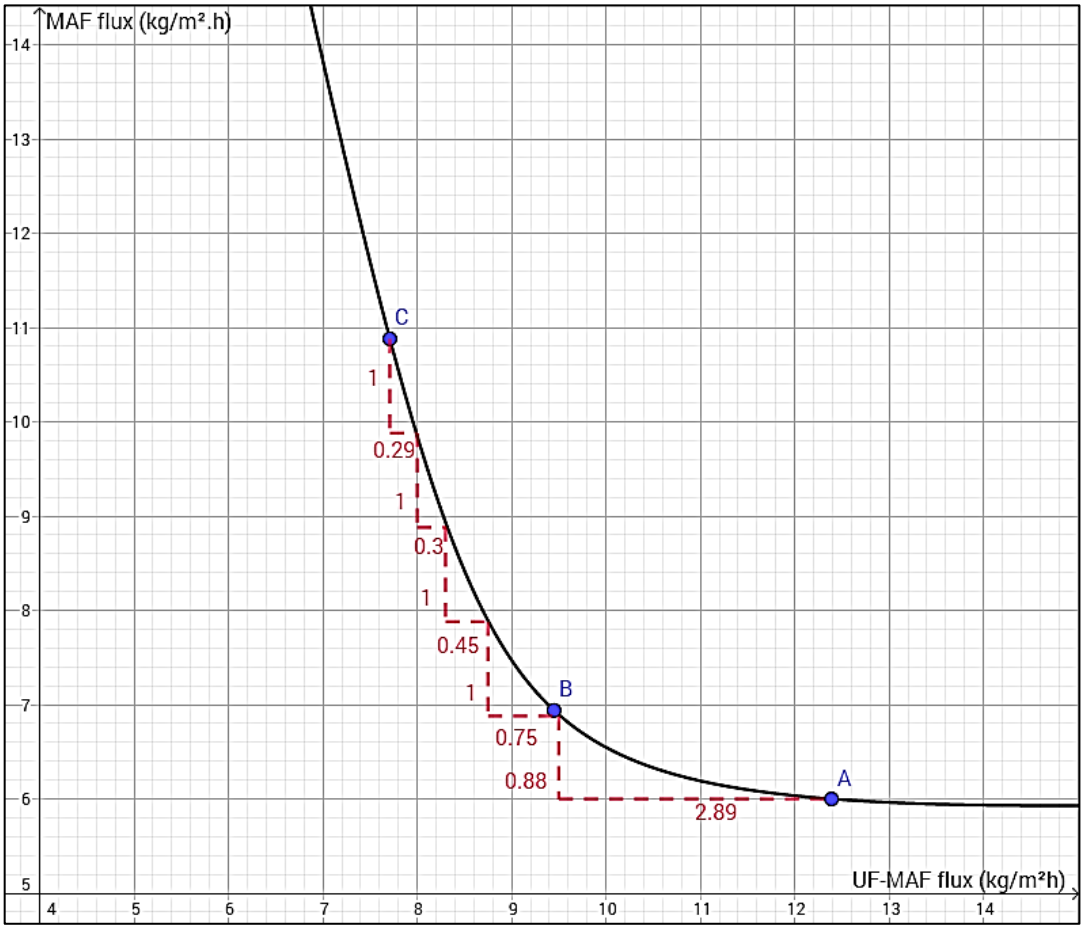

Figure 49*: Indifference curve between the MAF and UF-MAF pretreatment technologies in terms of DCMD permeate flux and the improvement provided by UF-MAF.*

Hence, we reach the practical use of this indifference curve which consists in mapping every point in **Figure 47** for scenarios 1, 2, and 3 to the corresponding point as if it was obtained from scenarios 4, 5, and 6; respectively (this is to preserve the same experimental condition in this mapping). This is achieved using the hyperbolic equation of **Figure 48**. Through this mapping, we reconstruct the values of time corresponding to the flux values that were not experimentally reached in scenarios 4, 5, and 6.

Using the results of **Figure 47**, we interpolate the evolution of time with respect to one of the six scenarios of **Table 12**.

Figure 50 shows the result of such interpolation in the case where the values of Scenario 1 are considered. For example, it underlined that it is possible to estimate the time corresponding to a flux equal to 7 kg/m^2.h.

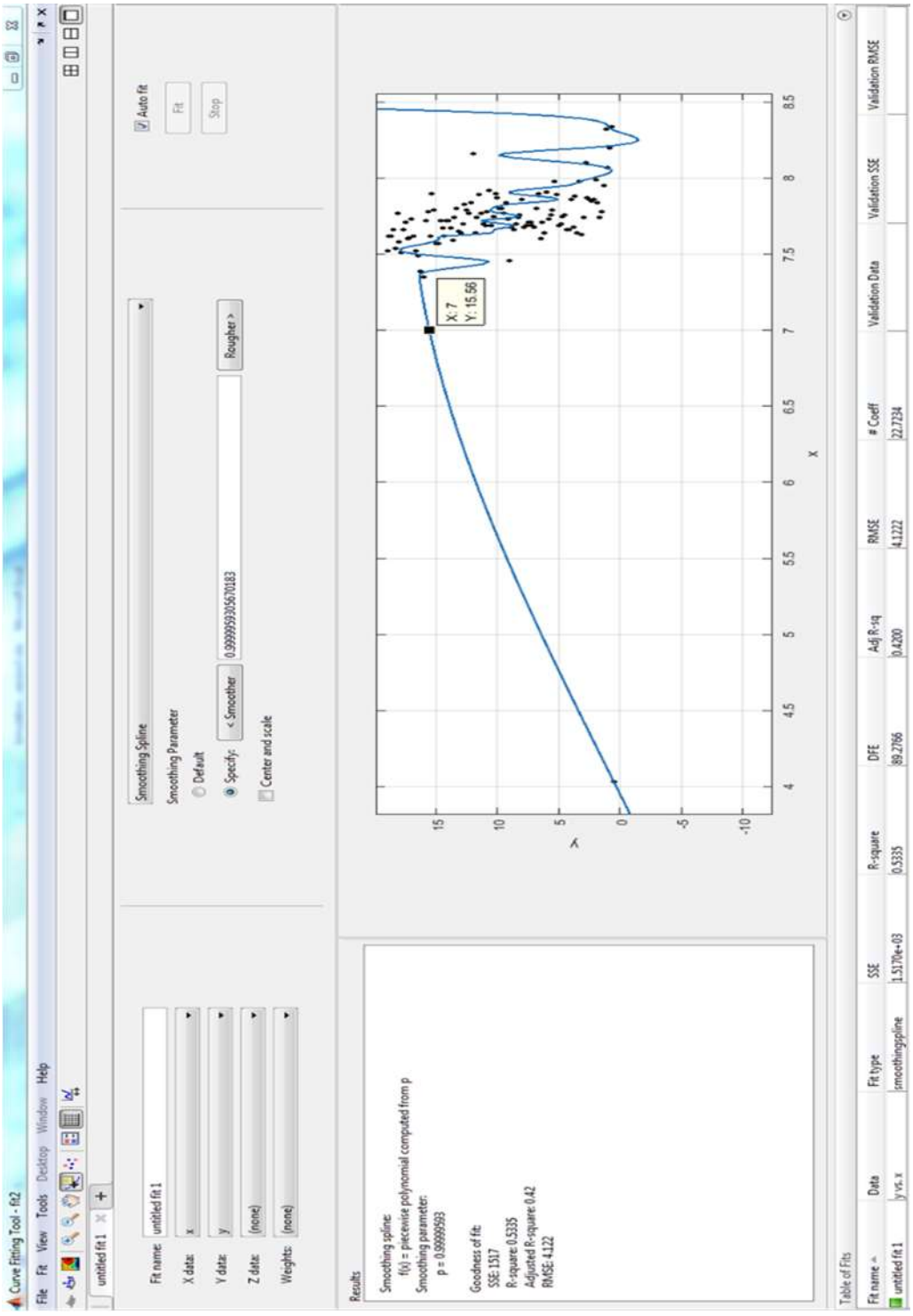

Figure 50: *Interpolation of time with respect to flux.*

By combining the results of **Figure 49** and **Figure 50,** it is possible to identify the time overhead needed to achieve the same performance as UF-MAF, in terms of flux, using MAF under the assumption of an indifferent user (this means that the MAF and UF-MAF techniques are not compared in similar experimental conditions). It is found that this overhead is equal in average to 43%. It reaches as a maximum 72 % and as minimum 28%.

This result is important from the cost-effectiveness perspective since it provides information about the cost overhead corresponding to the same value of flux. It gives a complementary view on the performances of the two pretreatment techniques (UF-MAF and MAF) in terms of the additional cost that would be spent for a similar performance and regardless of the requirement to have similar experimental conditions. Obviously, we considered the operation time as an indicator of cost because most of the OPEX (Operational Expenditure) are often function of time (e.g., energy, manpower).

The next evaluated indicator that impacts the DCMD treatment applicability is the membrane's void ratio that describes the available membrane surface on the utilized samples which could reflect its lifetime. The calculated void ration is also closely linked to the membrane fouling and consequently, to the process performance in terms of permeate flux.

Similarly, the indifference curve illustrating the relationship between the effects of the two pretreatment scenarios on DCMD performance, in terms of membrane void ration, is plotted in **Figure 51**.

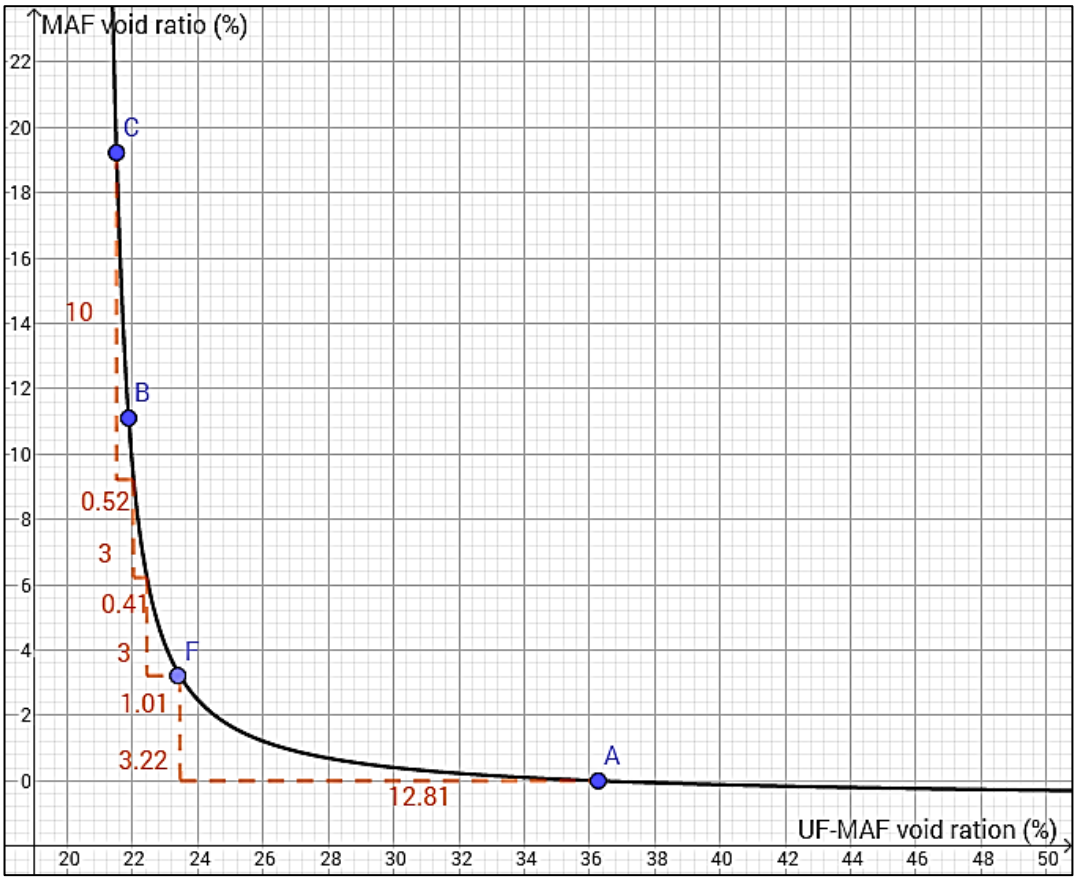

Figure 51: *Indifference curve between the MAF and UF-MAF pretreatment technologies in terms of membrane void ratio.*

According to the mapped local improvements, we calculate the average global improvement which is 12.6%, taking into consideration both positive and negative performances of UF-MAF with respect to MAF. In terms of neat improvement (taking only the positive performances into consideration), the permeate flux improvement ratio that we can obtain by UF-MAF pretreatment have a minimum of 66.3% and a maximum of 94.8%.

3.3.6 Conclusions

In this third section, DCMD treatment of saline dairy effluent has been investigated. The treatment with two pore sized PTFE membranes showed that using tighter pore sizes could lead to higher process performances for all feed qualities. Raw effluent pretreatment by ultrafiltration has a positive effect on both the final permeate flux and the permeate quality which indicates that the feed content and organic load has a direct and significant effect on the DCMD performance which is mainly linked to the fouling layer deposition on the membrane surface and therefore to the membrane wetting that becomes more severe when treating the raw or the macrofiltrated effluent. Besides, it was found that the fouling layer composition has been different after treating the three feed qualities with respect mainly to the salts involved in the fouling layer protein interactions.

Reducing the flow rate during the experiment compromised more the membrane hydrophobicity in all treated feeds. However, when lower temperature difference was applied by increasing the permeate stream temperature, the membrane hydrophobicity improved though lower flux values have been obtained. In all tested operating conditions, DCMD of the pretreated effluent by macrofiltration-ultrafiltration has led to the best permeate quality with stable flux levels and better thermal efficiencies.

The membrane cleaning in our study did contribute in the hydrophobicity loss which could be further investigated to determinate the most suitable cleaning procedure relatively to the fouling layer nature and composition.

In our study, some observations have raised questions and need further investigation such as the impact of the membrane pore size, feed velocity and temperature difference on the fouling layer formation and thickness during dairy effluents DCMD treatment.

The utility theory has been applied in this work to assess the performance and cost-effectiveness of the saline dairy effluent DCMD treatment with respect to two types of pretreatments: MAF and UF-MAF. The obtained results have shown that, in terms of DCMD permeate flux, the neat improvement ratio that we can obtain by UF-MAF pretreatment have a minimum of 25% and a maximum of 71% in comparison to MAF.

This improvement is associated with an average time overhead of 43% that is needed when utilizing MAF to achieve the same performance of UF-MAF, under the assumption of an indifferent user.

With respect to the process cost-effectiveness, this time overhead, which is directly linked to the additional cost that has to be provided when utilizing MAF, have as maximum 72% and as minimum 28%. Regarding the membrane void ratio, the permeate flux improvement ratio that we can obtain by UF-MAF pretreatment have a minimum of 66.3% and a maximum of 94.8%, in terms of neat improvement. This analysis could be extended using the same procedure in order to evaluate and investigate all the listed indicators that impact the DCMD treatment applicability, which requires more precise experimental data.

4 CONCLUSIONS AND PERSPECTIVES

Saline wastewater treatment is a current and growing issue that is getting an increasing attention due to the water resources scarcity worldwide. These effluents have the particularity of containing important salt and organic contents which creates the complexity of their treatment. Besides, the conventional wastewater treatment processes have shown in some cases limited performances that mainly linked to the effluents salt concentration. In order to address these issues, new alternatives for saline effluents treatment and water recovery have to be investigated and analyzed to overcome the present challenges.

To achieve this objective, this research work is focusing on the treatment of saline wastewater and saline dairy effluents obtained from a cheese industry. First, the limitations of biological and membrane processes saline wastewater were studied. Then, comes the main objective of this thesis which is the examination of the feasibility, performance and application of direct contact membrane distillation (DCMD) of the aforementioned effluents. For this purpose, DCMD is applied at different experimental conditions and combined with various pretreatments, namely macrofiltration and ultrafiltration. The cost-effectiveness of the industrial effluent DCMD treatment is also considered in this work.

In the first section, different treatment processes and wastewater qualities were analyzed and investigated to show the effect of the NaCl mass percentage and the treatment characteristics on the final water quality and the processes performances. According to this investigation, the aerobic treatment was more efficient when combined to the ceramic membrane microfiltration since we have obtained higher water quality with good overall performance: the microfiltration led to COD removal of 96%, 76% and 81% for aerobically treated feed of 0.5%, 1% and 2% NaCl, respectively. Concerning the ultrafiltration, the COD removal reached 96 %, 74%, 85% for saline feed concentrations of 0.5%, 1% and 2% NaCl, respectively. In our study, the anaerobic biological treatment didn’t lead to sufficiently good COD removal when compared to the aerobic process which didn’t improve significantly after the filtration processes. In all the studied processes, the main COD removal rates were achieved mainly by the biological treatments. Besides, the final water qualities were very similar in the case of low salt concentrations (0% NaCl and 0.5% NaCl) in comparison to the higher concentrations (1%, 2% and 3% NaCl).

In the second section, the issue of saline effluents treatments is addressed using DCMD. For this purpose, the response surface methodology was applied to optimize the DCMD treatment of saline synthetic wastewater via the optimization of the permeate flux (*Jp*). The studied process has led to the obtention of a remarkable high quality permeate in terms of electrical conductivity reduction (99.9%) and COD removal rate (>99.9%). The DCMD optimization was provided by the application of the response surface methodology in which four different variables were considered to create the optimization model. The four different variables are namely: temperature difference ΔT, feed velocity *Vf*, NaCl concentration [*NaCl*] and glucose concentration [*Gluc*]. The developed regression model demonstrated a good level of effectiveness and ability to predict the process response with $R^2 = 0.967$ and $R^2_{Adj} = 0.932$. The statistical evaluation and analysis of the model showed that it has a high significance and that the most influencing variable in the studied ranges are the temperature difference and the feed flow rate followed by the glucose concentration with lower significant effect. The optimization procedure has led to the prediction of the maximum permeate flux (34.14 L/m^2.h) that could be achieved under the following optimum experimental conditions: $\Delta T = 55.23$°C, *Vf* = 0.086 m/s, *[NaCl]* = 10.08 g/L and *[Gluc]* = 20.01 g/L. As a final step, the experimental verification of the developed regression model showed its validity and suitability within the studied range of variables.

The dairy industries are one of the food processing industrial activities that contribute in the pressure applied on the environment. This contribution starts from the reception of raw materials and milk processing to the packaging of the finished products. The dairy industries are characterized by consuming and discharging massive quantities of water and wastewater, respectively. Among them, we find the cheese industry that is also characterized by the production of a particular by-product, the cheese whey. This by-product is one of the most important components of the discharged saline effluents which increases our need to treat them.

In the third section of this thesis, DCMD treatment of saline dairy effluent has been investigated. The treatment with two PTFE membranes with two different pore sizes showed that using tighter pore sizes could lead to higher process performances for all feed qualities. The raw effluent pretreatment by ultrafiltration has showed a positive effect on both the final permeate flux and the permeate quality which indicates that the feed content and organic load has a direct and significant effect on the DCMD performance that is mainly linked to the fouling layer deposition on the membrane surface. Besides, it was found that the fouling layer composition was different following the treatment of three different feed qualities, mainly with respect to the salts involved in the fouling layer protein interactions.

The variation of the experimental parameters has led to different outcomes in terms of permeate flux and membrane quality. Reducing the flow rate during the experiment compromised more the membrane hydrophobicity in all treated feeds. However, when lower temperature difference was applied by increasing the permeate stream temperature, the membrane hydrophobicity improved though lower flux values have been obtained. In all tested operating conditions, DCMD of the pretreated effluent by macrofiltration-ultrafiltration has led to the best permeate quality with stable flux levels and better thermal efficiencies.

The performance analysis of saline dairy wastewater DCMD process is extended in this work so as to consider its cost-effectiveness when in it is associated with two types of pretreatment. To this purpose, a set of parameters (i.e. criteria) that impact the applicability of the DCMD process in industry are taken into consideration in order to assess its performance. The utility theory has been applied to assess the performance of the saline dairy effluent DCMD treatment with respect to two types of pretreatments: MAF and UF-MAF. The obtained results have shown that, in terms of DCMD permeate flux, the neat improvement ratio that we can obtain by UF-MAF pretreatment have a minimum of 25% and a maximum of 71% in comparison to MAF. This improvement is associated with an average time overhead of 43% that is needed to achieve by MAF the same performance using UF-MAF, under the assumption of an indifferent user. With respect to the cost-effectiveness, this time overhead, which is directly linked to the additional cost that has to be provided when utilizing MAF, have as maximum 72% and as minimum 28%. Regarding the membrane void ratio, the permeate flux improvement ratio that we can obtain by UF-MAF pretreatment have a minimum of 66.3% and a maximum of 94.8%, in terms of neat improvement.

This analysis could be extended using the same procedure in order to evaluate and investigate all the listed indicators that impact the DCMD treatment applicability, which requires more precise experimental data.

In this research work, some observations have raised questions and need further investigation such as the impact of the membrane pore size, feed velocity and temperature difference on the fouling layer formation and thickness during dairy effluents DCMD treatment. Additionally, the membrane cleaning in our study did contribute in the hydrophobicity loss which could be further investigated to determinate the most suitable cleaning procedure relatively to the fouling layer nature and composition.

The tested treatment concept presents a possible alternative to the conventional treatment processes of saline dairy wastewater. This alternative is interesting when the valorization of the concentrated proteins is possible in addition to the water recovery.

In terms of energy consumption, further research could be also dedicated to investigate the possibility of using waste-heat in the DCMD treatment which could increase its cost-effectiveness and create an appealing alternative for industrial saline effluents treatment.

REFERENCES

A. Alkhudhiri, N. Darwish, et N. Hilal. «Membrane distillation: A comprehensive review.» *Desalination* 287 (2012): 2–18.

A. Anglada , R. Ibanez, A. Urtiaga, et I. Ortiz. «Electrochemical oxidation of saline industrial wastewaters using boron-doped diamond anodes.» *Catalysis Today* 151 (2010): 178–184.

A. Bottino , G. Capannelli, O. Monticelli , et P. Piaggio . «Poly(vinylidene fluoride) with improved functionalization for membrane production.» *Journal of Membrane Science 166*, 2000: 23–29.

A. Boubakri , A. Hafiane , et S.A. Bouguecha . «Application of response surface methodology for modeling and optimization of membrane distillation desalination process.» *Journal of Industrial and Engineering Chemistry* 20 (2014): 3163–3169.

A. Hausmann , et al. «Fouling mechanisms of dairy streams during membrane distillation.» *Journal of Membrane Science* 441 (2013.a): 102–111.

A. Hausmann, et al. «Fouling of dairy components on hydrophobic polytetrafluoroethylene (PTFE) membranes for membrane distillation.» *Journal of Membrane Science* 442 (2013.b.): 149–159.

A. Kaminska . *Development and Implementation of a Liquid-Entry-Pressure Test Facility for Assessment of the Wettability of Hydrophobic Membranes.* University of Applied Sciences in Offenburg, 2014.

A. Lee , J.W. Elam , et S.B. Darling. «Membrane materials for water purification: design, development, and application.» *Environ. Sci.: Water Res. Technol.* 2 (2016): 17-42.

A. Pierre, J. Fauquant, Y. Le Graat, M. Piot , et J. L. Maubo. «Préparation de phosphocaséinate natif par microfiltration sur membrane.» *Lait 72* 75 (1992): 461–474.

A. Ventosa . «Taxonomy of moderately halophilic heterotrophic eubacteria». In: Halophilic bacteria.» *Boca Raton JFL CRC Press: 1*, 1988: 77-84.

A. Vijay, S. Aroraa , S. Guptab , et M. Chhabra. «Halophilic starch degrading bacteria isolated from Sambhar Lake, India, as potential anode catalyst in microbial fuel cell: A promising process for saline water treatment.» *Bioresource Technology 256*, 2018: 391-398.

A.I. Khuri , et S. Mukhopadhyay. «Response surface methodology.» *John Wiley & Sons, Inc.* 2 (2010): 128-149.

A.R. Dincer, et F. Kargi. «Performance of rotating biological disc system treating saline wastewater.» *Process Biochem* 36 (2001): 901–906.

A.T. Kivistö , et M.T. Karp. «Halophilic anaerobic fermentative bacteria.» *Arch Microbiol 170(5)*, 2011: 319–330.

A.W. Mohammad, R.K. Basha, et C.P. Leo,. «Nanofiltration of glucose solution containing salts: effects of membrane characteristics, organic component and salts on retention.» *J. Food Eng. 97*, 2010: 510–518.

B. Kempf, et E. Bremer. «Uptake and synthesis of compatible solutes as microbial stress responses to high-osmolality environments.» *Arch Microbiol* 170(5) (1998): 319–330.

B. Prado , et al. «Numerical Taxonomy of Moderately Halophilic Gram-negative Rods Isolated· from the Salar de Atacama, Chile.» *System. Appl. Microbiol. 14*, 1991: 275-281.

B.B. Ashoor, S. Mansour, A. Giwa, V. Dufour, et S.W. Hasan. «Principles and applications of direct contact membrane distillation (DCMD): A comprehensive review.» *Desalination* 398 (2016): 222–246.

B.R. Babu, N.K. Rastogi, et K.S.M.S. Raghavarao. «Mass transfer in osmotic membrane distillation of phycocyanin colorant and sweet-lime juice.» *Journal of Membrane Science*, 2006.

C. Antileo , E. Aspe , C. Zaror, M. Roeckel , H. Urrutia , et M.C. Marti. «Differential bacterial growth kinetic and nitrification of fisheries wastewaters containing high ammonium and organic matter concentration by using pure oxygen.» *Biotechnol. Lett. 19 (3)*, 1997: 241-244.

C. Charcosset. *A review of membrane processes and renewable energies for desalination.* Elsevier, 2009.

C. Gostoli, et G.C. Sarti. «Separation of liquid mixtures by membrane distillation.» *J. Membr. Sci.* 41 (1989): 211–224.

C. M. Bethke, et S. Marshak. «Brine migration across North America – The plate tectonics of groundwater.» *Annual Review of Earth Planetary Science* 18 (1990): 287–315.

C. Nuengjamnong, J.H. Kweon, J. Cho, C. Polprasert, et K.-H. Ahn. «Membrane fouling caused by extracellular polymeric substances during microfiltration processes.» *Desalination* 179 (2005): 117–124.

D. Cheng, W. Gong, et N. Li. «Response surface modeling and optimization of direct contact membrane distillation for water desalination.» *Desalination* 394 (2016): 108–122.

D. Jang, Y. Hwang, H. Shin, et W. Lee. «Effects of salinity on the characteristics of biomass and membrane fouling in membrane bioreactors.» *Bioresource Technology* 141 (2013): 50–56.

D. Singh, P. Prakash, et K.K. Sirkar. «Deoiled produced water treatment using direct contact membrane distillation.» *Ind. Eng. Chem. Res.* 52 (2013): 13439–13448.

D. Winter. *Membrane Distillation - a Thermodynamic, Technological and Economic Analysis.* Aachen, Germany.: Schriftenreihe der Reiner Lemoine-Stiftung. D 386. ISBN 978-3-8440-3706-7., 2015.

D. Winter, J. Koschikowski, D. Düver, P. Hertel, et U. Beuscher. «Evaluation of MD process performance: Effect of backing structures and membrane properties under different operating conditions.» *Desalination* 323 (2013): 120–133.

D.Y. Hou, J. Wang, B.Q. Wang, Z.K. Luan, X.C. Sun, et X.J. Ren. «Fluoride removal from brackish groundwater by direct contact membrane distillation.» *Water Sci. Technol.* 61 (2010): 3178–3187.

E. Corcoran, C. Nellemann, E. Baker, R. Bos, D. Osborn, et H. Sav. *Sick Water? The central role of wastewater management in sustainable development. A Rapid Response Assessment. United Nations Environment Programme,.* UN-HABITAT GRID-Arendal, 2010.

E. Drioli, A. Ali, et F. Macedonio. «Membrane distillation: Recent developments and perspectives.» *Desalination*, 2014.

E. Drioli, A. Criscuoli, et L.P. Molero. *Water And Wastewater Treatment Technologies Vol. III - Membrane Distillation.* Encyclopedia of Life Support Systems (EOLSS), 2009.

E. Quesada , A. Ventosa, F. Rodriguez-Valera, et A. Megias and Ramos-Cormenzana. «Numerical Taxonomy of Moderately Halophilic Gram-negative Bacteria from Hypersaline Soils.» *Journal of General Microbiology 129*, 1983: 2649-2657.

E. Reid, X. Liu, et S.J. Judd. «Effect of high salinity on activated sludge characteristics and membrane permeability in an immersed membrane bioreactor.» *J. Membr. Sci.* 283 (2006): 164–171.

F. Carvalho, A.R. Prazeres, et J. Rivas. «Cheese whey wastewater: Characterization and treatment.» *Science of the Total Environment* 445–446 (2013): 385–396.

F. He, J. Gilron, et K.K. Sirkar. «High water recovery in direct contact membrane distillation using a series of cascades.» *Desalination* 323 (2013): 48.

F. Jia, J. Li, J. Wang, et Y. Sun. «Removal of strontium ions from simulated radioactive wastewater by vacuum membrane distillation.» *Annals of Nuclear Energy* 103 (2017): 363–368.

F. Kargi, et A.R. Dincer. «Effect of salt concentration on biological treatment of saline wastewater by fed-batch operation.» *Enzyme Microb. Technol.* 19 (1996): 529–537.

F. Kargi, et A.R. Dincer. «Saline wastewater treatment by halophile-supplemented activated sludge culture in an aerated rotating biodisc contactor.» *Enzyme Microbiol Technol* 22(6) (1998): 427-433.

F. Laganà, G. Barbieri, et E. Drioli. «Direct contact membrane distillation: modelling and concentration experiments.» *Journal of Membrane Science* 166 (2000): 1–11.

G. Guan, X. Yang, R. Wang, et A.G. Fane. «Evaluation of heat utilization in membrane distillation desalination system integrated with heat recovery.» *Desalination* 366 (2015): 80–93.

G. Naidu, S. Jeong, S.-J. Kim, I. S. Kim, et S. Vigneswaran. «Organic fouling behavior in direct contact membrane distillation.» *Desalination* 347 (2014): 230–239.

G. Ozalp, C.Y. Gomec, I.Ozturk, S. Gonuldinc, et M. Altinbas. «Effect of high salinity on anaerobic treatment of low strength effluents.» *Water Science and Technology* 48 (2003): 207–212.

G. Rice, S.E. Kentish, A. O'Connor, A. Barber, et A. Philajama. «Analysis of separation and fouling behavior during nanofiltration of dairy ultrafiltration permeate.» *Desalination* 236 (2009): 23-29.

G. Tchobanoglous, F.F. Burton, et H.D. Stensel. *Wastewater engineering: Treatment and Reuse. 4th ed.* New York: Metcalf & Eddy, McGraw-Hill, 2003.

H. Lee, F. He, L. Song, J. Gilron,, et K. K. Sirkar. «Desalination with a Cascade of Cross-flow Hollow Fiber Membrane Distillation Devices Integrated with a Hollow Fiber Heat Exchanger.» *AIChE J.* 57 (7) (2011): 1780.

H. Singh, M. Boland, et A. Thompson. *Milk Proteins: from expression to food, second edition.* New Zealand: Food Science and Technology International Series, 2014.

H.H.P. Fang. «Treatment of wastewater from a whey processing plant using activated sludge and anaerobic processes.» *J Dairy Sci* 74 (6) (1991): 2015–2019.

I. Demir, et B. Seyler. «Chemical Composition and Geologic History of Saline Waters in Aux Vases and Cypress Formations, Illinois Basin.» *Aquatic Geochemistry* 5 (1999): 281–311.

I. Vyrides, et D.C. Stuckey. «Adaptation of anaerobic biomass to saline conditions: Role of compatible solutes and extracellular polysaccharides.» *Enzyme and Microbial Technology* 44 (2009.b): 46–51.

I. Vyrides, et D.C. Stuckey. «A modified method for the determination of chemical oxygen demand (COD) for samples with high salinity and low organics.» *Bioresource Technology* 100 (2009.a): 979–982.

I. Vyrides, et D.C. Stuckey. «Fouling cake layer in a submerged anaerobic membrane bioreactor treating saline wastewaters: curse or a blessing?» *Water Sci. Technol.* 63 (12) (2011): 2902–2908.

I. Vyrides, et D.C. Stuckey. «Saline sewage treatment using a submerged anaerobic membrane reactor (SAMBR): Effects of activated carbon addition and biogas-sparging time.» *Water Research* 43 (2009.c): 933-942.

I.K. Kapdan , et B. Erten. «Anaerobic treatment of saline wastewater by Halanaerobium lacusrosei.» *Process Biochemistry 42*, 2007: 449–453.

J. Deshpande, K. Nithyanandam, et R. Pitchumani. «Analysis and design of direct contact membrane distillation.» *Journal of Membrane Science* 523 (2017): 301–316.

J. Ge, Y. Peng, Z. Li, P. Chen, et S. Wang. «Membrane fouling and wetting in a DCMD process for RO brine concentration.» *Desalination* 344 (2014): 97–107.

J. J. Kehoe, et E. A. Foegeding. «Interaction between β-Casein and Whey Proteins as a Function of pH and Salt Concentration.» *J. Agric. Food Chem.* 59 (2011): 349–355.

J. Luo, S. Wei, Y. Su, X. Chen , et Y. Wan. «Desalination and recovery of iminodiacetic acid (IDA) from its sodium chloride mixtures by nanofiltration.» *J. Membr. Sci. 342*, 2009: 35–41.

J. Rivas, A.R. Prazeres, F. Carvalho, et F. Beltrán. «Treatment of cheese whey wastewater: combined coagulation–flocculation and aerobic biodegradation.» *J Agric Food Chem* 58 (13) ((2010)): 7871–7877.

J. Rivas, A.R. Prazeres, et F. Carvalho. «Aerobic biodegradation of precoagulated cheese whey wastewater.» *J Agric Food Chem* 59 (6) (2011): 2511–2517.

J. S. Mounsey, et B. T. O'Kennedy. «Stability of β-lactoglobulin/ micellar casein mixtures on heating in simulated milk ultrafiltrate at pH 6.0.» *Int. J. Dairy Technol.* 62 (4) (2009): 493-499.

J. Warczok, M. Gierszewskab, W. Kujawski, et C. Guell. «Application of osmotic membrane distillation for reconcentration of sugar solutions from osmotic dehydration.» *Separation and Purification Technology* 57 (2007): 425–429.

J.A. Prince , D. Rana , T. Matsuura, N. Ayyanar, T.S. Shanmugasundaram , et G. Singh. «Nanofiber based triple layer hydro-philic/-phobic membrane - a solution for pore wetting in membrane distillation.» *Sci. Rep. 4*, 2014.b: 6949.

J.A. Prince , D. Rana, G. Singh, T. Matsuura, T. Jun Kai , et T.S. Shanmugasundaram . «Effect of Hydrophobic Surface Modifying Macromolecules on Differently Produced PVDF Membranes for Direct Contact Membrane Distillation.» *Chemical Engineering Journal 242*, 2014.a: 387-396.

J.A. Prince, G. Singh , D. Rana , T. Matsuura, V. Anbharasi , et T.S. Shanmugasundaram. «Preparation and characterization of highly hydrophobic poly(vinylidene fluoride)–Clay nanocomposite nanofiber membranes (PVDF–clay NNMs) for desalination using direct contact membrane distillation.» *Journal of Membrane Science 397– 398*, 2012: 80– 86.

J.E. Efome , D. Rana, T. Matsuura , et C.Q. Lan. «Enhanced performance of PVDF nanocomposite membrane by nanofiber coating: A membrane for sustainable desalination through MD.» *Water Research, 89*, 2016: 39-49.

J.E. Miller. *Review of Water Resources and Desalination Technologies.* SAND 0800, 2003.

J.L. Cohon. *Multiobjective Programming and Planning.* California, United States: Volume 140, 1st Edition. ISBN: 9780080956497., 1978.

J.-L. Wang, X.-M. Zhan, Y.-C. Feng, et Y. Qian. «Effect of Salinity Variations on the Performance of Activated Sludge System.» *Biomedical and Environmental Sciences* 18 (2005): 5-8.

J.-S. Kim, C.-H. Lee, et I.-S. Chang. «Effect of pump shear on the performance of a crossflow membrane bioreactor.» *Water Research* 35 (2001): 2137–2144.

K. He , H.J. Hwang , M.W. Woo, et I.S. Moon. «Production of drinking water from saline water by direct contact membrane.» *Journal of Industrial and Engineering Chemistry* 17 (2011): 41–48.

K. Kezia, L. Judy, W. Mike, et S. Kentish. «Direct contact membrane distillation for the concentration of saline dairy effluent.» *Water Research* 81 (2015): 167-177.

K. Nakoa, A. Date , et A. Akbarzadeh. «A research on water desalination using membrane distillation.» *Desalination and Water Treatment.*, 2014: 1–13.

K. Yang, Y. Yu, et S. Hwang. «Selective optimization in thermophilic acidogenesis of cheese-whey wastewater to acetic and butyric acids: partial acidification and methanation.» *Water Research* 37(10) (2003): 2467–2477.

K.M. Blaschek, W.L. Wendorff, et S.A. Rankin. «Survey of salty and sweet whey composition from various cheese plants in Wisconsin.» *J. Dairy Sci.* 90 (4) (2007): 2029-2034.

K.W. Lawson, et D.R. Lloyd. «Direct contact membrane distillation.» *J. Membr. Sci.* 120 (1996): 123–133.

L. Jianquan, et W. Yinhua. «Desalination of effluents with highly concentrated salt by nanofiltration: From laboratory to pilot-plant.» *Desalination 315*, 2013: 91–99.

L. Martinez, et J.M. Rodriguez-Maroto. «On transport resistances in direct contact membrane distillation.» *Journal of Membrane Science* 295 (2007): 28–39.

L. Martinez-Diez, et M.I. Vazquez-Gonzalez. «Temperature and concentration polarization in membrane distillation of aqueous salt solutions.» *J. Membr. Sci. 156*, 1999: 265–273.

L.D. Tijing, Y. C. Woo, J.-S. Choi, S. Lee, S. H. Kim, et H. K. Shon. «Fouling and its control in membrane distillation—A review.» *Journal of Membrane Science* 475 (2015): 215-24.

L.M. Camacho, L. Dumée, , J. Zhang, J. De Li, M. Duke, et J. Gomez. «Advances in membrane distillation for water desalination and purification applications.» *Water* (Water) 5 (2013): 94–196.

M. A. Izquierdo-Gil, M. C. Garca-Payo , et C. Fernndez-Pineda. «Direct Contact Membrane Distillation of Sugar Aqueous Solutions.» *Separation Science and Technology* 349 (1999): 1773-1801.

M. Boukhriss, H. Ben Bacha, K Zarzoum, et k. Zhani. «Study of Modeling and Simulation of Direct Con-tact Membrane Distillation.» *International Journal of Scientific & Engineering Research* 6 (2015): 1317-1325.

M. Gryta. «Effectiveness of Water Desalination by Membrane Distillation Process.» *Journal of Membranes 2*, 2012: 415-429.

M. Gryta. «Fouling in direct contact membrane distillation process.» *Journal of Membrane Science* 325 (2008): 383–394.

M. Khaska, et al. «Origin of groundwater salinity (current seawater vs. saline deep water) in a coastal karst aquifer based on Sr and Cl isotopes. Case study of the La Clape. Case study of the La Clape massif (southern France).» *Applied Geochemistry* 37 (2013): 212–227.

M. Khayet, C. Cojocaru, et C. Garcia-Payo. «Application of Response Surface Methodology and Experimental Design in Direct Contact Membrane Distillation.» *Ind. Eng. Chem. Res.* 46 (2007): 5673-5685.

M. Khayet, et T. Matsuura. «Preparation and characterization of polyvinylidene fluoridemembranes for membrane distillation.» *Ind. Eng. Chem. Res. 40 (24)*, 2001: 5710–5718.

M. M. A. Saleh, et U. F. Mahmood. «Anaerobic digestion technology for industrial wastewater treatment.» *Eighth International Water Technology Conference, IWTC8.* Alexandria, Egypt, 2004.

M. Samblebe. «Wastewater re-use and desalination a summary of the drivers for, and technology evolution to satisfy the global push for sustainable water use.» *69th Annual Water Industry Engineers and Operators' Conference.* 2006. 52-58.

M. Wybult. *Characterization and Investigation of Conditions Influencing the Aging of Hydrophobic, Microporous Membranes for Membrane Distillation.* University of Applied Sciences in Offenburg, 2015.

M.A. De La Fuente, H. Singh, et Y. Hemar. «Recent advances in the characterization of heat induced aggregates and intermediates of whey proteins,.» *Trends Food Sci. Technol.* 13(8) (2002): 262–274.

M.A. Izquierdo-Gil, M.C. Garca-Payo, et C. Fernndez-Pineda. «Direct Contact Membrane Distillation of Sugar Aqueous Solutions.» *Separation Science and Technology* 34:9 (1999): 1773-1801.

M.C. Lai , et al. «Methanocalculus taiwanensis sp. nov., isolated from an estuarine environment.» *Int J Syst Evol Microbiol. 52*, 2002: 1799-806.

M.P.Diaz , K.G. Boyd, S.J.W. Grigson , et J.G. Burgess. «Biodegradation of crude oil across a wide range of salinities by an extremely halotolerant bacterial consortium MPD-M, immobilized onto polypropylene fibers.» *Biotechnol. Bioeng. 79 (2)*, 2002: 145–153.

M.S. El-Bourawi, Z. Ding, R. Ma, et M. Khayet. «A framework for better understanding membrane distillation separation process.» *Journal of Membrane Science* 285 (2006): 4–29.

M.S. Khayet, et T. Matsuura. *Membrane Distillation : Principles and Applications.* Elsevier 1st edition, 2011.

M.W. Shahzad, M. Burhan, L. Ang, et K. Choon Ng. «Energy-water-environment nexus underpinning future desalination sustainability.» *Desalination* 413 (2017): 52–64.

N. Argova, D.G. Lemaya, et J.B. German. «Milk Fat Globule structure & function; nanosciece comes to milk production.» *Trends Food Sci Technol* 19(12) (2008).

N. Rovirosa, E. Sanchez, M. Cruz, MC. Veiga, et R. Borja. «Coliform concentration reduction and related performance evaluation of a down-flow anaerobic fixed bed reactor treating low-strength saline wastewater.» *Bioresour Technol* 94 (2004): 119–1227.

N. Sundaresan, et L. Philip. «Performance evaluation of various aerobic biological systems for the treatment of domestic wastewater at low temperatures.» *Water Science & Technology* 58.4 (2008): 819-830.

O. Kaplinski. «The Utility Theory in Maintenance and Repair Strategy.» *Procedia Engineering 54*, 2013: 604 – 614.

O. Lefebvre, et R. Moletta. «Treatment of organic pollution in industrial saline wastewater: A literature review.» *Water Research* 40 (20) (2006.a): 3671–3682.

O. Lefebvre, N. Vasudevan, M. Torrijos, K. Thanasekaran, et R. Moletta. «Anaerobic digestion of tannery soak liquor with an aerobic post treatment.» *Water Research* 40 (2006.b): 1492–1500.

P. M. Kamrani, O. Bakhtiari, P. Kazemi, et T. Mohammadi. «Theoretical modeling of direct contact membrane distillation (DCMD): effects of operation parameters on flux.» *Desalination and Water Treatment*, 2014: 1-10.

P. Onsekizoglu. «Membrane Distillation: Principle, Advances, Limitations and Future Prospects in Food Industry.» Dans *Distillation - Advances from Modeling to Applications*, de Sina Zereshki (Ed.), 234-257. InTech, 2012.

P. Onsekizoglu. «Potential of membrane distillation for production of high quality fruit juice concentrate- A comprehensive review.» *Food Science and Nutrition*, 2013.

P.A. Hogan, R.P. Canning, P.A. Peterson, R.A. Johnson, et A.S. Mi. «A new option: Osmotic Distillation.» *Chemical Engineering Progress.*, 1998.

P.C. Fishburn. *Utility Theory. Management Science.* USA.: Vol. 14, No. 5, 335-378., 1968.

P.M. Kamrani, O. Bakhtiari , P. Kazemi , et T. Mohammadi . «Theoretical modeling of direct contact membrane distillation (DCMD): effects of operation parameters on flux.» *Desalination and Water Treatment*, 2014: 1-10.

R. Bura, et al. «Composition of extracellular polymeric substances in the activated sludge floc matrix.» *Water Sci. Technol.* 37 (1998): 325–333.

R. Dashtpour, et S.N. Al-Zubaidy. «Energy Efficient Reverse Osmosis Desalination Process.» *International Journal of Environmental Science and Development, Vol. 3, No. 4*, 2012: 339-345.

R. Gebauer. «Meosphilic anaerobic treatment of sludge from saline fish farm effluents with biogas production.» *Bioresour Technol* 93 (2004): 155–167.

R. Waninge, P. Walstra, J. Bastiaans, H. Nieuwenhuijse, et T. Nyl. «Competitive Adsorption between â-Casein or â-Lactoglobulin and Model Milk Membrane Lipids at Oil-Water Interfaces.» *J. Agric. Food Chem.* 53 (2005): 716-724.

R.B. Saffarini, B. Mansoor, R. Thomas, et H.A. Arafat. «Effect of temperature-dependent microstructure evolution on pore wetting in PTFE membranes under membrane distillation conditions.» *J. Membr. Sci.* 429 (2013): 282–294.

R.W. Schofield, A.G. Fane , C.J.D. Fell , et R. Macoun. «Factors affecting flux in membrane distillation.» *Desalination* 77 (0) (1990): 279-294.

R.W. Schofield, A.G. Fane, et C.J.D. Fell. «Heat and mass transfer in membrane distillation.» *Journal of Membrane Science* 33 (1987): 299-313.

S. Abdelkader , et al. «Application of direct contact membrane distillation for saline dairy effluent treatment: performance and fouling analysis.» *Environ Sci Pollut Res*, 2018: 1–14.

S. Al-Asheha, F. Banatb, M. Qtaishatc, et M. Al-Khateeb. «Concentration of sucrose solutions via vacuum membrane distillation.» *Desalination* 195 (2006): 60–68.

S. Lattemann, et T. Höpner. «Environmental impact and impact assessment of seawater desalination.» *Desalination* 220 (2008): 1-15.

S. Yarlagadda, V.G. Gude, L.M. Camacho, S. Pinappu, et S. Deng. «Potable water recovery from As, U, and F contaminated ground waters by direct contact membrane distillation process.» *Journal of Hazardous Materials 192*, 2011 : 1388–1394.

S.V. Kalyuzhnyi, E.P. Martinez, et J.R. Martinez. «Anaerobic treatment of high-strength cheese-whey wastewater in laboratory and pilot UASB-reactors.» *Bioresource Technologies* 60 (1) (1997): 59–65.

S.V. Panno, et al. «Source Identification of Sodium and Chloride Contamination in Natural Waters: Preliminary Results.» *The 12th Annual Conference of the Illinois Groundwater Conference of the Illinois Groundwater Consortium.* Makanda, 2002.

T.J. McGhee. *Treatment of Brackish and Saline Waters. Water Supply and Sewerage, 6th ed.* New York: McGraw-Hill, Inc., 1991.

V.P. Marel, A. Zwijnenburg, A.J.B. Kemperman, M. Wessling, H.Temmink, et W.G.J. van derMeer. «Influence of membrane properties on fouling in submerged membrane bioreactors.» *J. Membr. Sci.* 348 (2010): 66-74.

W. A. Zisman. *Relation of the Equilibrium Contact Angle to Liquid and Solid Constitution. Advances in Chemistry.* Washington, DC: American Chemical Society, 1964.

W. Guo, H.-H. Ngo, et J. Li. «A mini-review on membrane fouling.» *Bioresource Technology* 122 (2012): 27–34.

W. Janczukowicz, M. S. Zielin, et D. M. bowski . «Biodegradability evaluation of dairy effluents originated in selected sections of dairy production.» *Bioresource Technologies* 99 (10) (2008): 4199–41205.

W. Luo, et al. «Effects of salinity build-up on biomass characteristics and trace organic chemical removal: Implications on the development of high retention membrane bioreactors.» *Bioresource Technology* 177 (2015): 274-281.

Wastewater the Untapped Resource. France: The United Nations World Water Development, 2017.

Water and Energy. The United Nations World Water Development, 2014.

Water for Sustainable World. The United Nations Educational Scientific and Cultural Organization: The United Nations World Water Development, 2015.

X. Shi, O. Lefebvre, K. Kwang Ng, et H. Yong Ng. «Sequential anaerobic–aerobic treatment of pharmaceutical wastewater with high salinity.» *Bioresource Technology* 153 (2014): 79–86.

X. Zhang, J. Gao, F. Zhao, Y. Zhao, et Z. Li. «Characterization of a salt-tolerant bacterium Bacillus sp. from a membrane bioreactor for saline wastewater treatment.» *Journal of Environmental Sciences* 26 (2014): 1369–1374.

X. Zhang, Z. Guo, C. Zhang, et J. Luan. «Exploration and optimization of two-stage vacuum membrane distillation process for the treatment of saline wastewater produced by natural gas exploitation.» *Desalination* 385 (2016): 117–125.

LIST OF FIGURES

LIST OF TABLES

List of abbreviations

Abbreviation	Designation
CA	Contact angle.
CAPEX	Capital Expenditure.
CIP	Cleaning in place.
COD	Chemical oxygen demand.
DCMD	Direct contact membrane distillation.
EDX	Energy dispersive X-ray.
EPS	Extracellular polymeric substances.
LEP	Liquid entry pressure.
M1	0.45µm pore size membrane.
M2	0.2µm pore size membrane.
MAF	Macrofiltration.
MAF-UF-WW	Pretreated effluent by macrofiltration and ultrafiltration.
MAF-WW	Pretreated effluent by macrofiltration.
MLSS	Mixed liquor suspended solids.
OPEX	Operational Expenditure.
PP	Polypropylene.
PTFE	Polytetrafluoroethylene.
R-WW	Raw effluent.
SEM	Scanning electron microscopy.
TC	Total carbon.
TIC	Total inorganic carbon.
TOC	Total organic carbon.
UF	Ultrafiltration.
VoT	Value of time.

List of symbols

Symbol	Unit	Designation
[CH_4]	ml/L	Methane concentration.
[*Gluc*]	g/L	Glucose concentration.
[*NaCl*]	g/L; %	Nacl concentration.
Δp	bar	Transmembrane pressure.
Δt	hour (h)	DCMD operating time.
A	m^2	Membrane filtration area.
c	-	The cost corresponding to the demand function x.
EC	µS/cm	Electrical conductivity.
I_i	-	Indicator.
J	$kg/m^2.h$	Permeate flux.
J*p*,	$L/m^2.h$	Volumetric permeate flux.
LEP	bar	Liquid entry pressure.
ηth	%	Thermal efficiency.
P^0	bar	Pure water vapor.
Q	L/h	Flow rate.
S	m^2	Effective membrane surface.
T	°C	Water temperature.
t	h	Filtration time.
t	-	Time to conduct the process satisfying the demand x.
Tco	°C	Permeate outlet temperature.
Tei	°C	Feed inlet temperature.
TOC	mg/L	Total organic carbon.
V	m/s	Velocity.

Vc	m/s	Permeate velocity in the laboratory scale DCMD test cell.
Ve	m/s	Feed velocity in the laboratory scale DCMD test cell.
V*f*	m/s	Feed velocity in the bench scale DCMD test cell
Vol	L	Permeate volume.
x	-	Demand function.
ΔT	°C	Temperature difference in the DCMD test cell.